Lactoferrin: Structure, Function, Thermal Denaturation and Digestion

A thesis submitted in fulfilment of the requirements for

the degree of Doctor of Philosophy

Bo Wang

B.Tech. (Marine Bio-pharmaceutics), Shanghai Ocean University, China, 2013

School of Science

College of Science, Engineering and Health

RMIT University, Melbourne, Australia

September, 2017

Declaration

I certify that except where due acknowledgement has been made, the work is that of the author alone; the work has not been submitted previously, in whole or in part, to qualify for any other academic award; the content of the Thesis is the result of work which has been carried out since the official commencement date of the approved research program; and any editorial work, paid or unpaid, carried out by a third party is acknowledged; and ethics procedures and guidelines have been followed.

Bo Wang
15 September 2017

Copyright

Bo Wang

2017

Copyright Notices

Notice 1

Notice 2

Acknowledgements

First and foremost, I am indebted to my father Yuchuan Wang and mother Kun Liu for providing me with financial and emotional support in the entirety of my PhD study. Without their support, it would not be possible for me set out for this journey.

I wish to express my deepest gratitude to my Senior Supervisor Associate Professor Benu Adhikari for accepting me as his PhD student. With his kind and invaluable guidance, the journey became smooth and enjoyable. I am also thankful to my Co-Supervisor Professor Ewan Blanch for sharing his insightful knowledge and providing guidance. The patient supervision from both supervisors enabled me to complete this study in time.

I am thankful to Dr Yakindra Prasad Timilsena for providing me with professional support especially in the early stage of candidature.

The fresh lactoferrin samples, used in this PhD study, were provided by Tatura Milk Industries Ltd. (Subsidiary of Bega Cheese, Australia). I gratefully acknowledge the industry for this generous support.

I wish to acknowledge the technical staffs of RMIT University for providing support on instrument training and safety induction. I also thank my past and current colleagues of Bioscience and Food Technology disciplines including Dr. Md. Amdadul Haque, Dr. Naksit Panyoyai, Dr. Vilia Darma Paramita, Billy Lo, A K M Masum, Arissara Phosanam, Bao Loc Pham, Isaac Martinez Pardo and Nyok Ling Tai for friendship and also for sharing their experience.

RMIT UNIVERSITY

SGR-80

School of Graduate Research
Research outputs - declaration form

Explanation:

This form is used to record bibliographical details and authorship arrangements associated with research outputs produced during candidature that are included in the thesis/project for examination. This includes publications and non-traditional research outputs whether they are reproduced in part **or** in full.

Instructions:

1. All candidates should complete section 1.
2. If your thesis/project contains sole-authored research outputs, please complete section 2.
3. If your thesis/project contains outputs involving collaborators please complete section 3 and attach a statement for each output that clarifies your contribution to the work. This may be in the form of a description of your precise contributions to the research output and/or a statement of your percentage contribution. This statement must be signed by all contributors. If signatures from all the contributors cannot be obtained, the statement detailing your contribution to the output must be signed by your senior supervisor.
4. If your thesis/project contains **both** sole and co-authored outputs please complete sections 2 and 3.
5. To formally report your outputs please see the process at: http://www1.rmit.edu.au/staff/research/publish

Section 1. Name and details

Student ID: s3518917

Family Name: Wang Given Name: Bo

Program code: DR232

School/Centre: Science - Applied Sciences

Section 2. Sole-authored research outputs

This thesis/project contains published or publicly presented work and/or work prepared for publication/public presentation, which has been **sole-authored**. The bibliographical details of the work and where it appears are outlined below. (Attach a separate statement if necessary)

Section 3. Co-authored research outputs

This thesis/project contains published or publicly presented work and/or work prepared for publication/public presentation, which has been **co-authored**. The bibliographical details of the work, where it appears in the thesis/project, and what contribution I made to the work/s are explained in the attached statements. I have the permission of all co-authors to include this work in my thesis/project.

Statement/s attached. ☑

Senior supervisor's signature (only required if co-authors signatures have not been obtained):

Signature: Benu Adhikari Name: Benu Adhikari

Staff number: E10974 Date: 01/09/2017

Section 3. Candidate signature

Signature: Date: 01/09/2017

PUBLICATIONS

The following are the journal papers that form the part of this Thesis.

A list of Journal articles

Wang, B., Timilsena, Y. P., Blanch, E., & Adhikari, B. (2017). Lactoferrin: Structure, Function, Denaturation and Digestion. *Critical Reviews in Food Science and Nutrition*, http://dx.doi.org/10.1080/10408398.2017.1381583.
(This accepted version of review article is presented as **Chapter 2** in this Thesis)

Wang, B., Timilsena, Y. P., Blanch, E., & Adhikari, B. (2017). Drying and denaturation characteristics of three forms of bovine lactoferrin. *Drying Technology*, 35(5), 606-615.
(This published paper is presented as **Chapter 3** in this Thesis)

Wang, B., Timilsena, Y. P., Blanch, E., & Adhikari, B. (2017). Characteristics of bovine lactoferrin powders produced through spray and freeze drying processes. *International Journal of Biological Macromolecules*, 95, 985-994.
(This published paper is presented as **Chapter 4** in this Thesis)

Wang, B., Timilsena, Y. P., Blanch, E., & Adhikari, B. (2017). Mild thermal treatment and in-vitro digestion of three forms of bovine lactoferrin: Effects on functional properties. *International Dairy Journal*, 64, 22-30.
(This published paper is presented as **Chapter 5** in this Thesis)

Wang, B., Blanch, E., Barrow, C., & Adhikari, B. (2017). Preparation and study of digestion behavior of lactoferrin-sodium alginate complex coacervates. *Journal of Functional Foods*, 37, 97-106.
(This published paper is presented as the first part of **Chapter 6** in this Thesis)

School of Science
Chapter Declaration for Thesis with Publications

Chapter 2 is represented by the following paper:

[Lactoferrin: Structure, Function, Denaturation and Digestion]
[Bo Wang, Yakindra Prasad Timilsena, Ewan Blanch & Benu Adhikari]
[Critical Reviews in Food Science and Nutrition]
[In press]
[2017]

Declaration by candidate

I declare that I wrote the initial draft of this manuscript, and my overall contribution to this paper is detailed below:

Nature of contribution	**Extend of contribution (%)**
Performed all experiments unless duly acknowledged, analysed all of the data and prepared the graphs and tables, interpreted the results, prepared the manuscript draft, revised the manuscript.	75

The following co-authors contributed to the work. The undersigned declare that the contributions of the candidate and co-authors are correctly attributed below.

Author	**Nature of contribution**	**Extent of contribution (%)**
Benu Adhikari	Supervised the project, edited the first and final draft and approved the manuscript for submission, edited and approved the revised manuscript and submitted to the journal	15
Ewan Blanch	Edited the first and final draft	7
Yakindra Prasad Timilsena	Partially interpreted the results and edited the first draft	3

Candidate's Signature		Date 15/09/2017
Primary Supervisor's Signature		15/09/2017

School of Science
Chapter Declaration for Thesis with Publications

Chapter 3 is represented by the following paper:

[Drying and denaturation characteristics of three forms of bovine lactoferrin]
[Bo Wang, Yakindra Prasad Timilsena, Ewan Blanch & Benu Adhikari]
[Drying Technology]
[Volume 35, Issue 5, 606-615]
[2017]

Declaration by candidate

I declare that I wrote the initial draft of this manuscript, and my overall contribution to this paper is detailed below:

Nature of contribution	**Extend of contribution (%)**
Performed all experiments unless duly acknowledged, analysed all of the data and prepared the graphs and tables, interpreted the results, prepared the manuscript draft, revised the manuscript.	75

The following co-authors contributed to the work. The undersigned declare that the contributions of the candidate and co-authors are correctly attributed below.

Author	**Nature of contribution**	**Extent of contribution (%)**
Benu Adhikari	Supervised the project, edited the first and final draft and approved the manuscript for submission, edited and approved the revised manuscript and submitted to the journal	15
Ewan Blanch	Edited the first and final draft	7
Yakindra Prasad Timilsena	Partially interpreted the results and edited the first draft	3

Candidate's Signature		Date 15/09/2017
Primary Supervisor's Signature		15/09/2017

School of Science
Chapter Declaration for Thesis with Publications

Chapter 4 is represented by the following paper:

[Characteristics of bovine lactoferrin powders produced through spray and freeze drying processes]
[Bo Wang, Yakindra Prasad Timilsena, Ewan Blanch & Benu Adhikari]
[International Journal of Biological Macromolecules]
[Volume 95, 985-994]
[2017]

Declaration by candidate

I declare that I wrote the initial draft of this manuscript, and my overall contribution to this paper is detailed below:

Nature of contribution	**Extend of contribution (%)**
Performed all experiments unless duly acknowledged, analysed all of the data and prepared the graphs and tables, interpreted the results, prepared the manuscript draft, revised the manuscript.	75

The following co-authors contributed to the work. The undersigned declare that the contributions of the candidate and co-authors are correctly attributed below.

Author	**Nature of contribution**	**Extent of contribution (%)**
Benu Adhikari	Supervised the project, edited the first and final draft and approved the manuscript for submission, edited and approved the revised manuscript and submitted to the journal	15
Ewan Blanch	Edited the first and final draft	7
Yakindra Prasad Timilsena	Partially interpreted the results and edited the first draft	3

Candidate's Signature		Date 15/09/2017

Primary Supervisor's Signature		15/09/2017

School of Science
Chapter Declaration for Thesis with Publications

Chapter 5 is represented by the following paper:

[Mild thermal treatment and in-vitro digestion of three forms of bovine lactoferrin: Effects on functional properties]
[Bo Wang, Yakindra Prasad Timilsena, Ewan Blanch & Benu Adhikari]
[International Dairy Journal]
[Volume 64, 22-30]
[2017]

Declaration by candidate

I declare that I wrote the initial draft of this manuscript, and my overall contribution to this paper is detailed below:

Nature of contribution	**Extend of contribution (%)**
Performed all experiments unless duly acknowledged, analysed all of the data and prepared the graphs and tables, interpreted the results, prepared the manuscript draft, revised the manuscript.	75

The following co-authors contributed to the work. The undersigned declare that the contributions of the candidate and co-authors are correctly attributed below.

Author	**Nature of contribution**	**Extent of contribution (%)**
Benu Adhikari	Supervised the project, edited the first and final draft and approved the manuscript for submission, edited and approved the revised manuscript and submitted to the journal	15
Ewan Blanch	Edited the first and final draft	7
Yakindra Prasad Timilsena	Partially interpreted the results and edited the first draft	3

Candidate's Signature		Date 15/09/2017

Primary Supervisor's Signature		15/09/2017

School of Science
Chapter Declaration for Thesis with Publications

Chapter 6 is represented by the following paper:

[Preparation and study of digestion behaviour of lactoferrin-sodium alginate complex coacervates]
[Bo Wang, Ewan Blanch, Collin James Barrow & Benu Adhikari]
[Journal of Functional Foods]
[Volume 37, 97-106]
[2017]

Declaration by candidate

I declare that I wrote the initial draft of this manuscript, and my overall contribution to this paper is detailed below:

Nature of contribution	**Extend of contribution (%)**
Performed all experiments unless duly acknowledged, analysed all of the data and prepared the graphs and tables, interpreted the results, prepared the manuscript draft, revised the manuscript.	75

The following co-authors contributed to the work. The undersigned declare that the contributions of the candidate and co-authors are correctly attributed below.

Author	**Nature of contribution**	**Extent of contribution (%)**
Benu Adhikari	Supervised the project, edited the first and final draft and approved the manuscript for submission, edited and approved the revised manuscript and submitted to the journal	15
Ewan Blanch	Edited the first and final draft	5
Collin James Barrow	Partially interpreted the results and edited the first draft	5

Candidate's Signature		Date 15/09/2017

Primary Supervisor's Signature		15/09/2017

TABLE OF CONTENTS

LIST OF ABBREVIATIONS

*Sequence of abbreviations are arranged by their alphabetical order

Apo-LF	Iron depleted lactoferrin
ATR	Attenuated total reflectance
BCA	Bicinchoninic acid
BSA	Bovine serum albumin
CD	Circular dichroism
CD	Convective air drying
CY	Yiled of coacervates
DPPH	2,2-diphenyl-1-picrylhydrazyl
DSC	Differential scanning calorimeter
EDTA	Ethylenediaminetetraacetic acid
FD	Freeze drying
$FDLF_b$	Freeze-dried bovine lactoferrin
FeNTA	Ferric nitrilotriacetic acid
FTIR	Fourier transform infrared spectrometer
GAB model	Guggenheim-Anderson-de Boer model
GIT	Gastrointestinal tract
Holo-LF	Iron saturated lactoferrin
HPLC	High performance liquid chromatography
IHT	Isothermal heat treatment
LF	Lactoferrin
LF_b	Bovine lactoferrin
MR	Moisture ratio
MW	Molecular weight
NaAlg	Sodium Alginate
PC-ET	Proton coupled electron transfer
PEG	Polyethylene glycol
pH	The power of Hydrogen
pI	Isoelectric point
RP-HPLC	Reversed phase high performance liquid chromatography
SD	Spray drying
SDD	Single droplet drying

$SDLF_b$	Spray-dried bovine lactoferrin
$SDLF_{b70}$	Spray-dried bovine lactoferrin at outlet temperature of 70 ˚C
$SDLF_{b95}$	Spray-dried bovine lactoferrin at outlet temperature of 95 ˚C
SDS-PAGE	Sodium dodecyl sulphate polyacrylamide gel electrophoresis
SEI	Strength of electrostatic interaction
SGF	Simulated gastric fluid
SIF	Simulated intestinal fluid
SOF	Simulated oral fluid
TGA	Thermogravimetric analyzer
UV-Vis	Ultraviolet–visible

RMIT	Royal Melbourne institute of technology
CSIRO	Commonwealth Scientific and Industrial Research Organisation

EXPLANATORY NOTES

The following notes briefly delineate the points that were taken into consideration during the writing of this Thesis.

(i) Attempts have been made to use British spellings in the text except in the published journal articles where the journal guidelines have been followed.

(ii) Symbols or abbreviations, used in place of a lengthy name or expression, have been defined or explained in appropriate places as far as practicable.

(iii) Wherever possible, SI units have generally been used in expressing results throughout this Thesis.

(iv) APA referencing format has been followed in this Thesis except in the published articles where journal guidelines have been followed.

(v) Details of materials and reagents, method of calibration of equipment and experimental parameters used are depicted in each experimental chapter (Chapter 3-6) of this Thesis.

SUMMARY

The demand for foods possessing health benefits above and beyond calorie value is continuously increasing. In this context, lactoferrin (LF) has received considerable research attention because of its unique iron binding and delivering abilities. LF is a minor constituent of milk proteins which possesses antibacterial, antioxidant and anti-carcinogenic characteristics in addition to its iron-binding ability. For these reasons, it is increasingly used as an important ingredient in many foods (e.g. infant milk formula) and pharmaceutical products (e.g., Acne care drugs).

The functional properties of LF are highly dependent on its structural integrity. Since LF is sensitive to temperature and other chemical induced denaturation, the extraction, powder formation processes and processing parameters of LF and LF-containing products have to be optimised to minimise the undesired conformational changes (denaturation). The breakdown of structure and subsequent loss in the functional values of LF and LF-containing products in human digestive system also require systematic study. This understanding will help develop novel methods to best deliver LF to the targeted absorption sites in the human gastrointestinal tract in structurally and functionally stable form. Therefore, this study investigated the structure-function relationship of LF during thermal processing (convective air drying, spray drying and freeze drying) and digestion (*in-vitro* adult condition), and also studied its complex coacervation with sodium alginate (NaAlg) to preserve its structural integrity and functional properties and to slow down its premature digestion.

LF exits in 3 different forms, i.e., iron depleted apo form, iron saturated holo form and partially iron saturated mono form. In this study, apo and holo forms of LF were prepared in the laboratory. Native-LF is a mixture of all of these three forms. The native-LF was extracted by membrane processing technology and was made available to this work in fresh aqueous solution form by a local manufacturer. The level of iron saturation of apo-, native- and holo-LF was 1.4, 12.6 and 100.0%, respectively.

At the first stage of this study, single droplet drying was carried out to quantify the drying and denaturation kinetics of LF during particle formation process. The single droplet drying simulates the drying of a droplet subjected to spray drying. It was found that 10-30% of LF was denatured when convective air drying was carried out for 10 min primarily due to longer drying time. The actual spray drying operation (180^{o}C inlet and 70-95^{o}C outlet

temperatures) was found to cause no significant denaturation of LF due to characteristically short drying time. A commonly used freeze drying process was also found to cause no significant denaturation of LF. The secondary structural features of both spray- and freeze-dried LF were identical to those of fresh LF solution. No significant decrease of the antioxidant capacity of LF was observed in the spray-dried LF powders while up to 6% decrease was observed in the freeze-dried LF powders. These findings indicate that industries could produce LF powders without losing its structural integrity and functional properties by selecting suitably optimised spray- and freeze-drying processes.

The degradation patterns, alteration in the secondary structural features and changes in the functional properties of LF were determined *in-vitro* simulating the human adult digestion system. The results show that the structure-function characteristics of LF were not altered during the oral stage of digestion. However, the structure of LF was unable to resist gastric stage of digestion and it was completely broken down into <10 kDa peptide fractions. These fractions were further degraded during the intestinal stage of digestion. These findings conclusively show that LF cannot be delivered to the small intestine absorption sites in its structurally intact form through oral intake. The degraded peptides possessed <20% iron binding capacity compared to that of the intact LF. The antioxidant capacity of LF also decreased significantly during the gastric stage of digestion. The above observations indicated that LF must be protected from premature digestion in the gastric stage of digestion.

The LF-NaAlg complex coacervates were synthesised and the digestion behaviour of the complex coacervated LF was studied. The highest yield of the complex coacervates was achieved at pH 4.5 and LF-to-NaAlg ratios of 8:1. No changes in the secondary structural features of LF occurred due to the formation of these electrostatically driven LF-NaAlg complex coacervates. The optimised LF-NaAlg complex coacervates provided 27%–34% protection to LF during the gastric stage of digestion while the unprotected LF was completely decomposed. The secondary structural features of LF were protected to a significantly greater extent in the gastric digestion stage when it was in complex coacervated form. The antioxidant capacity of LF in the complex coacervated form was also fully retained during gastrointestinal tract. However, the effectiveness of LF as an iron transferring protein was not improved when it formed complex coacervates with NaAlg.

This study provides fundamental insights into the fact that the structural and functional properties of LF can be altered due to thermal, acidic and enzymatic stresses encountered

during thermal processing and digestion. It also shows that the undesirable changes in structure and functions of LF can be significantly reduced by optimising process parameters and forming complex coacervates as a more acid-stable matrix. Overall, this study paves a way for the production of structurally and functionally intact LF powders through spray and freeze drying process. The outcomes of this study help better utilisation of LF in high-value food products that aim to deliver LF through oral intake. The complex coacervation based approach, developed in this study to protect LF in gastric stage of digestion, can also be applied to other bioactive proteins.

CHAPTER 1

Introduction

1.1. Background

With increased awareness of consumers regarding their health and wellbeing, foods are no longer considered only as carriers of nutrients and energy. Instead, they are expected to enhance physical and mental wellbeing at various stages of life. Desired health benefits can be imparted to foods by incorporating biologically-active or functional ingredients. In general, these foods are known as functional foods and consumer demand for them has been continuously increasing in recent years (Betoret, Betoret, Vidal & Fito, 2011). In this context, a number of new bio-active proteins have been extracted from animals and plants and their functional efficacies have been investigated. One of such highly sought-after protein is lactoferrin (LF), which is also known as lactotransferrin.

LF is known for its characteristic iron binding and transferring abilities. Since iron deficiency is one of the most common nutritional deficiencies in the world (Centers for Disease Control and Prevention, 2002), LF is increasingly viewed as an effective and safe ingredient to deliver iron to people with iron deficiency (Paesano *et al.,* 2010). Apart from this commonly known iron binding ability, LF has also been reported to facilitate absorption of sugars (Artym & Zimecki, 2005), provide defense against infection and inflammation (Britigan *et al.,* 1994; EI-Loly & Mahfouz, 2011), modulate cell growth and inhibit the formation of several toxic compounds (Baveye *et al.,* 1999). Due to these reasons, industrial manufacturing of bovine LF is continuously increasing for last 25 years (Tomita *et al.,* 2009). The global market for LF has increased from 45 tons in 2001 to 185 tons in 2012 and it is projected to grow to 262 tons in 2017 (Synlait, 2013).

LF is found in relatively higher concentration in bovine milk than in other sources (Tomita *et al.,* 2009); however, the extraction process is costly. It has been reported that 10,000 litres of bovine milk can produce only 1 kg of LF by using sophisticated membrane filtration technologies. It is also called ‘pink gold’ due to its scarcity in the market and high cost. After extraction, LF is usually converted into powders in order to extend its shelf-life and to preserve its bio-functional properties. Commercially available LF powders are primarily produced by freeze drying and there is very limited knowledge about its spray drying process. Spray drying uses atmospheric air at high temperature and very low relative humidity as the drying medium. Droplets of submicron to 200 micron in diameter are brought into contact with inlet air of 180^{o}C or above (Woo & Bhandari, 2013). Thus, thermal and dehydration related stresses are quite strong and pervasive in spray drying process (Haque *et*

al., 2013) and these stresses are expected to denature LF when it is being converted into powder using spray drying. The extent and the nature of denaturation of LF in the spray drying (convective drying) environment and the impact of denaturation on solubility, iron binding/release ability and digestion characteristics are currently poorly understood. Quantification of drying kinetics (moisture loss, temperature histories and drying rate) as a function of temperature and relative humidity of drying air together with the denaturation kinetics and droplet/particle morphology are essential for determining best possible drying parameters to produce spray-dried LF powders. Lack of this information can lead to over processed LF particles with unacceptable low solubility and other suboptimal functional properties. Due to the above mentioned gap in knowledge, industries are using much more expensive freeze drying technology which is >5 times expensive in terms of capital cost and >8 time expensive in terms of operational cost compared to spray drying (Ratti, 2012). Thus, a thorough and systematic study is required to understand the quality and functional aspects of both spray-dried and freeze-dried LF. If LF powders with comparable characteristics of those of freeze-dried ones can be produced through spray dying, the cost of production can be reduced and LF can be made readily available and affordable.

LF is called 'pink gold' not only because of its high cost but also because of its important bio-functional properties. However, native-LF is unable to pass through the adult human gastric digestion stage in a molecularly intact and functionally sound form (David-Birman *et al.,* 2013; Furlund *et al.,* 2013). Since LF's functional properties are highly dependent on its unique structural conformation (Lönnerdal, & Kelleher, 2009; Pan *et al.,* 2007), there will be no benefit of taking LF unless it is protected from gastric pepsinolysis. Thus, LF must be protected to a suitable degree during its delivery to its absorption site of human intestine. One of the most widely used methods of protecting sensitive and unstable bioactive ingredients is to encapsulate them in a more stable matrix (Bokkhim *et al.,* 2016; Kanwar, Mahidhara, & Kanwar, 2012). Alternatively, formation of complex coacervates of LF with more stable polysaccharide gums is expected to increase its stability during gastro-intestinal delivery (Gulão *et al.,* 2014; Yan *et al.,* 2013).

Complex coacervation involves at least two oppositely charged biopolymers such as proteins and polysaccharides in aqueous medium. These polymers interact with each other electrostatically and form protein-polysaccharide insoluble complexes at a specific pH, ionic strength and protein-to-polysaccharide mixing ratios (De Kruif, Weinbreck & de Vries, 2004; Eratte *et al.,* 2014). These complex coacervates are more surface active and are considered as

better encapsulants compared to individual protein or polysaccharide gum. In addition, simple operation and easy to scale-up features are some of the advantages of the complex coacervation process. For these reasons, complex coacervation is widely used in food and pharmaceutical industries for encapsulation of unstable bioactive ingredients such as vitamins, flavour oils and polyunsaturated fatty acids (Junyaprasert *et al.,* 2001; Timilsena *et al.,* 2017; Yeo *et al.,* 2005). Sodium alginate is one of the most commonly used and readily available polysaccharides to synthesise protein-polysaccharide complex coacervates. This is because sodium alginate is relatively more stable than many other polysaccharides against thermal and acidic stressors (Bhardwaj *et al.,* 2000). It is expected that LF-alginate complex coacervates can be easily formed as sodium alginate possesses negative charges above pH 2.0 while LF possesses positive charges below pH 8.0 (Bokkhim *et al.,* 2013; Harnsilawat, Pongsawatmanit, & McClements, 2006). Thus, LF and sodium alginate could expediently form the complex coacervate in a wide pH range. However, optimisation of the complex coacervation parameters between LF and sodium alginate is essential to achieve highest yield of complex coacervates before they can be utilized for encapsulation and stabilization of LF.

1.2.Expected benefits of this study

If it can be proven, through this study, that structurally and functionally intact LF powders can be produced through spray drying and the spray-dried LF powders possess similar or better physicochemical properties to those of freeze-dried powders, industry is expected to produce LF powders at significantly low cost. Increased availability and affordability of LF powders will greatly broaden their application in many food and pharmaceutical formulations and thus contribute to the health and wellbeing of consumers. The *in-vitro* digestion studies carried out using LF and LF-sodium alginate complex coacervates will provide valuable information regarding how best to protect the LF in the acidically and enzymatically intense or harsh gastric stage of digestion and achieve targeted delivery and achieve best physiological utilization. Most importantly, this study will make notable advances in knowledge on four fronts. Firstly, it will provide fundamental insights into the drying and denaturation (unfolding and aggregation) behaviours of three forms (native, iron depleted and iron saturated) of LF in industrially important convective drying environment. Secondly, it will provide fundamental insights on the breaking down, iron binding and release behaviours of three forms of LF in simulated (*in-vitro*) gastrointestinal

conditions where acid/alkaline and enzymatic conditions vary considerably. Thirdly, it will provide a holistic picture of advantages and disadvantages associated with production of LF powders using spray and freeze drying processes. Lastly, and equally importantly, it will provide greater understanding of complex coacervation between LF and sodium alginate and digestion behaviour of the complex coacervated LF during gastrointestinal digestion.

1.3.Research hypotheses and research questions

This study hypothesizes that spray dying can be used to convert liquid LF into powder and that the spray-dried LF powders will have comparable quality characteristics and functional properties to those of freeze-dried ones. It also assumes that complex coacervates of LF produced using readily available anionic polysaccharides (e.g. sodium alginate) are capable of better protecting LF from undesired effects of acid and enzymes prevailing in gastric stage of digestion and deliver to the desired absorption site in intestine. It further hypothesizes that the iron saturation/depletion levels of LF could affect its drying and digestion behaviours.

In line with the above hypotheses, this thesis addresses the following research questions:

(1) How does the spray drying process alter the structural features (denaturation) of LF and what is the extent of this alteration?

(2) What are the differences in physicochemical characteristics and functional properties of LF powders obtained from spray drying and freeze drying processes?

(3) How does the mild thermal treatment alter digestion behaviour and functional properties of LF such as nature of polypeptides, iron binding and antioxidant capacities?

(4) Does complexation of LF with sodium alginate increase its resistance to undesired breakdown especially during gastric stage of digestion?

1.4. Research objectives

Overall, this study aimed at providing a fundamental understanding of spray and freeze drying behaviour of LF as well as providing fundamental understanding of its digestive breakdown pattern in a simulated (*in-vitro*) gastrointestinal environment. It also aimed at

providing understanding of complex coacervation of three forms of LF with a common anionic polysaccharide (sodium alginate) and the ability of these complex coacervates in enhancing stability of LF during drying and digestion. The specific objectives of this study were as follows:

1. To measure and interpret the drying and denaturation characteristics of LF during a convective drying process that simulates the spray drying environment.

2. To evaluate and compare the physicochemical characteristics and functional properties of spray-dried and freeze-dried LF powders.

3. To measure and interpret the effect of mild thermal treatment on the digestion and functional properties of LF.

4. To produce LF-alginate complex coacervates and to measure and compare the ability of the complexed LF to resist undesired breakdown during gastric digestion.

1.5. Outline of this research

This thesis is organized in 7 Chapters as listed below. The contents of Chapter 3, Chapter 4, Chapter 5 and Chapter 6 have been published in refereed journals. The contents of Chapter 2 have been accepted for publication in a well-regarded refereed journal. A brief outline of each chapter is provided below.

Chapter 1: This chapter presents relevant background information on LF and its function and stability. It highlights the gap in knowledge relevant to this work and the impact of this gap on the broader utilization of LF in industrial production. It also articulates the rationale and hypotheses of the research and lists the research questions explored during this PhD study. The specific objectives to be achieved in this research are also documented.

Chapter 2: This chapter provides a thorough and critical review of the literature relevant to this thesis. It includes the structural features of three forms of LF and their relationships to functional properties. Factors affecting the molecular conformational features of LF during thermal processing and digestion are discussed. The health benefits and current state of utilization of LF in food and pharmaceutical applications are also covered. Furthermore, the information available in the literature on the encapsulation and complex

coacervation of LF with commonly available anionic polysaccharides is also reviewed and documented. The contents of this chapter have been accepted for publication in a refereed journal (*Critical Reviews in Food Science and Nutrition*, in press, 2017).

Chapter 3: This chapter documents the drying and denaturation characteristics of three forms (native, iron saturated and iron depleted) of bovine LF during convective air drying. Single droplets of aqueous LF solutions were dried using a single droplet drying instrument which mimicked the spray drying process. Isothermal heat treatment of aqueous solution of lactoferrin was also carried out for comparison. The contents of this chapter have been published (Wang *et al.*, 2017a)

Chapter 4: This chapter reports the physicochemical and functional properties of spray- and freeze-dried native LF powders. The solubility in water, moisture sorption and denaturation characteristics of spray- and freeze-dried powders are measured, compared and explained. The residual antioxidant capacity of both powders is compared with that of liquid LF. The contents of this chapter have been published (Wang *et al.*, 2017b).

Chapter 5: This chapter documents the digestion behaviour of three forms of LF during simulated *in-vitro* digestion. The effects of mild thermal treatment on the digestion and functional properties of the three forms of LF are documented. The contents of this chapter have also been published (Wang *et al.*, 2017c).

Chapter 6: This chapter documents the complex coacervation behaviour and established parameters to produce LF-sodium alginate complex coacervates. The efficacy of LF-sodium alginate complex coacervate in protecting LF during gastrointestinal digestion is documented in this chapter as well. The objective of this Chapter is to slow down the premature breakdown of lactoferrin during gastric stage of digestion, which ultimately helps delivering functionally intact lactoferrin to human body. Potential applications of the lactoferrin-sodium alginate complex coacervates include nutritional supplements, infant milk formula products and therapeutic drugs which contain lactoferrin as the active ingredient. The contents of this chapter have been published (Wang *et al.*, 2017d).

Chapter 7: This chapter suitably integrates and puts the contents and findings presented in preceding four experimental chapters into context. It also documents the overall conclusions drawn from this thesis. The contributions made by this research to the relevant

body of knowledge are also articulated in this chapter. Finally, this chapter recommends or provides pointers for future research.

References:

Artym, J., & Zimecki, M. (2005). The role of lactoferrin in the proper development of newborns. *Advances in Hygiene and Experimental Medicine*, 59, 421-432

Baveye, S., Elass, E., Mazurier, J., Spik, G., & Legrand, D. (1999). Lactoferrin: A multifunctional glycoprotein involved in the modulation of the inflammatory process. *Clinical Chemistry and Laboratory Medicine*, 37, 281-286.

Bhardwaj, T. R., Kanwar, M., Lal, R., & Gupta, A. (2000). Natural gums and modified natural gums as sustained-release carriers. *Drug development and industrial pharmacy*, 26(10), 1025-1038.

Bokkhim, H., Bansal, N., GrØndahl, L., & Bhandari, B. (2013). Physico-chemical properties of different forms of bovine lactoferrin. *Food chemistry*, 141(3), 3007-3013.

Bokkhim, H., Bansal, N., Grøndahl, L., & Bhandari, B. (2016). *In-vitro* digestion of different forms of bovine lactoferrin encapsulated in alginate micro-gel particles. *Food Hydrocolloids*, 52, 231-242.

Britigan, B. E., Serody, J. S., & Cohen, M. S. (1994). The role of lactoferrin as an anti-inflammatory molecule. In William, H. T., Lonnerdal, B., & Rumball, V.S (Eds.), Lactoferrin: Structure and Function (pp. 143-156). New York, USA: Plenum Press.

Centers for Disease Control and Prevention (CDC. (2002). Iron deficiency--United States, 1999-2000. MMWR. *Morbidity and mortality weekly report*, 51(40), 897.

David-Birman, T., Mackie, A., & Lesmes, U. (2013). Impact of dietary fibers on the properties and proteolytic digestibility of lactoferrin nano-particles. *Food Hydrocolloids*, 31(1), 33-41.

De Kruif, C. G., Weinbreck, F., & de Vries, R. (2004). Complex coacervation of proteins and anionic polysaccharides. *Current Opinion in Colloid & Interface Science*, 9(5), 340-349.

EI-Loly, M. M., & Mahfouz, M. B. (2011). Lactoferrin in relation to biological functions and applications: a review. *International Journal of Dairy Science*. 6(2), 79-111.

Eratte, D., Wang, B., Dowling, K., Barrow, C. J., & Adhikari, B. P. (2014). Complex coacervation with whey protein isolate and gum Arabic for the microencapsulation of omega-3 rich tuna oil. *Food & function*, 5(11), 2743-2750.

Furlund, C. B., Ulleberg, E. K., Devold, T. G., Flengsrud, R., Jacobsen, M., Sekse, C. *et al.*, (2013). Identification of lactoferrin peptides generated by digestion with human gastrointestinal enzymes. *Journal of Dairy Science*, 96(1), 75-88.

Gulão, E. D. S., de Souza, C. J., da Silva, F. A., Coimbra, J. S., & Garcia-Rojas, E. E. (2014). Complex coacervates obtained from lactoferrin and gum Arabic: Formation and characterization. *Food Research International*, 65, 367-374.

Haque, M. A., Putranto, A., Aldred, P., Chen, J., & Adhikari, B. (2013). Drying and denaturation kinetics of whey protein isolate (WPI) during convective air drying process. *Drying Technology*, 31(13-14), 1532-1544.

Harnsilawat, T., Pongsawatmanit, R., & McClements, D. J. (2006). Characterization of β-lactoglobulin–sodium alginate interactions in aqueous solutions: a calorimetry, light scattering, electrophoretic mobility and solubility study. *Food Hydrocolloids*, 20(5), 577-585.

Junyaprasert, V. B., Mitrevej, A., Sinchaipanid, N., Boonme, P., & Wurster, D. E. (2001). Effect of process variables on the microencapsulation of vitamin A palmitate by gelatin-acacia coacervation. *Drug Development and Industrial Pharmacy*, 27(6), 561-566.

Kanwar, J. R., Mahidhara, G., & Kanwar, R. K. (2012). Novel alginate-enclosed chitosan-calcium phosphate-loaded iron-saturated bovine lactoferrin nanocarriers for oral delivery in colon cancer therapy. *Nanomedicine*, 7(10), 1521-1550.

Lönnerdal, B., & Kelleher, S. L. (2009). Micronutrient transfer: infant absorption. In Goldberg, G. R., Prentice, A., Prentice, A., Filteau, S., Simondon, K. (Eds.), Breast-Feeding: Early Influences on Later Health (pp. 29-40). New York, USA: Plenum Press.

McKenna, T., & Rawlin, G. (2005). Nutritional milk-managing the supply. *Australian journal of dairy technology*, 60(2), 154.

Paesano, R., Berlutti, F., Pietropaoli, M., Pantanella, F., Pacifici, E., Goolsbee, W., & Valenti, P. (2010). Lactoferrin efficacy versus ferrous sulfate in curing iron deficiency and iron deficiency anemia in pregnant women. *Biometals*, 23(3), 411-417.

Pan, Y., Rowney, M., Guo, P., & Hobman, P. (2007). Biological properties of lactoferrin: an overview. *Australian Journal of Dairy Technology*, 62(1), 31.

Ratti, C (2012). Freeze drying process design. In: Rahman, S., & Ahmed, J (Eds.), Handbook of food process design (pp. 621-647). New York: John Wiley & Sons.

Synlait. (2013). $15 Million investment in lactoferrin production. Retrieved from http://www.scoop.co.nz/.

Timilsena, Y. P., Adhikari, R., Barrow, C. J., & Adhikari, B. (2017). Digestion behaviour of chia seed oil encapsulated in chia seed protein-gum complex coacervates. *Food Hydrocolloids*, 66, 71-81.

Tomita, M., Wakabayashi, H., Shin, K., Yamauchi, K., Yaeshima, T., & Iwatsuki, K. (2009). Twenty-five years of research on bovine lactoferrin applications. *Biochimie*, 91(1), 52-57.

Wang, B., Timilsena, Y. P., Blanch, E., & Adhikari, B. (2017a). Drying and denaturation characteristics of three forms of bovine lactoferrin. *Drying Technology*, 35(5), 606-615.

Wang, B., Timilsena, Y. P., Blanch, E., & Adhikari, B. (2017b). Characteristics of bovine lactoferrin powders produced through spray and freeze drying processes. *International Journal of Biological Macromolecules*, 95, 985-994.

Wang, B., Timilsena, Y. P., Blanch, E., & Adhikari, B. (2017c). Mild thermal treatment and in-vitro digestion of three forms of bovine lactoferrin: Effects on functional properties. *International Dairy Journal*, 64, 22-30.

Wang, B., Blanch, E., Barrow, C., & Adhikari, B. (2017d). Preparation and study of digestion behavior of lactoferrin-sodium alginate complex coacervates. *Journal of Functional Foods*, 37, 97-106.

Woo, M. W., & Bhandari, B. (2013). Spray drying for food powder production. In B. Bhandari., N. Bansal., M. Zhang & P. Schuck (Eds.), Handbook of food powders (pp. 29-56). Cambridge, UK: Woodhead Publishing Limited.

Yan, Y., Kizilay, E., Seeman, D., Flanagan, S., Dubin, P. L., Bovetto, L *et al*. (2013). Heteroprotein complex coacervation: bovine β-lactoglobulin and lactoferrin. *Langmuir*, 29(50), 15614-15623.

Yeo, Y., Bellas, E., Firestone, W., Langer, R., & Kohane, D. S. (2005). Complex coacervates for thermally sensitive controlled release of flavor compounds. *Journal of Agricultural and Food Chemistry*, 53(19), 7518-7525.

CHAPTER 2

Literature Review

Accepted for publication in *Critical Reviews in Food Science and Nutrition*, 2017, in press

CRITICAL REVIEWS IN FOOD SCIENCE AND NUTRITION
2017, VOL. 0, NO. 0, 1–17
https://doi.org/10.1080/10408398.2017.1381583

Lactoferrin: Structure, function, denaturation and digestion

Bo Wang[a], Yakindra Prasad Timilsena[a,b], Ewan Blanch[a], and Benu Adhikari [a,b]

[a]Food Research and Innovation Centre, School of Science, RMIT University, Melbourne, VIC, Australia; [b]Materials Science and Engineering, CSIRO Manufacturing Flagship, Clayton South, VIC, Australia

ABSTRACT

Lactoferrin (LF) is a multifunctional protein occurring in many biological secretions including milk. It possesses iron binding/transferring, antibacterial, antiviral, antifungal, anti-inflammatory and anti-carcinogenic properties. These functional properties intimately depend on the structural integrity of LF especially its higher order conformation. LF is primarily extracted from bovine milk and it is subsequently added into many commercial products such as nutritional supplements, infant formula, cosmetics and toothpaste. LF is sensitive to denaturation induced by temperature and other physicochemical stresses. Hence, the extraction, powder formation processes of LF and processing parameters of LF-containing products have to be optimized to minimise its undesired denaturation. This review documents the advances made on structure-function relationships and discusses the effectiveness of methods used to preserve the structure of LF during thermal processing. Oral delivery, as the most convenient way for administering LF, is also discussed focusing on digestion of LF in oral, gastric and intestinal stages. The effectiveness of methods used to deliver LF to intestinal digestion stage in structurally intact form is also compared. Altogether, this work comprehensively reviews the fate of LF during thermal processing and digestion, and suggests suitable means to preserve its structural integrity and functional properties.

SCOPE OF REVIEW

The manuscript aims at providing a comprehensive review of the latest publications on four aspects of LF: structural features, functional properties, nature and extent of denaturation and gastrointestinal digestion. It also analyses how these publications benefit food and pharmaceutical industries.

KEYWORDS

Lactoferrin; Structure; Function; Drying; Denaturation; Digestion and Application

1. Introduction

Lactoferrin (LF) was first identified in 1939 as a red protein in whey (Sorensen and Sorensen 1940). In the year of 1960, it was isolated and purified from human and bovine milk (Groves 1960; Johanson 1960). The isolated protein was structurally similar to serum transferrin with ~60% sequence identity and can reversibly bind ferric (Fe^{3+}) ion (Baker 1994; Johanson 1960). Due to this reason, LF is classified as a member of transferrin family along with serum transferrin, melanotransferrin and ovotransferrin (Lambert, Perri and Meehan 2005).

LF is present in biological fluids including milk, saliva and seminal fluid (Cheng et al. 2008). It is also present in mucosal surfaces and in some granules of polymorphonuclear leukocytes. The most abundant source of LF is human and bovine milk. The concentration of LF in milk varies widely with lactation stages and across species. Human colostrum contains higher than 5 g/L of LF as compared to 2–3 g/L in mature breast milk. LF content in bovine colostrum is approximately 0.8 g/L; whereas bovine milk contains only 0.03–0.49 g/L (Table 1). The higher amount of LF in colostrum is believed to provide protections to breast-fed infants against bacterial infection and inflammation (Artym and Zimecki 2005).

LF promotes iron absorption in the human body (Paesano et al. 2010). It modulates cell growth, scavenges harmful free radicals and inhibits the formation of several toxic compounds (Baveye et al. 1999). Due to these reasons, LF is added in many commercial products including infant formula powders, therapeutic drinks, fermented milk, cosmetics and toothpaste (Tomita et al. 2009). The multiple health promoting functions of LF and its wide real-life applications has stimulated increased research interest.

2. Structure of lactoferrin

LF is a single polypeptide chain glycoprotein with a molecular weight of around 78 kDa. Detailed structural studies have reported that there are 691 and 696 amino acids in human and bovine LF, respectively (Baker et al. 2000; Moore et al. 1997). LF from mammalian species has similar amino acid sequence. Human and bovine LF share approximately 70% sequence identity whereas human and chimpanzee LF share almost 97% sequence identity (Yount et al. 2007). This pronounced similarity in primary structure of LF in various mammalian species

CONTACT Benu Adhikari benu.adhikari@rmit.edu.au Plenty Road, Bundoora 3083, VIC, Australia; Research Way, Clayton, 3168, VIC, Australia.
Color versions of one or more of the figures in the article can be found online at www.tandfonline.com/bfsn.

Table 1. Major sources and concentration of lactoferrin (LF).

Biological Fluids	Concentration (mg/mL)	References
Human colostrum	5.80 ± 4.30	Montagne 2001
Bovine colostrum	0.82 ± 0.54	Kehoe 2007
Camel colostrum	0.81 ± 0.31	Konuspayeva 2007
Goat colostrum	0.39 ± 0.07	Hiss 2008
Human milk	2.00 – 3.30	Montagne 2001
Bovine milk	0.03 – 0.49	Cheng 2008
Camel milk	0.06 – 0.89	Konuspayeva 2007
Goat milk	0.17– 0.59	Chen, 2004
Human tears	1.13 ± 0.29	Balasubramanian, Pye and Willcox 2012

indicates that it performs identical biological functions in different species. LF has ordered secondary structural features comprising 33–34% helices and 17–18% strands (Table 2). The tertiary structures of LF, as determined by X-ray crystallography (Figure 1A), consists of two symmetric lobes (N-lobe and C- lobe) joined by a short α-helix. These two lobes are globular and can be further divided into two similarly sized subdomains: N_1 and N_2; C_1 and C_2, respectively. In bovine LF, sub lobe N_1 is composed of residues 1–90 & 251–333; N_2 is made up of residues 91–250. Similarly, C_1 sub lobe is comprised of 345–431 & 593–676 residues and the C2 sub lobe is comprised of 432–592 residues. Residues 334–344 make a small 3-turn helix that connects the N and C lobes. This small (3-turn) helix behaves as a flexible hinge during opening and closing of the domains when LF releases/binds iron (Baker and Baker 2009; Steijns and van Hooijdonk 2000). Bovine LF contains 17 disulfide bonds (Moore et al. 1997).

One of the most noteworthy features of LF's structure is that its surface is positively charged. This facilitates the binding of LF with anionic bio-compounds. The positively charged moieties of LF are mainly concentrated on the outer region of first helix of the N_1 domain and towards the end of C terminal (Figure 1B). Another, much smaller, but intensely positively charged spot exists in the inter lobe region where two lobes are connected by a helix. The basic region surrounding the N-terminus is shown to be responsible for binding DNA, heparin, and lipopolysaccharide (He and Furmanski 1995; Lizzi et al. 2016; van Berkel et al. 1997). Sugars (mainly high mannose and N-Acetyleglucosamine) are associated with LF through N-linked glycosylation (Moore et al. 1997). In human LF, approximately 5% of the molecules are glycosylated at one site (Asn 479), 85% of the molecules are glycosylated at two sites (Asn138 and 479) and 9% of the molecules are glycosylated at three sites (Asn138, 479 and 624) (van Berkel et al. 1996). In bovine LF, 5 potential glycosylation sites have been reported. Most bovine LF molecules are glycosylated with sugars at Asn 233, 281, 368, 476, while only 15–30% of LF molecules make use of the Asn281 glycosylation site (Spik et al. 1994; Wei et al. 2000; Yoshida el al. 2000). The number of N-linked glycosylation sites and the types of sugar attached to LF are precisely regulated by gene expression. These variations in glycosylation sites affect the susceptibility of LF to proteolysis and thermal denaturation (Moore et al. 1997; van Veen et al. 2004). The glyco-variation is also involved in modulating the association of pathogens with LF (Barboza et al. 2012).

Table 2. Amino acids composition and secondary structural features of human and bovine lactoferrin (LF) (Baker et al. 2000, Moore et al. 1991).

Amino acids residues			Secondary structural features (%)		
	Bovine LF	Human LF		Bovine LF	Human LF
Ala (A)	67	63	Alpha helix	30.6	29.4
Arg (R)	37	45	3–10 helix	2.6	4.6
Asn (N)	29	33	Strand	17.4	18.1
Asp (D)	36	38	Others	49.3	47.9
Cys (C)	34	32			
Glu (E)	40	41			
Gln (Q)	29	28			
Gly (G)	49	54			
His (H)	10	9			
Ile (I)	16	16			
Leu (L)	66	58			
Lys (K)	54	45			
Met (M)	4	5			
Phe (F)	27	30			
Pro (P)	30	35			
Ser (S)	45	50			
Thr (T)	36	31			
Trp (W)	13	10			
Tyr (Y)	21	21			
Val (V)	46	48			
Total	689	691			

3. Function and applications of lactoferrin

The unique structural characteristics of LF provide a variety of nutritional and medicinal values. In terms of nutritional function, LF transport iron and detoxify free radicals in biological fluids. Since iron deficiency is one of the most common nutritional deficiencies in the world (Gupta et al. 2016; Lopez et al. 2016), LF is increasingly considered to be a safe and effective ingredient to deliver iron to deficient people. Earlier study conducted by Kawakami et al. (1988) compared the iron absorption from bovine LF and ferrous sulphate in iron deficient anaemic rats. It was found that the iron from bovine LF was more easily absorbed across the intestinal mucosa compared to the iron from ferrous salts. A recently reported clinical research on pregnant women showed that oral administration of bovine LF increased iron absorption whereas the iron from ferrous salts was not absorbed in the same level (Paesano et al. 2010). The more efficient iron absorption from LF than that from iron salts might be due to the presence of specific LF receptors on human mucosa cells, which generate a receptor-mechanism pathway (Cox et al. 1979; Iyer and Lönnerdal 1993; Lönnerdal et al. 2015). Nevertheless, conflicting results have been presented in infants. Some researches demonstrated that oral administration of LF promotes iron absorption of newborns whereas other studies did not observe any significant effect (Davidsson et al. 1994; Hernell and Lönnerdal 2002; Ke et al. 2015). One of the possible reasons for these contradictory results is that LF might not be recognized by mucosal LF receptors due to the difference in state of iron in individuals (Hernell and Lönnerdal 2002; Lönnerdal 2015). Another hypothesis put forward by Sánchez. (1992a) is that LF regulates rather than promoting the absorption of iron in infants. This hypothesis was further

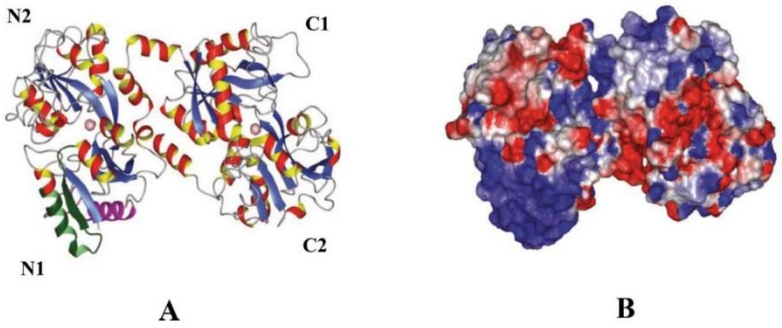

Figure 1. (A) 3D crystal structure and (B) surface charge distribution of iron saturated bovine LF (protein databank code: 1BLF) in the same orientation. N1, N2, C1 and C2 represent the four subdomains of LF. The blue, white and red colors correspond to net positive, neutral and negative charges, respectively (Vogel 2012). This figure is reproduced with permission of the publisher.

tested and verified by Davidsson et al. (1994), Scarino (2007) and Lönnerdal et al. (2015).

LF also possesses antimicrobial, anti-inflammatory and anti-carcinogenic activities, highlighting the therapeutic values of this multifunctional protein. Many vaccines, therapeutic drugs and oral health care products are developed making use of the medicinal functions of LF. These functions and applications are further discussed in section 3.2–3.3.

3.1. Iron transferring function

LF has very high affinity to iron with an equilibrium dissociation constant value (K_D) of $\sim 10^{-20}$ M (Baker and Baker 2004; Steijns and van Hooijdonk 2000). Two ferric ions (Fe^{3+}) can covalently bind to a LF molecule in the presence of 2 carbonate ions (CO_3^{2-}). Based on the iron-saturation levels, LF has been found to exist in three different forms: iron depleted (apo) form (both C lobe and N lobe are free from iron), iron saturated (holo) form (1 iron atom is attached to both C and N lobes) and partially iron saturated (mono) form (1 iron atom is attached to either C or N lobe). In practice, if the iron saturation level of LF lies in between 0–6%, it is considered as apo form whereas the holo forms of LF have an iron saturation level between 76–100% (Bokkhim et al. 2013; Sui et al. 2010; Voswinkel et al. 2016). The apo and holo forms of LF are prepared in small scale for research purpose. Commercially available LF (native-LF) is primarily extracted from bovine milk, which has an iron saturation level of 10–20%.

3.1.1. Iron binding and iron release mechanisms

The iron binding mechanism of human and bovine LF has been thoroughly studied (Baker and Baker 2009; Moore et al. 1997; Rastogi et al. 2016). The metal-ligand bonds and hydrogen bonds in the iron binding domains were found to be identical for bovine and human LF. Four different amino acid residues are involved in binding Fe^{3+} ion. Asp60, Tyr92, Tyr192, His253 covalently bind with Fe^{3+} ion in N lobe (Figure 2). The two oxygen atoms of carbonate ion also covalently attach with Fe^{3+}. In the C lobe, Asp395, Tyr433, Tyr526, His595 and carbonate ion bind with Fe^{3+} in the similar fashion. Both the N and C lobes of LF bind to carbonate ion (CO_3^{2-}) first and then they bind the Fe^{3+}. The CO_3^{2-} binding sites are located in a positively charged pocket in N_2 and C_2 domain. These pockets are supported by the α-helix structure in the vicinity of the iron binding cleft (121–131 residues in N lobe and 395–407 in C lobe). The side-chains of arginine and threonine residues (Arg121 and Thr117 in the N lobe, Arg463 and Thr459 in the C lobe) are also involved in the CO_3^{2-} binding pocket. This positively charged pocket satisfies the full hydrogen bonding potential of the carbonate ion, and allows it to fit perfectly between the Fe^{3+} atom and anion binding sites (Moore et al. 1997). The iron binding by LF is a cooperative type of binding where C-lobe first binds with Fe^{3+} and then stimulates the N-lobe for iron binding (Abdallah and Chahine 2000). It has been reported that after iron binding, the inter domain hydrogen bonding occurs at the lips of the iron binding cleft. In this way the Fe^{3+} molecule is enclosed within the iron binding domains. The inclusion of Fe^{3+} atoms in both two lobes makes the structure of iron saturated LF more compact compared to that of the iron-depleted LF. The structurally compact iron saturated (holo) form of LF is, thus, more stable against external stressors (Abdallah and Chahine 2000).

Iron release from LF follows a reverse path of iron binding. In this case, structural changes at the iron binding site, i.e., the opening of the closed iron binding domains occurs first followed by the release of iron. There are three factors that cause the structural changes essential for the release of iron: firstly, presence of specific receptors similar to that in serum

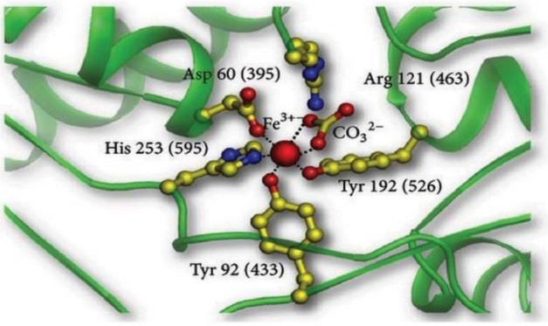

Figure 2. Schematic figure of the iron-binding site of bovine lactoferrin (Sharma et al. 2013). The iron atom is shown as a red sphere, while the interacting amino acid residues of lactoferrin are in yellow. The residue numbers correspond to N-lobe, while the corresponding residues of C-lobe are in brackets (with permission of the publisher).

transferrin; secondly, reduction of Fe^{3+} to Fe^{2+} (LF has much lower affinity to Fe^{2+}); and thirdly, decrease of the pH in the environment (Baker and Baker 2009; Baker, Baker and Kidd. 2002). The pH trigged release of iron has been studied to a considerable detail using crystallographic and iron release kinetics (Abdallah and Chahine 2000; Baker and Baker 2009; Rastogi et al. 2016). The carbonate ion, tyrosine and/or histidine ligands present in the iron binding domain are protonated at certain low pH values depending on the source of LF. This lowering of pH weakens the iron coordination to a point at which it cannot hold the two LF domains together. When this happens, the iron binding domains will open and interact with positive charges prevailing in the environment and ultimately result in the release of iron. Rastogi et al. (2016) reported that the N-lobe of bovine LF started to lose iron at pH 6.5 while C-lobe began to lose iron at pH 5.5. N-lobe and C-lobe showed identical iron release behaviour below pH 4.0. In the case of human LF, the N lobe started to release iron at ∼pH 5.0 while the C lobe retained iron at pH as low as 3.5 (Baker 1994; Baker and Baker 2004). Therefore, the iron binding ability of LF is fully retained at prevailing pH values of fresh human and bovine milk (pH 6.5–6.8). Interestingly, the iron binding ability or affinity to hold iron of other transferrins (e.g. serum transferrin and ovotransferrin) already starts to lose at these pH values; thus, their bacteriostatic ability is greatly reduced (Abdallah and Chahine 2000; Erickson et al. 2013; Tsioulpas et al. 2007). The receptor-driven iron release pathway of LF is involved in the iron metabolism and regulation iron content in human body. Human LF is absorbed through the apical membrane of the intestinal cell by a specific LF receptor and internalized with its bound iron (Lönnerdal et al. 2015). The absorbed LF is then transported by microsomes and ultimately participates in the redox reactions of the iron cycle (Lönnerdal et al. 2015).

3.1.2. Iron delivery function

Iron is an essential mineral for growth and survival of all living organisms because it is required as a cofactor for essential enzymes that are involved in many basic cellular functions and metabolic pathways. Iron deficiency causes fatigue and decreased immunity. Excess of iron is also toxic as free irons catalyses reactions that produce free oxygen radicals, which are highly toxic to cells (Bokare and Choi 2014; Phaniendra et al. 2015). Most of the required iron in human body can be obtained from the recycling metabolism, thus, absorption of 1–2 mg of iron is sufficient in balancing the iron recycling cycle (Camaschella 2015). Despite of this highly efficient system, iron deficiency is one of the most common nutritional deficiencies in the world (Gupta et al. 2016; Lopez et al. 2016). As a transporter of iron in iron recycling cycle, LF is expected to maintain the balance of iron within the normal range, and help avoid both iron deficiency and iron overload. This is the reason why a large number of studies have been conducted to investigate the nutritional and therapeutic benefits of LF.

It has been shown that oral delivery of bovine LF is effective in preventing iron deficiency anaemia in pregnant women (Paesano et al. 2010; Rezk et al. 2015). Hence, it is expected that LF can be used as an effective iron source to people suffering from iron deficiency. LF has also been added into functional beverages to compensate the loss of iron during professional sport training and excise (sweating) (Özer and Kirmaci 2010; Tang et al. 2016). In order to use LF as an effective vehicle of iron delivery, it has to be stabilised both in liquid and solid forms. Cao and Maas (2015) have reported that when the LF-containing functional beverages were heated (80–100°C, 15–60 s) under acidic conditions (pH 2.0–5.0) with adequate amount of stabilizers (35–70% mannitol, w/w) and sugars (>30% sucrose, w/w), the shelf life of LF was extended to >4 weeks as indicated by the preservation of primary structure and iron binding capacity. This means that when the formulation and the processing condition are carefully chosen LF can be delivered through beverages. Although the question of whether or not the LF promotes absorption of iron in infants is still not conclusively answered, it is commonly used to fortify infant formula products. The increased incorporation of LF in infant formula products also stems from its additional benefits such as promotion of bone growth (Cornish et al. 2004), modulation of immune functions (Legrand 2016) and anti-pathogenic effects (Chen et al. 2016). Furthermore, LF also helps better absorption of other nutrients such as calcium and magnesium (Lönnerdal 2016; Liao et al. 2012).

3.2. Antibacterial and antiviral activities

3.2.1. Antibacterial property of intact LF

LF demonstrated bacteriostatic effects against a variety of Gram-positive (Francesca et al. 2004; Lee et al. 2005; Rodriguez-Franco et al. 2004) and Gram-negative (Beeckman et al. 2007;Ostan et al. 2017; Rogan et al. 2004) bacteria. In earlier researches, it was believed that the antibacterial activity of LF is due to its high affinity to iron. The iron-free form of LF (apo-LF) is expected to impede iron utilization and cause iron deficiency in iron requiring microorganisms. This finally results into a slower bacterial growth rate (Law and Reiter 1977). However, later studies found that even iron-saturated form of LF (holo-LF) inhibits the growth of many bacterial strains (Ellison 3rd and Giehl 1991; Ochoa and Cleary 2009; Ostan et al. 2017). This means that antibacterial property of LF is not fully dependent on iron binding or scavenging.

Recent research findings show that the bactericidal effect is directly related to the interaction between LF and bacteria (Jenssen and Hancock 2009; Orsi 2004; Ostan et al. 2017). Ostan et al. 2017 reported that C-lobe of LF associates with a bi-lobed outer membrane-bound lipoprotein in two different sites of Gram-negative bacterial cells and forms receptor complexes. The binding of LF in these two sites either inhibits the iron intake of bacteria or removes the protective effect membrane bound lipoprotein against antimicrobial cationic peptides. Other researches (Coughlin et al. 1983; González-Chávez et al. 2009) suggested that the highly positively charged N-lobe of LF could prevent the interaction between lipopolysaccharide and the cations (Ca^{2+} and Mg^{2+}) required for bacterial growth. LF causes release of lipopolysaccharide from cell wall, increases permeability of membrane and finally obliterates the Gram-negative bacteria. LF binds the anionic molecules (e.g. lipoteichoic acid) on the cell surface of Gram-positive bacteria. This electrostatic binding reduces the overall negative charge of cell wall and facilitates effectiveness of antibacterial compounds

such as lysozyme and antibiotics (Barbiroli et al. 2012; González-Chávez et al. 2009; Leitch and Willcox 1999).

LF prevents the interaction between bacteria and host cells. It inhibits bacterial adhesion to host cells by occupying the surface of bacterial cells (Francesca et al. 2004; Oho et al. 2002; Valenti and Antonini 2005). Although the detailed mechanism of this effect has not been adequately understood, it has been shown that the (oligo) mannoside glycan of LF is involved in binding with bacterial cells through adhesion (Barboza et al. 2012; da Motta Willer et al. 2004; Gomez et al. 2003).

3.2.2. Antibacterial peptides of LF

Bacteriostatic effect of LF is not restricted to its structurally intact form. In fact, the peptides obtained from LF have higher bacteriostatic efficiency. Lactoferricin is a small bactericidal peptide obtained from cleavage of human and bovine LF structure by gastric pepsin (Bellamy et al. 1992). Lactoferricin derived from human LF (lactoferricin H) contains the 1–47 amino acid residue sequence of N- terminus and it has a molecular weight of ~5.6 kDa. Similarly, the peptide derived from bovine LF (lactoferricin B) is comprised of 17–41 amino acid sequence and it has a molecular weight of ~3.2 kDa (Table 3). It was found that both lactoferricins (H and B) had 9–25 fold higher efficiency in inhibiting the growth of common pathogenic bacteria such as *Escherichia coil, Klebsiella pneumoniae*, and *Listeria monocytogenes* compared to intact LF (Bellamy et al. 1992; Lizzi et al. 2016). Interestingly, lactoferricin B was found to possess stronger antimicrobial activity than lactoferricin H which might be due to differences in their primary and secondary structural features. It has also been reported that the residues 1 to 17 in lactoferricin H are not responsible for antibacterial activity while the 25–30 amino acid residues (sequence in intact LF) had strong bacteriostatic activity (Bellamy et al. 1992).

Another antibacterial peptide, called lactoferampin, has also been derived from the N-terminal lobe of LF. It is comprised of the amino acids residues of 269–285 in human LF and amino acids residues of 265–284 in bovine LF. These lactoferampins have slightly weaker bactericidal activity compared to lactoferricin (Haney et al. 2009; van der Kraan et al. 2004). Similar to the case of lactoferricin, lactoferampin obtained from bovine LF is found to have stronger antibacterial activity than the one obtained from human LF. This might be due to structural differences and higher net positive surface charge in bovine lactoferampin than in human lactoferampin (van der Kraan et al. 2004). Both properties play important roles in membrane-mediated activities (van der Kraan et al. 2004). It has been shown that the bactericidal effect of both peptides can be correlated to their ability to disturb membrane integrity (permeabilization and depolarization) of bacteria (Sijbrandij et al. 2017).

Table 3. Amino acids sequence of antibacterial peptides derived from human and bovine lactoferrin (LF). The primary structure of human and bovine LF is determined by Baker et al. (2000) and Moore et al. (1997), respectively. The sequence of amino acid residues is based on the intact form of human or bovine lactoferrin.

Antibacterial peptides	Sequences in lactoferrin	Primary structure
Human lactoferricin	1–47	GRRRRSVQWCAVSNPEATKCFQWQ RNMRKVRGPPVSCIKRDSPIQCI
Human lactoferampin	269–285	WKLLSKAQEKFGKNKSR
Bovine lactoferricin	17–41	FKCRRWQWRMKKLGAPSITCVRRAF
Bovine lactoferampin	265–284	DLIWKLLSKAQEKFGKNKSR
Bovine lactoferrin chimera	—	DLIWKLLSKAQEKFGKNKSR | FKCRRWQWRMKKLG — K

3.2.3. Antiviral activity of LF

The antiviral effect of LF lies in the early phase of infection. LF not only prevents the infection of host cells by viruses (Beljaars et al. 2004; Hasegawa et al. 1994; Marchetti et al. 1999) but also inhibits the growth of viruses after the host cells have been infected (Ikeda et al. 2000; Superti et al. 1997). The domain in LF which acts against viruses seems to be different from the domain that acts against bacteria. This is the reason why the bacteriostatic peptide lactoferricin was not found to be effective against viruses (van der Strate et al. 2001). Earlier studies indicated that LF only inhibits the infection of enveloped viruses; however, recent studies have found that it also inhibits non-enveloped species (Lin et al. 2002; Seganti et al. 2004). The most widely reported hypothesis for the antiviral activity of LF is that it binds to and blocks glycosaminoglycan viral receptors, especially the heparan sulphate. The binding of LF with viral receptors prevents the first contact between virus and host cell, thus preventing the infection (González-Chávez et al. 2009; Shimizu et al. 1996).

3.2.4. LF in antibacterial and antiviral drugs

The bacteriostatic and other antimicrobial effects of LF and LF derived peptides are studied to considerable details. These studies have led to the development of vaccines, antimicrobial drugs and oral health care products using LF as the main agent.

LF is used in oral care products (e.g. toothpaste, mouth-rinses and chewing gums) to inhibit the growth of oral pathogens (e.g. *Streptococcus mutans*) and supress oral malodour (Francesca et al. 2004; Shin et al. 2011). LF is also used in vaccines and antimicrobial drugs. It has been shown that injection of bovine LF is a safe and efficient method in producing antibody against *H1N1 influenza virus* (Sherman et al. 2015). The administration of bovine and human LF also generated a stronger T-cell helper 1 response and boosted the effectiveness of vaccines against *Mycobacterium tuberculosis* infection (Hwang et al. 2005; Hwang et al. 2015). No detrimental effects have been reported when LF is in above mentioned and other vaccines (Nevison 2014). Regarding its application as a drug, the therapeutic potential of LF has demonstrated against a number of diseases caused by bacteria and viruses. For example, it has been reported that LF could reduce the number of pathogens in *Helicobacter pylori* induced gastric infection (Wada et al. 1999). LF has also shown to be effective against a number of human and animal viruses such as *hepatitis* B (Hara et al. 2002), *hepatitis* C (Kaito et al. 2007), *cytomegalovirus* (van der Strate et al. 2001) and human immunodeficiency viruses (Wang et al. 2016).

3.3. Other functional properties

Besides the intensively studied iron transferring, antibacterial and antiviral properties, LF also possesses other functional values such as antifungal, anti-inflammatory and anti-carcinogenic activities. These functional properties are briefly discussed.

3.3.1. Antifungal activity

LF and LF derived peptides can effectively act on a broad spectrum of fungal species due to their strong iron (Fe^{3+}) scavenging property. It has been observed that LF kills *Candida albicans* and *Candida krusei* (Kirkpatrick et al. 1971; Al-Sheikh 2009). It has been reported that the sequestration of iron by apo-LF was essential for the host defence against *Aspergillus fumigatus* (Zarember et al. 2007). Apart from the iron depriving effect, LF directly binds on the surface of fungal cells, disrupts the surface and causes increased membrane permeability leading to their death. Thus, LF is incorporated in a number of antifungal drugs including those used to cure oral candidiasis (Takakura et al. 2003). The combination of LF with other antifungal compounds significantly enhanced the inhibitory activity against Candida species (Wakabayashi et al. 1998; Venkatesh and Rong 2008; Kobayashi et al. 2011) and *Cryptococcus neoformans* (Lai et al. 2016).

3.3.2. Anti-inflammatory activity

LF is secreted in mucosa environment of human and animal body. Since many pathogens tend to enter the body via the mucosa, LF plays a key role in the host defence system (Wiesner and Vilcinskas 2010). Its anti-inflammatory effect can be evidenced by the sharp increase of LF content in body fluids during inflammation (Sagel et al. 2009; Pfefferkorn et al. 2010). Clinical trials have shown that LF can help cure or prevent the inflammation of lung (Hwang et al. 2016; Valenti et al. 2016), gut (Brimelow et al. 2017; Drago-Serrano et al. 2017), intestine (MacManus et al. 2017; Nguyen et al. 2016) etc. The anti-inflammatory activity of LF can be attributed to its positively charged surface. LF interacts with negatively charged moieties (e.g. proteoglycans) on the surface of immune cells. This association can trigger signalling pathways that lead to physiological anti-inflammatory response (González-Chávez et al. 2009; Legrand 2016). The incorporation of LF in anti-inflamation drugs can minimise their side effects. For example, indomethacin (a non-steroidal anti-inflammatory drug) inhibits human tenocyte growth and proliferation at high concentration (100 μM) whereas LF helps the survival and growth of human tenocytes. The side effect of indomethacin was reversed when LF was administered together with indomechacin (Zhang et al. 2014).

3.3.3. Anti-carcinogenic activity

LF and peptides derived from it have demonstrated notable therapeutic potential in treatment of cancer. Studies have shown that LF and its peptides possess inhibitory effect against lung (A549), gastric (AGS), intestinal (HT-29) and breast (MDA-MB-231, MCF-7) cancer cell lines (Amiri, Moradian and Rafiei. 2015; Gibbons et al. 2015; Jiang and Lönnerdal 2016; Tung et al. 2013). Bovine LF inhibited the expression of survivin (a protein enhances survival rate of cancer cell) and modulated the apoptosis of cancer cells both *in-vitro* and *in-vivo* (Gibbons et al. 2015; Kanwar et al. 2015). In a rat model, vascular endothelial growth factor, a major angiogenic factor in tumours, was significantly reduced by oral administration of bovine LF (Norrby et al. 2001). It was found that orally administrated recombinant human LF inhibited the growth of cancer (head and neck carcinoma) cells (60–80% inhibition) through direct cellular inhibition and systemic immunomodulation (Wolf et al. 2007). The carcinoma inhibition effect of LF and its peptides is that they trigger a variety of signalling pathways (apoptosis, and angiopoietin signalling) in human body (Jiang and Lönnerdal 2016; Tomita et al. 2002) and increase the expression of tumour suppression proteins (Jiang and Lönnerdal 2016). Lactoferricin obtained during its *in-vitro* gastrointestinal digestion also show anti-carcinogenic effect (Khan et al. 2015; Jiang ans Lönnerdal 2016). Thus, oral administration of LF could be used as a chemotherapeutic agent together with other anticancer drugs.

4. Thermal denaturation of lactoferrin

Denaturation occurs when proteins are subjected to harsh environmental conditions such as strong acid/base, elevated or sub-zero temperatures and concentrated organic/inorganic salt. These conditions alter the conformation of the protein and cause the breakdown of forces (e.g. hydrogen and disulphide bonds) that give rise and stabilise higher order (secondary, tertiary and quaternary) structural features. In general, denaturation of LF is not desired as it alters its 3D structure and compromises functional properties (e.g. iron binding and antibacterial activities). Thus, during the extraction and production processes, the extent of denaturation of LF has to be carefully considered and the processing parameters have to be optimized to preserve its biological activity. Thus, the effect of pH, temperature and drying (dehydration) conditions on the denaturation characteristics of LF are discussed in the ensuing sections.

4.1. Effect of temperature and pH on the denaturation of lactoferrin

LF is present in milk and other physiological fluids in dissolved state. In aqueous form, it is stabilized by hydrogen bonding, hydrophobic/hydrophilic interactions, disulphide bonds and ligand binding. These structure stabilising forces could be affected at a certain pH and temperature conditions. The pH affects salt bridges and hydrogen bonding whereas temperature changes the kinetic energy of hydrogen bonds, non-polar hydrophobic and intermolecular thiol/disulphide interactions (Brisson et al. 2007; Hendsch and Tidor 1994; Privalov and Khechinashvili 1974).

The isoelectric point (pI) of LF falls within 8.0–9.0 pH range (Hirai et al. 1990; Bokkhim et al. 2013; Wang et al. 2017a). LF is soluble in water at any pH other than the pI range. It is shown that solubility of LF was >92% at pH 7.0 at ambient temperature (25°C) (Wang et al. 2017b). The structural and functional properties of LF in between 2.0 and 8.0 pH values have been documented. Baker and Baker (2004) and Rastogi et al. (2016) reported that LF started losing iron at pH 5.0–6.5 and >90% of its iron was released at pH 2.0. The loss of iron was found to depend on the alteration in tertiary structure. As the depletion of iron was complete when the tertiary or higher order structures were altered, there is no need for the secondary structural features to be altered for complete depletion of iron (Bokkhim et al. 2013; Wang et al. 2017b). It was found that the thermal stability of apo-LF was severely affected and it gelled at

neutral and alkaline pH when it was heated at 80–100°C for 5min (Abe et al. 1991). However, the apo-LF was relatively stable at pH 4.0 under the same heating condition (Abe et al. 1991). Thus, the pH of LF solution has to be maintained > 6.5 in order to retain its iron content even though its thermal stability is highest at pH 4.0.

In addition to the temperature, thermal denaturation of LF depends on the environment factors such as pH, ionic strength, and the presence of other proteins and polysaccharides (Bengoechea et al. 2011; Li and Zhao 2017; Sreedhara et al. 2010). A number of studies have been carried out to determine the denaturation temperature of LF by using differential scanning calorimeter. It was found that the pure apo-LF denatured at ~70°C whereas the pure holo-LF denatured at ~90°C at pH 6.0–7.0 (Bokkhim et al. 2013; Sreedhara et al. 2010; Wang et al. 2017c). The higher denaturation temperature of holo-LF is attributed to its more compact structure formed by the binding of iron (Rastogi et al. 2016; Stănciuc et al. 2013). Therefore, iron saturation increases its resistance to thermally induced denaturation. This finding was verified by a kinetic study (72–85°C, pH 7.4) that apo-LF denatured faster than holo-LF (Sánchez 1992b). It has also been reported that thermal stability of LF in milk is lower than its stability in buffered aqueous solutions (Sánchez 1992b). Temperatures higher than ambient are commonly used during extraction and other processes such as pasteurization, sterilization and ultra-heat treatment (UHT). Thus, it is essential to understand the nature and degree of denaturation of LF during these thermal processes. A study conducted by Elagamy (2000) reported that heating bovine, camel and buffalo milk at 65°C for 30 min at their natural pH did not denature LF in significant degree. However, heating of above milks at 85°C for 30 min significantly denatured LF and substantially reduced its biological activity. Abe et al. (1991) preheated bovine LF at 70°C for 3 min and then subjected it to a UHT process at 130°C for 2 s (pH 4.0). These authors reported that the iron binding ability of bovine LF was almost fully retained, indicating the fact the denaturation of LF in commonly applied UHT process is negligible. By contrast, Saito et al. (1991) reported that bovine LF was thermally degraded and its iron biding ability was irreversibly lost when it was heated at 120°C for 15min (pH 2.0). These two observations indicate that exposure time is critical factor causing denaturation of LF. The effect of commonly used temperature-time combination of pasteurization (72°C, 15 s) and UHT treatment (135°C, 4 s) on denaturation of LF has also been investigated. It was found that bacteriostatic activity of bovine and human LF was retained after pasteurization (72°C, 15 s); however, this functional property was lost after the UHT (135°C, 4 s) treatment (Conesa et al. 2009; Paulsson et al. 1993). It is essential to enhance the thermal stability of LF in many food processing operations which can be achieved forming complexes or complex coacervates with other proteins or polysaccharides (Bengoechea et al. 2011; Li and Zhao 2017).

It is also important to understand the denaturation and loss of functional properties of LF at sub zero temperatures. Rollo et al. (2014) reported that human LF was stable at −18 to −20°C for 5 days; however, loss due to denaturation of the order of 37% was observed when stored for 3 months. Wang et al. (2017b) carried out freezing of bovine LF at −30°C for 24 h before freeze drying and reported that the loss of intact LF due to denaturation was < 2% at the end of combined freezing-freeze drying process. These studies implied that LF adequately resists chilling/freezing induced denaturation at short storage period (< 5 days).

4.2. Effect of powder formation process on the denaturation of lactoferrin

LF in aqueous form is very sensitive to chemical and microbial degradation when it is stored at ambient temperature. Therefore, it is generally converted into powder form to extend its shelf-life and to preserve its functional properties. Freeze drying is overwhelmingly preferred in industry to transfer LF into powder form in order to preserve its functional properties to the best possible degree (Sharbafi et al. 2011; Tomita et al. 2002). However, long drying time, batch mode of production and higher capital and operational costs are major drawbacks of this process (Haque and Adhikari 2015; Peters et al. 2016). Alternatively, spray drying can be used industrially to produce LF powders (Wang et al. 2017b; Wang et al. 2017c). The challenge of this drying method is that LF encounters thermal, interfacial and rapid evaporation-related stresses. These stresses can lead to conformation changes (denaturation) and also affect the functional attributes of the dried LF powders if the process parameters are not carefully chosen. Therefore, the understanding of the denaturation characteristics of LF in drying processes (especially freeze drying and spray drying) is important. The understanding of extent and nature of denaturation of LF in spray and freeze drying processes helps optimisation of the process parameters and minimise the extent of denaturation of LF powders. This will ultimately benefits the application of LF in many food and pharmaceutical formulations.

The drying and denaturation characteristics of three forms of bovine LF (apo-, native- and holo-LF) during convective air drying has been determined by Wang et al. (2017c) using a single droplet drying (SDD) apparatus. SDD produces and dries a single LF droplet under a controlled convective drying environment. This method mimics the spray drying process. It allows measurement of drying and denaturation kinetics of bioactive compound contained in the droplet at chosen time interval (Che et al. 2012; Fu et al. 2012; Mezhericher et al. 2007). Wang et al. (2017c) reported the drying and denaturation kinetics of three forms of LF measured using single droplet drying (Figure 3). Their work has shown that 10 (holo-LF) to 30% (apo-LF) of LF was denatured during convective air drying of 70 and 95°C when dried for 10 min. The alteration of secondary structural features (α-helix, β-sheet, β-turn and random coil) of all the three forms of LF in the above study was of the order of 10%. This study also showed that iron-saturated holo form of LF is more suitable than native or apo forms to produce LF powders through convective air drying (spray drying) system. Wang et al. (2017b) also studied the extent of denaturation of native bovine LF during spray and freeze drying processes. The denaturation profiles of spray and freeze dried LF powders

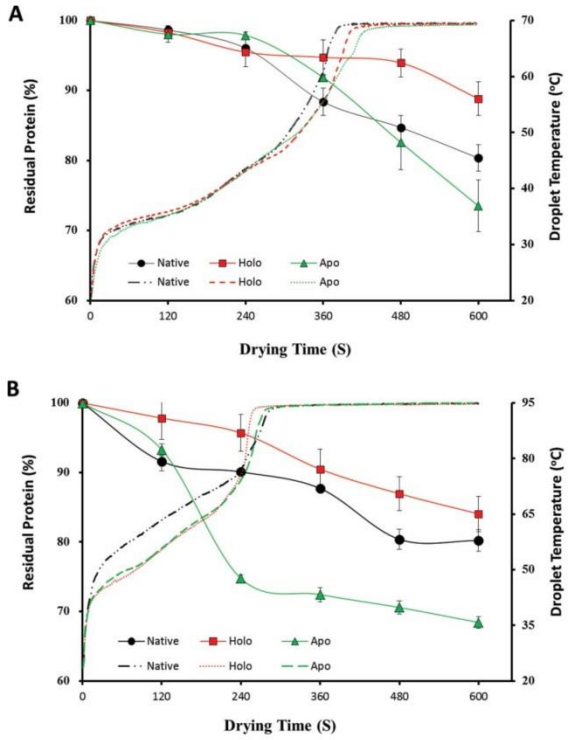

Figure 3. Denaturation profiles of three forms of bovine lactoferrin (LF) at (A) 70°C and (B) 95°C convective drying temperature. The black, red and green colors represent native (native-), iron saturated (holo-) and iron depleted (apo-) LF forms, respectively (Wang et al. 2017c).

are reported by these authors which are presented in Figure 4. The spray drying was carried out at 180°C inlet temperature and 70 and 95°C outlet temperatures. The freeze drying process was comprised of pre-frozen (−30°C, 24 h), primary (0°C, 12 h) and secondary (20°C, 6 h) drying stages. Interestingly, the results of this study showed both the spray- and freeze-dried LF powders had negligible denaturation (< 2%)

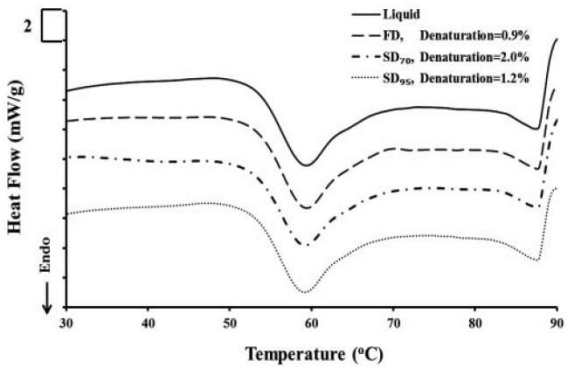

Figure 4. Differential scanning calorimetric thermograms of liquid, spray-dried (SD) and freeze-dried (FD) bovine LF powders. SD_{70} = spray-dried LF powder at outlet drying temperature of 70°C, SD_{95} = spray-dried LF powder at outlet drying temperature of 95°C. The inlet drying temperature was 180°C. The extent of denaturation was determined using decrease in the enthalpy (ΔH) due to denaturation (Wang et al. 2017b).

and conformation changes when compared to the fresh membrane-filtered LF solution (Figure 4). The antioxidant activity of spray-and freeze-dried powders was similar to that of fresh membrane-filtered LF sample. Although the inlet and outlet temperatures of the spray drying process were within the denaturation temperature of native-LF, the very short drying and exposure time (<2 s) helped to avoid the denaturation during spray drying. The combination of low temperature and reasonably short freezing and drying time of the freeze drying process also avoided the denaturation. Thus, denaturation of LF was avoided in both spray- and freeze-drying conditions. The result of this study implied that industries could produce LF powders without losing its structural integrity and functional properties by selecting suitably optimised spray- and freeze-drying process parameters.

5. Digestion of lactoferrin

Dietary proteins including LF are digested into small molecules in human body. It ensures nutrients (e.g. essential amino acids and small molecular weight peptides) are absorbed by the intestine and then transported in the blood. Human digestion system is comprised of three digestion phases: salivary, gastric and intestinal digestion. The salivary phase plays a role in mastication and, to some extent digestion of starch whereas gastric and intestinal phases are the stages where digestion of protein occurs.

It is expected that the functional properties of LF (e.g. iron transporting, antibacterial and antioxidant activity) could be affected at gastric and intestinal stage of digestion. Since the functional domains of LF (e.g. iron binding) are highly dependent on its unique 3D structural conformation, the gastrointestinal breakdown of LF causes undesirable loss of its functional properties. Nevertheless, the degradation of LF during gastrointestinal tract also could be beneficial. As mentioned earlier, it has been reported that strong antibacterial peptides such as lactoferricin and lactoferrampin are produced by pepsin hydrolysis (Bellamy et al. 1992; Lizzi et al. 2016). Therefore, the understanding of the digestion behaviour of LF is important which provides essential information (e.g. degradation patterns and changes in functional properties) of LF and peptides derived from LF at different digestion stages (gastric and intestinal digestion). This information further benefits the utilization of LF in high value food products such as infant formula, nutritional supplements and other formulations that aims at delivering LF through oral administration.

5.1. Fate of lactoferrin during digestion

The *in-vivo* digestion of LF in human digestive system is poorly understood and there are many mutually contradictory claims. Troost et al. (2002) investigated the digestion behaviour of recombinant human LF in 43–57 year-old female volunteers. The recombinant human LF was in iron depleted (apo) form which had the identical 3-D structure as that of human LF. It was found that the recombinant human LF was completely degraded at upper gastrointestinal tract. Another *in-vivo* digestion study carried out on 20–22 year-old volunteers used 20% and 100% iron saturated bovine LF as the test specimen (Troost

et al. 2001). It reported that >60% of orally administered bovine LF passed through the gastric (stomach) stage in structurally intact form. In the above mentioned *in-vivo* digestion study, the gastric emptying time was ~30 min and the intragastric pH was decreased from 7.0 to 4.0 during the digestion period. The pH range (4.0–7.0) is substantially higher than the optimum pH (1.5–2.0) required for pepsin digestion. In fasting stage, the intragastric pH of adults is in the range of 5.0–6.0 and it takes up to 100 minutes to generate enough hydrochloric acid to reach the optimum pH of pepsin digestion (Kong and Singh 2010). Hence, the gastric emptying rate and the buffering capacity of food play an important role in the *in-vivo* digestion of LF. LF in liquid products has faster gastric emptying time than that in solid products. The nature of glycosylation and source of LFs also affect their stability in gastrointestinal environment. For example, glycosylation at Asn281 protects bovine LF against cleavage by trypsin at Lys282 while the glycosylation of human LF did not show any protection (van Veen et al. 2004). The information regarding the digestion of LF in human infant and newborns is less controversial. As the digestive system in infants and newborns is not mature enough (e.g. the intragastric pH and the gastric emptying rate is higher than adults), LF could not be completely digested in this condition. This hypothesis is confirmed by measuring the unhydrolysed LF in faecal extracts of babies (Spik et al. 1982; Gisbert et al. 2009). However, to date, there is no *in-vivo* study which conclusively shows the extent and nature of digestion of LF at different stages of digestion and the chemical structure and functional properties of the resultant digesta.

In-vitro studies of LF simulating the digestion of LF in adult/infant gastrointestinal systems are quite abundant as these studies are faster and are also easier to carry out. The parameters including types of enzymes and their activities, enzyme to substrate ratio, time and pH must confirm to the age, the fasting/ feeding stage and other physicochemical conditions in human digestive system. The most commonly used digestion conditions chosen in *in-vitro* digestion studies of LF and the percentage of structurally intact or undigested LF in different stages of gastrointestinal tract are given in (Table 4). These *in-vitro* digestion studies of LF can be classified into two types: a) study on the digestion behaviour of LF to assess the effects of heat treatment and encapsulation and b) generation of new peptides and determine their sequence and functional properties. Currently, most of the *in-vitro* digestion studies indicate that LF gets completely degraded during gastric stage of digestion (Table 4) and hence it cannot reach the absorption sites of intestine. Due to the proteolysis and pH induced degradation, the iron binding ability of LF was lost and its antioxidant capacity was also decreased before it reached intestinal stage (Wang et al. 2017a). Moreover, it has been reported that mild thermal treatment (70°C, 10 min) of bovine LF before subjecting it to the *in-vitro* digestion did not have any significant effect on its digestion behaviour compared to the unheated sample as shown by the degradation pattern of LF(SDS-PAGE, Figure 5). Furlund et al. 2013 showed that small-molecular-weight peptides (<10 kDa) are generated when bovine LF is subjected to *in-vivo* and *in-vitro* digestion for 30 min. The *in-vivo* digestion produced more than 40 peptides with 6–22 amino acid residues with molecular weight of less than 2.5 kDa whereas the *in-vitro* digestion generated 4–33 peptides of similar molecular weight depending on the digestion conditions used. The bioactive peptide-lactoferricin was not produced from bovine LF during *in-vivo* and *in-vitro* digestions by human gastric and duodenal juices (Furlund et al. 2013). In contrast, Kuwata et al. (1998) reported the detection of high concentration ($5.7 \pm 0.7 \times 10^{-5}$ mol/L) of lactoferricin in the gastric fluids after 10 min of gastric digestion of bovine LF. Therefore, although the bioactive peptides are produced from the digestion of LF, their production depends greatly on the prevailing digestion conditions such as intragastric pH, gastric emptying times and type and activity of enzymes. For example, lactoferricin can be degraded at longer gastric emptying time and its health benefit may not be achieved.

5.2. Protection of LF from premature digestion

The important receptors of LF are located at the intestinal mucosa and lymphatic tissue cells in the gut (Jiang et al. 2011; Takeuchi et al. 2006; Yamano et al. 2010; Yao et al. 2015). Hence, the delivery of LF through oral administration requires that it is protected so that it passes through stomach and is delivered to the absorption sites in functionally active form. The most commonly used methods to protect LF during its passage through the gastrointestinal tract are: a) iron saturation b) microencapsulation and c) PEGylation. The various methods used to protect the LF during oral and gastric (stomach) stages of gastrointestinal tract and their effectiveness are presented in (Table 5).

Crystallographic studies have shown that the binding of iron to LF made the structural conformation of LF more compact (Baker et al. 2000; Baker and Baker 2012; Moore et al. 1997; Rastogi et al. 2016). This change in LF structure offers higher resistance to pepsin induced proteolysis (Kuwata et al. 2001; Troost et al. 2001; Bokkhim et al. 2016). However, the protection of LF by iron saturation alone is not sufficient. It has been reported that iron saturation is able to protect about 80% LF (increased from 60% to 80%) in the gastric fluid without encapsulation (Troost et al. 2001; Bokkhim et al. 2016). In contrast, other studies have shown that unprotected or unencapsulated LFs, whether they are iron saturated or depleted, cannot pass through stomach (gastric stage) in their structurally intact form (Chan and Li-Chan 2007; Wang et al. 2017a). Therefore, although iron saturation could be considered as an optional method to slow down the enzymatic hydrolysis of LF, it is not adequately effective in delivering LF to small intestine in its structurally intact form through oral administration.

A more commonly acceptable method to protect LF during digestion is microencapsulation. In this method, a protective (shell) matrix is created around the LF core. Food grade proteins (e.g. bovine serum albumin, β- lactoglobulin) and polysaccharides (e.g. pectin, carrageenan, sodium alginate, gum Arabic) are commonly used as the shell materials. This core-shell structure excellently protects LF from the harsh environment prevailing in human digestive system. Microencapsulation also helps achieve targeted and controlled release of LF by simply using shell materials with suitable properties. For example, sodium alginate is resistant to pepsin attack but breaks down during intestinal digestion

Table 4. Digestion conditions and percentage of structurally intact lactoferrin (LF) during gastrointestinal digestion. Apo-LF = iron depleted LF, holo-LF = iron saturated LF, native-LF = natural form of LF with an iron saturation level of 10–20%. GI = gastrointestinal tract, G = Gastric tract, I = Intestinal tract.

Material	Study Model	Volunteers	pH	Emptying time in GI	Percentage of structurally intact LF in stomach	Percentage of structurally intact LF in intestine	References
Recombinant human apo-LF	*In-vivo, GI*	Adult	—	24 h	—	0	Troost 2002
Bovine native-LF	*In-vivo, GI*	Rats	—	< 0.4 h in stomach < 1 h in upper small intestine < 12 h in lower small intestine	0	0	Kuwata 2001
Bovine native-LF	*In-vivo, G*	Adult	7.0→4.0	< 0.5 h	60–80%	—	Troost 2001
Bovine holo-LF	*In-vivo, G*	Adult	7.0→4.0	< 0.5 h	80–100%	—	Troost 2001
Bovine LF	*In-vivo, GI*	—	2.3 in stomach 6.5→7.5 in intestine	0.5 h in stomach 0.5 h in intestine	0	0	Furlund 2013
Bovine LF	*In-vitro, I*	—	7.4	6 h	—	0	Yao 2014
Bovine apo-, native- and holo-LF	*In-vitro, GI*	—	7.0 in mouth 2.0 in stomach 7.0 in intestine	2 min in oral 2 h in stomach 2 h in intestine	0	0	Wang 2017a
Bovine apo-, native- and holo-LF	*In-vitro, GI*	—	2.0→3.5 in stomach 7.5 in intestine	2 h in stomach 2 h in intestine	54% (apo), 57%, (native) and 96% (holo)	0	Bokkhim 2016
Bovine LF	*In-vitro, G*	—	6.8 in mouth 4.5→1.7 in stomach	2 s in oral 2 h in stomach	0	—	Shimoni 2013
Bovine LF	*In-vitro, G*	—	3.2	100 min	0	—	Nojima 2008; Nojima 2009
Bovine LF	*In-vitro, GI*	—	2.5 in stomach 6.5 in intestine	1 h in stomach 0.5 h in intestine	0	0	David-Birman 2013
Bovine LF	*In-vitro, GI*	—	2.5 in stomach 7.0 in intestine	0.5 h in stomach 0.5 h in intestine	0	0	Furlund 2013
Bovine LF	*In-vitro, GI*	—	2.0 in stomach 8.0 in intestine	0.5 h in stomach 0.5 h in intestine	< 6%, porcine enzyme digestion <19%, human juices digestion	< 6%	Eriksen 2010
Bovine, caprine, human and equine LF	*In-vitro, GI*	—	2.5 in stomach 8.0 in intestine	0.5 h in stomach 0.5 h in intestine	—	~0	Inglingstad 2010

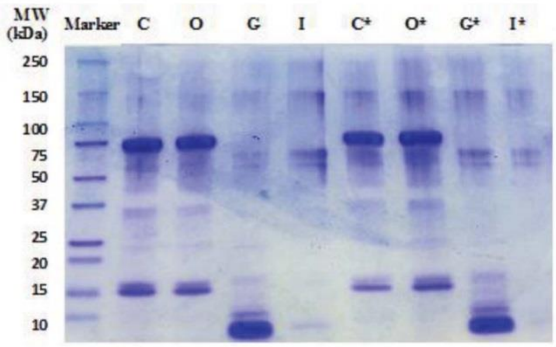

Figure 5. Degradation patterns of native bovine LF at different stages of adult human digestion (*in vitro*) determined using SDS-PAGE. "C" indicates the control sample without any treatment; "O" represents the sample after oral digestion. "G" and "I" are the samples after successive oral+gastric and oral+gastic+intestinal digestion stages, respectively. The samples subjected to isothermal heat treatment (70°C for 10min) prior to digestion are labeled with * (Wang et al. 2017a). The band at ~75 kDa corresponds to the intact form of (non-degraded) LF.

and releases the LF which is desirable (Chater et al. 2015). Kilic et al. (2017) prepared a bilayer (bovine serum albumin-tannic acids) capsules loaded with bovine LF. It achieved >76% protection efficiency during gastric digestion. The shell of this capsule was degraded and the LF was released during intestinal digestion. The released LF was further absorbed by intestine. Consequently, the level of LF in the blood stream of subjects who were administered with these capsules was 2–4 times higher than those who were administered with unencapsulated native bovine LF. It was found that the percentage of structurally intact (protected) bovine LF encapsulated in sodium alginate (during gastric digestion) increased from 57% to 79% (Bokkhim et al. 2016). Liu et al. (2013) encapsulated bovine LF in liposomes prepared from milk fat globule membrane-derived phospholipids and reported that liposomes could prevent gastric degradation of bovine LF. The liposomes also reduced the rate of hydrolysis of bovine LF under intestinal conditions. Therefore, encapsulation could be used to modulate the digestion behaviour of LF and hence achieve sufficient bioavailability through oral administration.

The covalent attachment of polyethylene glycol (PEG) has been reported in protecting LF against harsh gastric environment. This technique, known as PEGylation, is expected to increase the resistance of LF against proteolysis by steric hindrance. It also inhibits the renal clearance due to the increased molecular mass after PEGylation (Yao et al. 2013). Nojima et al. (2008) synthesized a bovine LF-PEG (20 kDa) conjugate and determined its digestion behaviour. It was found that the proteolytic half-life (*in-vitro* gastric stage) of LF was prolonged by ~2-fold and the amount of absorption of LF through the intestinal mucosa increased by ~10-fold compared to the unPEGylated LF. At a further study, Nojima et al. (2009) prepared a covalently linked conjugate of LF with a branched 40 kDa PEG and reported that this conjugate fully retained the iron binding and anti-inflammatory activity of LF during gastric stage of digestion and delivered almost 100% structurally intact LF to the intestine. Furthermore, the 40kDa PEGylated LF had 8-fold longer plasma half-life than that of the unPEGylated bovine LF in rat model. Hence, PEGylation is also efficient in protecting LF in oral delivery route.

The electrostatic complexation (complex coacervation) of LF with acid-stable gums and proteins also increases its stability and hence this system has good potential in delivering LF through oral route. The complex coacervation process involves at least two oppositely charged biopolymers such as proteins and polysaccharides in aqueous medium. Positively charged proteins undergo complex coacervation with negatively charged polysaccharides and form insoluble complex coacervates at some specific pH, ionic strength and protein-to-polysaccharide mixing ratios (De Kruif et al. 2004; Eratte et al. 2014). The complex coacervates are more surface active and are considered as better encapsulants compared to individual protein or polysaccharide gum. In addition, simple operation and easy to scale-up features are some of the advantages of complex coacervation process. Due to these reasons, complex coacervates are widely used in food and pharmaceutical industries for encapsulation of unstable bioactive ingredients such as vitamins, flavour oils and polyunsaturated fatty acids (Junyaprasert et al. 2001; Timilsena et al. 2017; Yeo et al. 2005). Since LF is positively charged at large pH range (<8.0) it can easily undergo

Table 5. Methods applied to protect the orally administrated LF during digestion.

Methods	Source of LF	Protecting materials	Protection in stomach	References
Iron saturation	Bovine	—	Increased from 57% to 79%	Bokkhim 2016
Iron saturation	Bovine	—	Increased from 60% to 80%	Troost 2001
Encapsulation	Bovine	Bovine serum albumin, tannic acids	≥ 76%	Kilic 2017
Encapsulation	Bovine	Sodium alginate	Increased from 57% to ≥ 76%	Bokkhim 2016
Encapsulation	Bovine	Milk fat globule membrane-derived phospholipids	100%	Liu 2013
Encapsulation	Bovine	High-methoxypectin, Low-methoxy pectin, Sodium alginate, Iota-carrageenan	0 (slower degradation)	David-Birman 2013
Oil-LF-polysaccharide emulsion	Bovine	I-carrageenan, alginate	~0 (slower degradation)	Shimoni 2013
Polyethylene glycol (PEG) conjunction	Bovine	PEG molecule (2 × 10 kDa)	>0 (proteolytic half-life prolonged from 17 min to 35 min)	Nojima 2008
Polyethylene glycol (PEG) conjunction	Bovine	PEG molecule (40 kDa)	100%	Nojima 2009

complex coacervation with many polysaccharides (including gums). As sodium alginate is negatively charged over a large pH range (>2.0) it is expected that it can form stable complex coacervates with relative ease. Research is needed to ascertain the efficiency of LF-sodium alginate complex coacervates in avoiding premature digestion of LF in gastric digestion stage and delivering it to the intestinal stage.

6. Concluding remarks

LF is a multifunctional protein with well-documented conformational features. The iron transferring/binding and antibacterial properties of LF and peptides obtained from it have been studied to a considerable detail. This has led to a range of nutritional and pharmaceutical applications of LF such as infant formula, functional beverages and toothpaste. Other functional properties of LF (e.g. antiviral and anti-carcinogenic activity) have also raised research attentions, showing potential in developing new drugs and vaccines. The functional properties of LF depend on its higher order (secondary and tertiary) structural conformation. Therefore, denaturation of the native structure must be taken into consideration during its processing. The pH, temperature and drying conditions involved in extraction and production of LF and processing of LF-containing products have to be optimized to avoid or minimise the denaturation of LF. Although oral administration of LF is the most widely adopted method of its delivery into human body, it still possesses some challenges that must be addressed to get highest benefit from its intake. To date, most of literature indicates that LF cannot pass through the stomach (gastric stage) in its structurally intact form and hence protection is required. Microencapsulation and PEGylation are the most effective methods used to deliver LF to the intestinal absorption sites. Formation of complex coacervates of LF with oppositely charged biopolymers such as polysaccharide gums is technologically convenient and useful method for oral delivery of LF.

Acknowledgments

The first author acknowledges the fee-waiver scholarship provided to him by the Royal Melbourne Institute of Technology (RMIT) University.

ORCID

Benu Adhikari http://orcid.org/0000-0002-7571-7968

References

Abdallah, F. B., and J. M. E. H. Chahine. 2000. Transferrins: iron release from lactoferrin. *Journal of Molecular Biology* 303 (2):255–266. doi:10.1006/jmbi.2000.4101.

Abe, H., H. Saito, H. Miyakawa, Y. Tamura, S. Shimamura, E. Nagao, and M. Tomita. 1991. Heat stability of bovine lactoferrin at acidic pH. *Journal of Dairy Science* 74 (1):65–71. doi:10.3168/jds.S0022-0302(91)78144-7.

Al-Sheikh, H. 2009. Effect of lactoferrin and iron on the growth of human pathogenic Candida species. *Pakistan Journal of Biological Sciences* 12 (1):91. doi:10.3923/pjbs.2009.91.94.

Amiri, F., F. Moradian, and A. Rafiei. 2015. Anticancer effect of lactoferrin on Gastric Cancer Cell Line AGS. *Research in Molecular Medicine* 3 (2):11–16.

Artym, J., and M. Zimecki. 2005. The role of lactoferrin in the proper development ofnewborns. *Advances in Hygiene and Experimental Medicine* 59:421–432.

Baker, E. N. 1994. Structure and reactivity of transferrins. *Advances in Inorganic Chemistry* 41:389–463. doi:10.1016/S0898-8838(08)60176-2.

Baker, E. N., and H. M. Baker. 2009. A structural framework for understanding the multifunctional character of lactoferrin. *Biochimie* 91 (1):3–10. doi:10.1016/j.biochi.2008.05.006.

Baker, E. N., H. M. Baker, and R. D. Kidd. 2002. Lactoferrin and transferrin: functional variations on a common structural framework. *Biochemistry and Cell Biology* 80 (1):27–34. doi:10.1139/o01-153.

Baker, H. M., C. J. Baker, C. A. Smith, and E. N. Baker. 2000. Metal substitution in transferrins: specific binding of cerium(IV) revealed by the crystal structure of cerium-substituted human lactoferrin. *Journal of Biological Inorganic Chemistry* 5:692–698. doi:10.1007/s007750000157.

Baker, H. M., and E. N. Baker. 2004. Lactoferrin and iron: structural and dynamic aspects of binding and release. *Biometals* 17 (3):209–216. doi:10.1023/B:BIOM.0000027694.40260.70.

Baker, H. M., and E. N. Baker. 2012. A structural perspective on lactoferrin function. *Biochemistry and Cell Biology* 90 (3):320–328. doi:10.1139/o11-071.

Balasubramanian, S. A., D. C. Pye, and M. D. P. Willcox. 2012. Levels of lactoferrin, secretory IgA and serum albumin in the tear film of people with keratoconus. *Experimental Eye Research* 96 (1):132–137. doi:10.1016/j.exer.2011.12.010.

Barbiroli, A., F. Bonomi, G. Capretti, S. Iametti, M. Manzoni, L. Piergiovanni, and M. Rollini. 2012. Antimicrobial activity of lysozyme and lactoferrin incorporated in cellulose-based food packaging. *Food Control* 26 (2):387–392. doi:10.1016/j.foodcont.2012.01.046.

Barboza, M., J. Pinzon, S. Wickramasinghe, J. W. Froehlich, I. Moeller, J. T. Smilowitz, et al. 2012. Glycosylation of human milk lactoferrin exhibits dynamic changes during early lactation enhancing its role in pathogenic bacteria-host interactions. *Molecular & Cellular Proteomics* 11 (6):M111–015248. doi:10.1074/mcp.M111.015248.

Baveye, S., E. Elass, J. Mazurier, G. Spik, and D. Legrand. 1999. Lactoferrin: A multifunctional glycoprotein involved in the modulation of the inflammatory process. *Clinical Chemistry and Laboratory Medicine* 37:281–286. doi:10.1515/CCLM.1999.049.

Beeckman, D. S. A., C. M. Van Droogenbroeck, B. J. De Cock, P. Van Oostveldt, and D. C. Vanrompay. 2007. Effect of ovotransferrin and lactoferrins on Chlamydophila psittaci adhesion and invasion in HD11 chicken macrophages. *Veterinary Research* 38 (5):729–739. doi:10.1051/vetres:2007028.

Beljaars, L., B. W. van der Strate, H. I. Bakker, C. Reker-Smit, F. C. Wiegmans, M. C. Harmsen, et al. 2004. Inhibition of cytomegalovirus infection by lactoferrin in vitro and in vivo. *Antiviral Research* 63 (3):197–208. doi:10.1016/j.antiviral.2004.05.002.

Bellamy, W., M. Takase, K. Yamauchi, H. Wakabayashi, K. Kawase, and M. Tomita. 1992. Identification of the bactericidal domain of lactoferrin. *Biochimica et Biophysica Acta (BBA)-Protein Structure and Molecular Enzymology* 1121 (1–2):130–136. doi:10.1016/0167-4838(92)90346-F.

Bengoechea, C., O. G. Jones, A. Guerrero, and D. J. McClements. 2011. Formation and characterization of lactoferrin/pectin electrostatic complexes: Impact of composition, pH and thermal treatment. *Food Hydrocolloids* 25 (5):1227–1232. doi:10.1016/j.foodhyd.2010.11.010.

Bokare, A. D., and W. Choi. 2014. Review of iron-free Fenton-like systems for activating H_2O_2 in advanced oxidation processes. *Journal of Hazardous Materials* 275:121–135. doi:10.1016/j.jhazmat.2014.04.054.

Bokkhim, H., N. Bansal, L. GrØndahl, and B. Bhandari. 2013. Physico-chemical properties of different forms of bovine lactoferrin. *Food Chemistry* 141 (3):3007–3013. doi:10.1016/j.foodchem.2013.05.139.

Bokkhim, H., N. Bansal, L. Grøndahl, and B. Bhandari. 2016. In-vitro digestion of different forms of bovine lactoferrin encapsulated in alginate micro-gel particles. *Food Hydrocolloids* 52:231–242. doi:10.1016/j.foodhyd.2015.07.007.

Brimelow, R. E., N. P. West, L. T. Williams, A. W. Cripps, and A. J. Cox. 2017. A role for whey-derived lactoferrin and immunoglobulins in the

attenuation of obesity-related inflammation and disease. *Critical Reviews in Food science and Nutrition* 57 (8):1593–1602. doi:10.1080/10408398.2014.995264.

Brisson, G., M. Britten, and Y. Pouliot. 2007. Heat-induced aggregation of bovine lactoferrin at neutral pH: Effect of iron saturation. *International Dairy Journal* 17 (6):617–624. doi:10.1016/j.idairyj.2006.09.002.

Camaschella, C. 2015. Iron-deficiency anemia. *New England Journal of Medicine* 372 (19):1832–1843. doi:10.1056/NEJMra1401038.

Cao, L., and H. Maas. 2015. U.S. Patent No. 8,999,923. Washington, DC: U.S. Patent and Trademark Office.

Chan, J. C., and E. C. Li-Chan. 2007. Production of lactoferricin and other cationic peptides from food grade bovine lactoferrin with various iron saturation levels. *Journal of Agricultural and Food Chemistry* 55 (2):493–501. doi:10.1021/jf0625149.

Chater, P. I., M. D. Wilcox, I. A. Brownlee, and J. P. Pearson. 2015. Alginate as a protease inhibitor in vitro and in a model gut system; selective inhibition of pepsin but not trypsin. *Carbohydrate Polymers* 131:142–151. doi:10.1016/j.carbpol.2015.05.062.

Che, L., D. Li, and X. D. Chen. 2012. Convective drying kinetics of single droplets of aqueous glucose. *Drying Technology* 30 (10):1029–1036. doi:10.1080/07373937.2012.663844.

Chen, P. W., W. C. Chen, and F. C. Mao. 2004. Increase of lactoferrin concentration in mastitic goat milk. *Journal of Veterinary Medical Science* 66 (4):345–350. doi:10.1292/jvms.66.345.

Chen, R., N. Cole, D. Dutta, N. Kumar, and M. D. Willcox. 2016. Antimicrobial activity of immobilized lactoferrin and lactoferricin. *Journal of Biomedical Materials Research Part B: Applied Biomaterials* doi:10.1002/jbm.b.33804.

Cheng, J. B., J. Q. Wang, D. P. Bu, G. L. Liu, C. G. Zhang, H. Y. Wei, et al. 2008. Factors affecting the lactoferrin concentration in bovine milk. *Journal of Dairy Science* 91 (3):970–976. doi:10.3168/jds.2007-0689.

Conesa, C., C. Rota, E. Castillo, M. D. Perez, M. Calvo, and L. Sanchez. 2009. Antibacterial activity of recombinant human lactoferrin from rice: effect of heat treatment. *Bioscience, Biotechnology, and Biochemistry* 73 (6):1301–1307. doi:10.1271/bbb.80814.

Cornish, J., K. E. Callon, D. Naot, K. P. Palmano, T. Banovic, U. Bava, et al. 2004. Lactoferrin is a potent regulator of bone cell activity and increases bone formation in vivo. *Endocrinology* 145 (9):4366–4374. doi:10.1210/en.2003-1307.

Coughlin, R. T., S. Tonsager, and E. J. McGroarty. 1983. Quantitation of metal cations bound to membranes and extracted lipopolysaccharide of Escherichia coli. *Biochemistry* 22 (8):2002–2007. doi:10.1021/bi00277a041.

Cox, T. M., J. Mazurier, G. Spik, J. Montreul, and T. J. Peters. 1979. Iron binding proteins and influx of irom across the duodenal brush border: Evidence for specific lactotransferrin receptors in the human intestine. *Biochimica et Biophysica Acta (BBA)-General Subjects* 588 (1):120–128. doi:10.1016/0304-4165(79)90377-5.

da Motta Willer, E., R. de Lourenço Lima, and L. G. Giugliano. 2004. In vitro adhesion and invasion inhibition of Shigella dysenteriae, Shigella flexneri and Shigella sonnei clinical strains by human milk proteins. *BMC Microbiology* 4 (1):18. doi:10.1186/1471-2180-4-18.

David-Birman, T., A. Mackie, and U. Lesmes. 2013. Impact of dietary fibers on the properties and proteolytic digestibility of lactoferrin nano-particles. *Food Hydrocolloids* 31 (1):33–41. doi:10.1016/j.foodhyd.2012.09.013.

Davidsson, L., P. Kastenmayer, M. Yuen, B. O. Lönnerdal, and R. F. Hurrell. 1994. Influence of lactoferrin on iron absorption from human milk in infants. *Pediatric Research* 35 (1):117–124. doi:10.1203/00006450-199401000-00025.

De Kruif, C. G., F. Weinbreck, and R. de Vries. 2004. Complex coacervation of proteins and anionic polysaccharides. *Current Opinion in Colloid & Interface Science* 9 (5):340–349. doi:10.1016/j.cocis.2004.09.006.

Drago-Serrano, M. E., R. Campos-Rodríguez, J. C. Carrero, and M. De La Garza. 2017. Lactoferrin: Balancing Ups and Downs of Inflammation Due to Microbial Infections. *International Journal of Molecular Sciences* 18 (3):501. doi:10.3390/ijms18030501.

Elagamy, E. I. 2000. Effect of heat treatment on camel milk proteins with respect to antimicrobial factors: a comparison with cows' and buffalo milk proteins. *Food Chemistry* 68 (2):227–232. doi:10.1016/S0308-8146(99)00199-5.

3rd, E., R. T. , and T. J. Giehl. 1991. Killing of gram-negative bacteria by lactoferrin and lysozyme. *Journal of Clinical Investigation* 88 (4):1080. doi:10.1172/JCI115407.

Eratte, D., B. Wang, K. Dowling, C. J. Barrow, and B. P. Adhikari. 2014. Complex coacervation with whey protein isolate and gum Arabic for the microencapsulation of omega-3 rich tuna oil. *Food & Function* 5 (11):2743–2750. doi:10.1039/C4FO00296B.

Erickson, T., G. Gill, and G. M. Chan. 2013. The effects of acidification on human milk's cellular and nutritional content. *Journal of Perinatology* 33 (5):371–373. doi:10.1038/jp.2012.117.

Eriksen, E. K., H. Holm, E. Jensen, R. Aaboe, T. G. Devold, M. Jacobsen, and G. E. Vegarud. 2010. Different digestion of caprine whey proteins by human and porcine gastrointestinal enzymes. *British Journal of Nutrition* 104 (03):374–381. doi:10.1017/S0007114510000577.

Francesca, B., M. Ajello, P. Bosso, C. Morea, P. Andrea, A. Giovanni, and V. Piera. 2004. Both lactoferrin and iron influence aggregation and biofilm formation in Streptococcus mutans. *Biometals* 17 (3):271–278. doi:10.1023/B:BIOM.0000027704.53859.d3.

Fu, N., M. W. Woo, and X. D. Chen. 2012. Single droplet drying technique to study drying kinetics measurement and particle functionality: a review. *Drying Technology* 30 (15):1771–1785. doi:10.1080/07373937.2012.708002.

Furlund, C. B., E. K. Ulleberg, T. G. Devold, R. Flengsrud, M. Jacobsen, C. Sekse, et al. 2013. Identification of lactoferrin peptides generated by digestion with human gastrointestinal enzymes. *Journal of Dairy Science* 96 (1):75–88. doi:10.3168/jds.2012-5946.

Gibbons, J. A., J. R. Kanwar, and R. K. Kanwar. 2015. Iron-free and iron-saturated bovine lactoferrin inhibit survivin expression and differentially modulate apoptosis in breast cancer. *BMC Cancer* 15 (1):425. doi:10.1186/s12885-015-1441-4.

Gisbert, J. P., A. G. Mcnicholl, and F. Gomollon. 2009. Questions and answers on the role of fecal lactoferrin as a biological marker in inflammatory bowel disease. *Inflammatory bowel diseases* 15 (11):1746–1754. doi:10.1002/ibd.20920.

Gomez, H. F., T. J. Ochoa, L. G. Carlin, and T. G. Cleary. 2003. Human lactoferrin impairs virulence of Shigella flexneri. *Journal of Infectious Diseases* 187 (1):87–95. doi:10.1086/345875.

González-Chávez, S. A., S. Arévalo-Gallegos, and Q. Rascón-Cruz. 2009. Lactoferrin: structure, function and applications. *International Journal of Antimicrobial Agents* 33 (4):301–e1. doi:10.1016/j.ijantimicag.2008.07.020.

Groves, M. L. 1960. The Isolation of a Red Protein from Milk2. *Journal of the American Chemical Society* 82 (13):3345–3350. doi:10.1021/ja01498a029.

Gupta, P. M., C. G. Perrine, Z. Mei, and K. S. Scanlon. 2016. Iron, anemia, and iron deficiency anemia among young children in the United States. *Nutrients* 8 (6):330. doi:10.3390/nu8060330.

Hasegawa, K., W. Motsuchi, S. Tanaka, and S. I. Dosako. 1994. Inhibition with lactoferrin of in vitro infection with human herpes virus. *Japanese Journal of Medical Science and Biology* 47 (2):73–85. doi:10.7883/yoken1952.47.73.

Haney, E. F., K. Nazmi, F. Lau, J. G. Bolscher, and H. J. Vogel. 2009. Novel lactoferrampin antimicrobial peptides derived from human lactoferrin. *Biochimie* 91 (1):141–154. doi:10.1016/j.biochi.2008.04.013.

Haque, M. A., and B. Adhikari. 2015. Drying and denaturation of proteins in spray drying process. In A.S. Mujumdar (Ed.), Handbook of Industrial Drying (pp. 971–985). Florida, US, CRC Press.

Hara, K., M. Ikeda, S. Saito, S. Matsumoto, K. Numata, N. Kato, et al. 2002. Lactoferrin inhibits hepatitis B virus infection in cultured human hepatocytes. *Hepatology Research* 24 (3):228–235. doi:10.1016/S1386-6346(02)00088-8.

He, J., and P. Furmanski. 1995. Sequence specificity and transcriptional activation in the binding of lactoferrin to DNA. *Nature* 373 (6516):721. doi:10.1038/373721a0.

Hendsch, Z. S., and B. Tidor. 1994. Do salt bridges stabilize proteins? A continuum electrostatic analysis. *Protein Science* 3 (2):211–226. doi:10.1002/pro.5560030206.

Hernell, O., and B. Lönnerdal. 2002. Iron status of infants fed low-iron formula: no effect of added bovine lactoferrin or nucleotides. *The American Journal of Clinical Nutrition* 76 (4):858–864.

Hirai, Y., N. Kawakata, K. Satoh, Y. Ikeda, S. Hisayasu, H. Orimo, and Y. Yoshino. 1990. Concentrations of lactoferrin and iron in human milk at different stages of lactation. *Journal of Nutritional Science and Vitaminology* 36 (6):531–544. doi:10.3177/jnsv.36.531.

Hiss, S., T. Meyer, and H. Sauerwein. 2008. Lactoferrin concentrations in goat milk throughout lactation. *Small Ruminant Research* 80 (1):87–90. doi:10.1016/j.smallrumres.2008.07.027.

Hwang, S. A., M. L. Kruzel, and J. K. Actor. 2005. Lactoferrin augments BCG vaccine efficacy to generate T helper response and subsequent protection against challenge with virulent Mycobacterium tuberculosis. *International Immunopharmacology* 5 (3):591–599. doi:10.1016/j.intimp.2004.11.006.

Hwang, S. A., M. L. Kruzel, and J. K. Actor. 2015. CHO expressed recombinant human lactoferrin as an adjuvant for BCG. *International Journal of Immunopathology and Pharmacology* 28 (4):452–468. doi:10.1177/0394632015599832.

Hwang, S. A., M. L. Kruzel, and J. K. Actor. 2016. Oral recombinant human or mouse lactoferrin reduces mycobacterium tuberculosis TDM induced granulomatous lung pathology. *Biochemistry and Cell Biology* 95 (1):148–154. doi:10.1139/bcb-2016-0061.

Ikeda, M., A. Nozaki, K. Sugiyama, T. Tanaka, A. Naganuma, K. Tanaka, et al. 2000. Characterization of antiviral activity of lactoferrin against hepatitis C virus infection in human cultured cells. *Virus Research* 66 (1):51–63. doi:10.1016/S0168-1702(99)00121-5.

Inglingstad, R. A., T. G. Devold, E. K. Eriksen, H. Holm, M. Jacobsen, K. H. Liland, et al. 2010. Comparison of the digestion of caseins and whey proteins in equine, bovine, caprine and human milks by human gastrointestinal enzymes. *Dairy Science & Technology* 90 (5):549–563. doi:10.1051/dst/2010018.

Iyer, S., and B. Lönnerdal. 1993. Lactoferrin, lactoferrin receptors and iron metabolism. *European Journal of Clinical Nutrition* 47 (4):232–41.

Jenssen, H., and R. E. Hancock. 2009. Antimicrobial properties of lactoferrin. *Biochimie* 91 (1):19–29. doi:10.1016/j.biochi.2008.05.015.

Jiang, R., and B. Lönnerdal. 2016. Bovine lactoferrin and lactoferricin exert antitumor activities on human colorectal cancer cells (HT-29) by activating various signaling pathways. *Biochemistry and Cell Biology* 95 (1):99–109. doi:10.1139/bcb-2016-0094.

Jiang, R., V. Lopez, S. L. Kelleher, and B. Lönnerdal. 2011. Apo−and holo−lactoferrin are both internalized by lactoferrin receptor via clathrin−mediated endocytosis but differentially affect ERK−signaling and cell proliferation in caco−2 cells. *Journal of Cellular Physiology* 226 (11):3022–3031. doi:10.1002/jcp.22650.

Johanson, B. 1960. Isolation of an Iron containing red protein from Human milk. *Acta Chemica Scandinavica* 14 (2):510–512. doi:10.3891/acta.chem.scand.14-0510.

Junyaprasert, V. B., A. Mitrevej, N. Sinchaipanid, P. Boonme, and D. E. Wurster. 2001. Effect of process variables on the microencapsulation of vitamin A palmitate by gelatin-acacia coacervation. *Drug Development and Industrial Pharmacy* 27 (6):561–566. doi:10.1081/DDC-100105181.

Kaito, M., M. Iwasa, N. Fujita, Y. Kobayashi, Y. Kojima, J. Ikoma, et al. 2007. Effect of lactoferrin in patients with chronic hepatitis C: combination therapy with interferon and ribavirin. *Journal of gastroenterology and hepatology* 22 (11):1894–1897. doi:10.1111/j.1440-1746.2007.04858.x.

Kanwar, J. R., G. Mahidhara, K. Roy, S. Sasidharan, S. Krishnakumar, N. Prasad, et al. 2015. Fe-bLf nanoformulation targets survivin to kill colon cancer stem cells and maintains absorption of iron, calcium and zinc. *Nanomedicine* 10 (1):35–55. doi:10.2217/nnm.14.132.

Kawakami, H., M. Hiratsuka, and S. I. Dosako. 1988. Effects of iron-saturated lactoferrin on iron absorption. *Agricultural and Biological Chemistry* 52 (4):903–908.

Ke, C., Z. Lan, L. Hua, Z. Ying, X. Humina, S. Jia, et al. 2015. Iron metabolism in infants: influence of bovine lactoferrin from iron-fortified formula. *Nutrition* 31 (2):304–309. doi:10.1016/j.nut.2014.07.006.

Kehoe, S. I., B. M. Jayarao, and A. J. Heinrichs. 2007. A survey of bovine colostrum composition and colostrum management practices on Pennsylvania dairy farms. *Journal of Dairy Science* 90 (9):4108–4116. doi:10.3168/jds.2007-0040.

Khan, A. R., and P. A. N.K A. J. Taneja. 2015. Cationic Peptide Lactoferricin B inhibits glutathione S-transferase P1 from human placenta and breast cancer cell line MDA-MB-231 preventing anticancer drug metabolism. *International Journal of Pharmacy and Pharmaceutical Sciences* 7:238–241.

Kilic, E., M. V. Novoselova, S. H. Lim, N. A. Pyataev, S. I. Pinyaev, O. A. Kulikov, et al. 2017. Formulation for Oral Delivery of Lactoferrin Based on Bovine Serum Albumin and Tannic Acid Multilayer Microcapsules. *Scientific Reports* 7:44159. doi:10.1038/srep44159.

Kirkpatrick, C. H., I. Green, R. R. Rich, and A. L. Schade. 1971. Inhibition of growth of Candida albicans by iron-unsaturated lactoferrin: relation to host-defense mechanisms in chronic mucocutaneous candidiasis. *Journal of Infectious Diseases* 124 (6):539–544. doi:10.1093/infdis/124.6.539.

Kobayashi, T., H. Kakeya, T. Miyazaki, K. Izumikawa, K. Yanagihara, H. Ohno, et al. 2011. Synergistic antifungal effect of lactoferrin with azole antifungals against Candida albicans and a proposal for a new treatment method for invasive candidiasis. *Japanese Journal of Infectious Diseases* 64 (4):292–296.

Kong, F., and R. P. Singh. 2010. A human gastric simulator (HGS) to study food digestion in human stomach. *Journal of Food Science* 75 (9):E627–E635. doi:10.1111/j.1750-3841.2010.01856.x.

Konuspayeva, G., B. Faye, G. Loiseau, and D. Levieux. 2007. Lactoferrin and immunoglobulin contents in camel's milk (Camelus bactrianus, Camelus dromedarius, and hybrids) from Kazakhstan. *Journal of Dairy Science* 90 (1):38–46. doi:10.3168/jds.S0022-0302(07)72606-1.

Kuwata, H., K. Yamauchi, S. Teraguchi, Y. Ushida, Y. Shimokawa, T. Toida, and H. Hayasawa. 2001. Functional fragments of ingested lactoferrin are resistant to proteolytic degradation in the gastrointestinal tract of adult rats. *The Journal of Nutrition* 131 (8):2121–2127.

Kuwata, H., T. T. Yip, M. Tomita, and T. W. Hutchens. 1998. Direct evidence of the generation in human stomach of an antimicrobial peptide domain (lactoferricin) from ingested lactoferrin. *Biochimica et Biophysica Acta (BBA)-Protein Structure and Molecular Enzymology* 1429 (1):129–141. doi:10.1016/S0167-4838(98)00224-6.

Lai, Y. W., L. T. Campbell, M. R. Wilkins, C. N. I. Pang, S. Chen, and D. A. Carter. 2016. Synergy and antagonism between iron chelators and antifungal drugs in Cryptococcus. *International Journal of Antimicrobial Agents* 48 (4):388–394. doi:10.1016/j.ijantimicag.2016.06.012.

Lambert, L. A., H. Perri, and T. J. Meehan. 2005. Evolution of duplications in the transferrin family of proteins. *Comparative Biochemistry and Physiology Part B: Biochemistry and Molecular Biology* 140 (1):11–25. doi:10.1016/j.cbpc.2004.09.012.

Law, B. A., and B. Reiter. 1977. The isolation and bacteriostatic properties of lactoferrin from bovine milk whey. *Journal of Dairy Research* 44 (03):595–599. doi:10.1017/S0022029900020550.

Lee, H. Y., J. H. Park, S. H. Seok, M. W. Baek, D. J. Kim, B. H. Lee, et al. 2005. Potential antimicrobial effects of human lactoferrin against oral infection with Listeria monocytogenes in mice. *Journal of Medical Microbiology* 54 (11):1049–1054. doi:10.1099/jmm.0.45918-0.

Legrand, D. 2016. Overview of Lactoferrin as a Natural Immune Modulator. *The Journal of Pediatrics* 173:S10–S15. doi:10.1016/j.jpeds.2016.02.071.

Leitch, E. C., and M. D. P. Willcox. 1999. Elucidation of the antistaphylococcal action of lactoferrin and lysozyme. *Journal of Medical Microbiology* 48 (9):867–871. doi:10.1099/00222615-48-9-867.

Li, Q., and Z. Zhao. 2017. Formation of lactoferrin/sodium caseinate complexes and their adsorption behaviour at the air/water interface. *Food Chemistry* 232:697–703. doi:10.1016/j.foodchem.2017.04.072.

Liao, Y., R. Jiang, and B. Lönnerdal. 2012. Biochemical and molecular impacts of lactoferrin on small intestinal growth and development during early life. *Biochemistry and Cell Biology* 90 (3):476–484. doi:10.1139/o11-075.

Lin, T. Y., C. Chu, and C. H. Chiu. 2002. Lactoferrin inhibits enterovirus infection of human embryonal rhabdomyosarcoma cells in vitro. *Journal of Infectious Diseases* 186 (8):1161–1164. doi:10.1086/343809.

Liu, W., A. Ye, W. Liu, C. Liu, and H. Singh. 2013. Stability during in vitro digestion of lactoferrin-loaded liposomes prepared from milk fat globule membrane-derived phospholipids. *Journal of Dairy Science* 96 (4):2061–2070. doi:10.3168/jds.2012-6072.

Lizzi, A. R., V. Carnicelli, M. M. Clarkson, C. Nazzicone, B. Segatore, G. Celenza, et al. 2016. Bovine lactoferrin and its tryptic peptides: Antibacterial activity against different species. *Applied Biochemistry and Microbiology* 52 (4):435––440. doi:10.1134/S0003683816040116.

Lönnerdal, B. 2016. Bioactive proteins in human milk: health, nutrition, and implications for infant formulas. *The Journal of Pediatrics* 173:S4–S9. doi:10.1016/j.jpeds.2016.02.070.

Lönnerdal, B., M. K. Georgieff, and O. Hernell. 2015. Developmental physiology of iron absorption, homeostasis and metabolism in the healthy term infant. *The Journal of Pediatrics* 167 (40):S8. doi:10.1016/j.jpeds.2015.07.014.

Lopez, A., P. Cacoub, I. C. Macdougall, and L. Peyrin-Biroulet. 2016. Iron deficiency anaemia. *The Lancet* 387 (10021):907–916. doi:10.1016/S0140-6736(15)60865-0.

MacManus, C. F., C. B. Collins, T. T. Nguyen, R. W. Alfano, P. Jedlicka, and E. F. de Zoeten. 2017. VEN-120, a Recombinant Human Lactoferrin, Promotes a Regulatory T Cell [Treg] Phenotype and Drives Resolution of Inflammation in Distinct Murine Models of Inflammatory Bowel Disease. *Journal of Crohn's and Colitis* 11 (9):1101–1112. doi:10.1093/ecco-jcc/jjx056.

Marchetti, M., F. Superti, M. G. Ammendolia, P. Rossi, P. Valenti, and L. Seganti. 1999. Inhibition of poliovirus type 1 infection by iron-, manganese-and zinc-saturated lactoferrin. *Medical Microbiology and Immunology* 187 (4):199–204. doi:10.1007/s004300050093.

Mezhericher, M., A. Levy, and I. Borde. 2007. Theoretical drying model of single droplets containing insoluble or dissolved solids. *Drying Technology* 25 (6):1025–1032. doi:10.1080/07373930701394902.

Montagne, P., M. L. Cuilliere, C. Mole, M. C. Bene, and G. Faure. 2001. Changes in lactoferrin and lysozyme levels in human milk during the first twelve weeks of lactation. In D.S. Newburg(Ed.), *Bioactive Components of Human Milk* (pp. 241–247). New York, US, Springer.

Moore, S. A., B. F. Anderson, C. R. Groom, M. Haridas, and E. N. Baker. 1997. Three-dimensional structure of diferric bovine lactoferrin at 2.8 Å resolution. *Journal of Molecular Biology* 274 (2):222–236. doi:10.1006/jmbi.1997.1386.

Nevison, C. D. 2014. A comparison of temporal trends in United States autism prevalence to trends in suspected environmental factors. *Environmental Health* 13 (1):73. doi:10.1186/1476-069X-13-73.

Nguyen, D. N., P. Jiang, A. Stensballe, E. Bendixen, P. T. Sangild, and D. E. Chatterton. 2016. Bovine lactoferrin regulates cell survival, apoptosis and inflammation in intestinal epithelial cells and preterm pig intestine. *Journal of Proteomics* 139:95–102. doi:10.1016/j.jprot.2016.03.020.

Nojima, Y., Y. Suzuki, K. Iguchi, T. Shiga, A. Iwata, T. Fujimoto, et al. 2008. Development of poly (ethylene glycol) conjugated lactoferrin for oral administration. *Bioconjugate Chemistry* 19 (11):2253–2259. doi:10.1021/bc800258v.

Nojima, Y., Y. Suzuki, K. Yoshida, F. Abe, T. Shiga, T. Takeuchi, et al. 2009. Lactoferrin conjugated with 40-kDa branched poly (ethylene glycol) has an improved circulating half-life. *Pharmaceutical Research* 26 (9):2125–2132. doi:10.1007/s11095-009-9925-z.

Norrby, K., I. Mattsby−Baltzer, M. Innocenti, and S. Tuneberg. 2001. Orally administered bovine lactoferrin systemically inhibits VEGF165−mediated angiogenesis in the rat. *International Journal of Cancer* 91 (2):236–240. doi:10.1002/1097-0215(200002)9999:9999%3c::AID-IJC1024%3e3.3.CO;2-K.

Ochoa, T. J., and T. G. Cleary. 2009. Effect of lactoferrin on enteric pathogens. *Biochimie* 91 (1):30–34. doi:10.1016/j.biochi.2008.04.006.

Oho, T., M. Mitoma, and T. Koga. 2002. Functional domain of bovine milk lactoferrin which inhibits the adherence of Streptococcus mutans cells to a salivary film. *Infection and Immunity* 70 (9):5279–5282. doi:10.1128/IAI.70.9.5279-5282.2002.

Orsi, N. 2004. The antimicrobial activity of lactoferrin: current status and perspectives. *Biometals* 17 (3):189–196. doi:10.1023/B:BIOM.0000027691.86757.e2.

Ostan, N. K., R. H. Yu, D. Ng, C. C. L. Lai, A. K. Pogoutse, V. Sarpe, et al. 2017. Lactoferrin binding protein B–a bi-functional bacterial receptor protein. *PLoS Pathogens* 13 (3):e1006244. doi:10.1371/journal.ppat.1006244.

Özer, B. H., and H. A. Kirmaci. 2010. Functional milks and dairy beverages. *International Journal of Dairy Technology* 63 (1):1–15. doi:10.1111/j.1471-0307.2009.00547.x.

Paesano, R., F. Berlutti, M. Pietropaoli, F. Pantanella, E. Pacifici, W. Goolsbee, and P. Valenti. 2010. Lactoferrin efficacy versus ferrous sulfate in curing iron deficiency and iron deficiency anemia in pregnant women. *Biometals* 23 (3):411–417. doi:10.1007/s10534-010-9335-z.

Paulsson, M. A., U. Svensson, A. R. Kishore, and A. S. Naidu. 1993. Thermal behavior of bovine lactoferrin in water and its relation to bacterial interaction and antibacterial activity. *Journal of Dairy Science* 76 (12):3711–3720. doi:10.3168/jds.S0022-0302(93)77713-9.

Peters, B. H., L. Staels, J. Rantanen, F. Molnár, T. De Beer, V. P. Lehto, and J. Ketolainen. 2016. Effects of cooling rate in microscale and pilot scale freeze-drying–Variations in excipient polymorphs and protein secondary structure. *European Journal of Pharmaceutical Sciences* 95:72–81. doi:10.1016/j.ejps.2016.05.020.

Pfefferkorn, M. D., J. H. Boone, J. T. Nguyen, B. E. Juliar, M. A. Davis, and K. K. Parker. 2010. Utility of fecal lactoferrin in identifying Crohn disease activity in children. *Journal of Pediatric Gastroenterology and Nutrition* 51 (4):425–428. doi:10.1097/MPG.0b013e3181d67e8f.

Phaniendra, A., D. B. Jestadi, and L. Periyasamy. 2015. Free radicals: properties, sources, targets, and their implication in various diseases. *Indian Journal of Clinical Biochemistry* 30 (1):11–26. doi:10.1007/s12291-014-0446-0.

Privalov, P. L., and N. N. Khechinashvili. 1974. A thermodynamic approach to the problem of stabilization of globular protein structure: a calorimetric study. *Journal of Molecular Biology* 86 (3):665–684. doi:10.1016/0022-2836(74)90188-0.

Rastogi, N., A. Singh, P. K. Singh, T. K. Tyagi, S. Pandey, K. Shin, et al. 2016. Structure of iron saturated C−lobe of bovine lactoferrin at pH 6.8 indicates a weakening of iron coordination. *Proteins: Structure, Function, and Bioinformatics* 84 (5):591–599. doi:10.1002/prot.25004.

Rezk, M., M. Kandil, R. Dawood, A. E. Shaheen, and A. Allam. 2015. Oral lactoferrin versus ferrous sulphate and ferrous fumerate for the treatment of iron deficiency anemia during pregnancy. *Journal of Advanced Nutrition and Human Metabolism* 1.

Rodriguez-Franco, D. A., L. Vazquez-Moreno, and M. G. Ramos-Clamont. 2004. Antimicrobial mechanisms and potential clinical application of lactoferrin. *Revista Latinoamericana de Microbiologia* 47 (3-4):102–111.

Rogan, M. P., C. C. Taggart, C. M. Greene, P. G. Murphy, S. J. O'neill, and N. G. McElvaney. 2004. Loss of microbicidal activity and increased formation of biofilm due to decreased lactoferrin activity in patients with cystic fibrosis. *Journal of Infectious Diseases* 190 (7):1245–1253. doi:10.1086/423821.

Rollo, D. E., P. G. Radmacher, R. M. Turcu, S. R. Myers, and D. H. Adamkin. 2014. Stability of lactoferrin in stored human milk. *Journal of Perinatology* 34 (4):284–286. doi:10.1038/jp.2014.3.

Sagel, S. D., M. K. Sontag, and F. J. Accurso. 2009. Relationship between antimicrobial proteins and airway inflammation and infection in cystic fibrosis. *Pediatric Pulmonology* 44 (4):402–409. doi:10.1002/ppul.21028.

Saito, H., H. Miyakawa, Y. Tamura, S. Shimamura, and M. Tomita. 1991. Potent bactericidal activity of bovine lactoferrin hydrolysate produced by heat treatment at acidic pH. *Journal of Dairy Science* 74 (11):3724–3730. doi:10.3168/jds.S0022-0302(91)78563-9.

Sánchez, L., M. Calvo, and J. H. Brock. 1992a. Biological role of lactoferrin. *Archives of Disease in Childhood* 67 (5):657. doi:10.1136/adc.67.5.657.

Sánchez, L., J. M. Peiro, H. Castillo, M. D. Perez, J. M. Ena, and M. Calvo. 1992b. Kinetic parameters for denaturation of bovine milk lactoferrin. *Journal of Food Science* 57 (4):873–879. doi:10.1111/j.1365-2621.1992.tb14313.x.

Scarino, M. L. 2007. A sideways glance: Take it or leave it? The role of lactoferrin in iron sequestration and delivery within the body. *Genes & Nutrition* 2 (2):161–162. doi:10.1007/s12263-007-0054-1.

Seganti, L., A. M. Di Biase, M. Marchetti, A. Pietrantoni, A. Tinari, and F. Superti. 2004. Antiviral activity of lactoferrin towards naked viruses. *Biometals* 17 (3):295–299. doi:10.1023/B:BIOM.0000027708.27142.bc.

Sharbafi, R., F. Moradian, A. R. Rafiei, and A. Barzegar. 2011. Isolation and purification of Bovine lactoferrin. *Journal of Mazandaran University of Medical Sciences* 21 (84):44–51.

Sharma, S., M. Sinha, S. Kaushik, P. Kaur, and T. P. Singh. 2013. C-lobe of lactoferrin: the whole story of the half-molecule. *Biochemistry Research International*. doi:10.1155/2013/271641.

Sherman, M. P., C. J. Pritzl, C. Xia, M. M. Miller, H. Zaghouani, and B. Hahm. 2015. Lactoferrin acts as an adjuvant during influenza vaccination of neonatal mice. *Biochemical and Biophysical Research Communications* 467 (4):766–770. doi:10.1016/j.bbrc.2015.10.067.

Shimizu, K., H. Matsuzawa, K. Okada, S. Tazume, S. Dosako, Y. Kawasaki, et al. 1996. Lactoferrin-mediated protection of the host from murine cytomegalovirus infection by a T-cell-dependent augmentation of natural killer cell activity. *Archives of Virology* 141 (10):1875–1889. doi:10.1007/BF01718201.

Shimoni, G., C. S. Levi, S. L. Tal, and U. Lesmes. 2013. Emulsions stabilization by lactoferrin nano-particles under in vitro digestion conditions. *Food Hydrocolloids* 33 (2):264–272. doi:10.1016/j.foodhyd.2013.03.017.

Shin, K., K. Yaegaki, T. Murata, H. Ii, T. Tanaka, I. Aoyama, et al. 2011. Effects of a composition containing lactoferrin and lactoperoxidase on oral malodor and salivary bacteria: a randomized, double-blind, crossover, placebo-controlled clinical trial. *Clinical Oral Investigations* 15 (4):485–493. doi:10.1007/s00784-010-0422-x.

Sijbrandij, T., A. J. Ligtenberg, K. Nazmi, E. C. Veerman, J. G. Bolscher, and F. J. Bikker. 2017. Effects of lactoferrin derived peptides on simulants of biological warfare agents. *World Journal of Microbiology and Biotechnology* 33 (1):3. doi:10.1007/s11274-016-2171-8.

Sorensen, M., and S. Sorensen. 1940. The proteins in whey. *Compte rendu des Travaux du Laboratoire de Carlsberg Ser. Chim* 23:55–99.

Spik, G., B. Brunet, D. C. Mazurier, G. Fontaine, and J. Montreuil. 1982. Characterization and properties of the human and bovine lactotransferrins extracted from the faeces of newborn infants. *Acta Paediatrica* 71 (6):979–985. doi:10.1111/j.1651-2227.1982.tb09560.x.

Spik, G., B. Coddeville, J. Mazurier, Y. Bourne, C. Cambillaut, and J. Montreuil. 1994. Primary and three-dimensional structure of lactotransferrin (lactoferrin) glycans. In T.W. Hutchens, S.V. Rumball and B. Lönnerdal(Ed.), *Lactoferrin* (pp. 21–32). New York, US: Springer.

Sreedhara, A., R. Flengsrud, V. Prakash, D. Krowarsch, T. Langsrud, P. Kaul, et al. 2010. A comparison of effects of pH on the thermal stability and conformation of caprine and bovine lactoferrin. *International Dairy Journal* 20 (7):487–494. doi:10.1016/j.idairyj.2010.02.003.

Stănciuc, N., I. Aprodu, G. Râpeanu, I. Van der Plancken, G. Bahrim, and M. Hendrickx. 2013. Analysis of the thermally induced structural changes of bovine lactoferrin. *Journal of Agricultural and Food Chemistry* 61 (9):2234–2243. doi:10.1021/jf305178s.

Steijns, J. M., and A. C. M. Van Hooijdonk. 2000. Occurrence, structure, biochemical properties and technological characteristics of lactoferrin. *British Journal of Nutrition* 84 (S1):11–17. doi:10.1017/S0007114500002191.

Sui, Q., H. Roginski, R. P. Williams, C. Versteeg, and J. Wan. 2010. Effect of pulsed electric field and thermal treatment on the physicochemical properties of lactoferrin with different iron saturation levels. *International Dairy Journal* 20 (10):707–714. doi:10.1016/j.idairyj.2010.03.013.

Superti, F., M. G. Ammendolia, P. Valenti, and L. Seganti. 1997. Antirotaviral activity of milk proteins: lactoferrin prevents rotavirus infection in the enterocyte-like cell line HT-29. *Medical Microbiology and Immunology* 186 (2):83–91. doi:10.1007/s004300050049.

Takakura, N., H. Wakabayashi, H. Ishibashi, S. Teraguchi, Y. Tamura, H. Yamaguchi, and S. Abe. 2003. Oral lactoferrin treatment of experimental oral candidiasis in mice. *Antimicrobial Agents and Chemotherapy* 47 (8):2619–2623. doi:10.1128/AAC.47.8.2619-2623.2003.

Takeuchi, T., T. Jyonotsuka, N. Kamemori, G. Kawano, H. Shimizu, K. Ando, and E. Harada. 2006. Enteric−formulated lactoferrin was more effectively transported into blood circulation from gastrointestinal tract in adult rats. *Experimental Physiology* 91 (6):1033–1040. doi:10.1113/expphysiol.2006.034876.

Tang, Y. M., D. G. Wang, J. Li, X. H. Li, Q. Wang, N. Liu, et al. 2016. Relationships between micronutrient losses in sweat and blood pressure among heat-exposed steelworkers. *Industrial Health* 54 (3):215–223. doi:10.2486/indhealth.2014-0225.

Timilsena, Y. P., R. Adhikari, C. J. Barrow, and B. Adhikari. 2017. Digestion behaviour of chia seed oil encapsulated in chia seed protein-gum complex coacervates. *Food Hydrocolloids* 66:71–81. doi:10.1016/j.foodhyd.2016.12.017.

Tomita, M., H. Wakabayashi, K. Yamauchi, S. Teraguchi, and H. Hayasawa. 2002. Bovine lactoferrin and lactoferricin derived from milk: production and applications. *Biochemistry and Cell Biology* 80 (1):109–112. doi:10.1139/o01-230.

Tomita, M., H. Wakabayashi, K. Shin, K. Yamauchi, T. Yaeshima, and K. Iwatsuki. 2009. Twenty-five years of research on bovine lactoferrin applications. *Biochimie* 91:52–57. doi:10.1016/j.biochi.2008.05.021.

Troost, F. J., J. Steijns, W. H. Saris, and R. J. M. Brummer. 2001. Gastric digestion of bovine lactoferrin in vivo in adults. *The Journal of Nutrition* 131 (8):2101–2104.

Troost, F. J., W. H. Saris, and R. J. M. Brummer. 2002. Orally ingested human lactoferrin is digested and secreted in the upper gastrointestinal tract in vivo in women with ileostomies. *The Journal of Nutrition* 132 (9):2597–2600.

Tsioulpas, A., M. J. Lewis, and A. S. Grandison. 2007. A study of the pH of individual milk samples. *International Journal of Dairy Technology* 60 (2):96–97. doi:10.1111/j.1471-0307.2007.00308.x.

Tung, Y. T., H. L. Chen, C. C. Yen, P. Y. Lee, H. C. Tsai, M. F. Lin, and C. M. Chen. 2013. Bovine lactoferrin inhibits lung cancer growth through suppression of both inflammation and expression of vascular endothelial growth factor. *Journal of Dairy Science* 96 (4):2095–2106. doi:10.3168/jds.2012-6153.

Valenti, P., A. Frioni, A. Rossi, S. Ranucci, I. De Fino, A. Cutone, et al. 2016. Aerosolized bovine lactoferrin reduces neutrophils and pro-inflammatory cytokines in mouse models of Pseudomonas aeruginosa lung infections. *Biochemistry and Cell Biology* 95 (1):41–47. doi:10.1139/bcb-2016-0050.

van Berkel, P. H., M. E. Geerts, and J. H. Nuijens. 1996. Heterogeneity in utilization of N-glycosylation sites Asn624 and Asn138 in human lactoferrin: a study with glycosylation-site mutants. *Biochemical Journal* 319 (1):117–122. doi:10.1042/bj3190117.

van Berkel, P. H., E. M. Geerts, A. H. van veen, M. Mericskay, A. H. de Boer, and H. J. Nuijens. 1997. N-terminal stretch Arg2, Arg3, Arg4 and Arg5 of human lactoferrin is essential for binding to heparin, bacterial lipopolysaccharide, human lysozyme and DNA. *Biochemical Journal* 328 (1):145–151. doi:10.1042/bj3280145.

van der Kraan, M. I., J. Groenink, K. Nazmi, E. C. Veerman, J. G. Bolscher, and A. V. N. Amerongen. 2004. Lactoferrampin: a novel antimicrobial peptide in the N1-domain of bovine lactoferrin. *Peptides* 25 (2):177–183. doi:10.1016/j.peptides.2003.12.006.

van der Strate, B. W. A., L. Beljaars, G. Molema, M. C. Harmsen, and D. K. F. Meijer. 2001. Antiviral activities of lactoferrin. *Antiviral Research* 52 (3):225–239. doi:10.1016/S0166-3542(01)00195-4.

van Veen, H. A., M. E. Geerts, P. H. van Berkel, and J. H. Nuijens. 2004. The role of N−linked glycosylation in the protection of human and bovine lactoferrin against tryptic proteolysis. *European Journal of Biochemistry* 271 (4):678–684. doi:10.1111/j.1432-1033.2003.03965.x.

Valenti, P., and G. Antonini. 2005. Lactoferrin: An important host defence against microbial and viral attack. *Cellular and Molecular Life Sciences* 62 (22):2576–87. doi:10.1007/s00018-005-5372-0.

Venkatesh, M. P., and L. Rong. 2008. Human recombinant lactoferrin acts synergistically with antimicrobials commonly used in neonatal practice against coagulase-negative staphylococci and Candida albicans causing neonatal sepsis. *Journal of Medical Microbiology* 57 (9):1113–1121. doi:10.1099/jmm.0.2008/001263-0.

Vogel, H. J. 2012. Lactoferrin, a bird's eye view. *Biochemistry and Cell Biology* 90 (3):233–244. doi:10.1139/o2012-016.

Voswinkel, L., T. Vogel, and U. Kulozik. 2016. Impact of the iron saturation of bovine lactoferrin on adsorption to a strong cation exchanger membrane. *International Dairy Journal* 56:134–140. doi:10.1016/j.idairyj.2016.01.008.

Wada, T., Y. Aiba, K. Shimizu, A. Takagi, T. Miwa, and Y. Koga. 1999. The therapeutic effect of bovine lactoferrin in the host infected with Helicobacter pylori. *Scandinavian Journal of Gastroenterology* 34 (3):238–243. doi:10.1080/00365529950173627.

Wakabayashi, H., S. Abe, S. Teraguchi, H. Hayasawa, and H. Yamaguchi. 1998. Inhibition of hyphal growth of azole-resistant strains of Candida albicans by triazole antifungal agents in the presence of lactoferrin-related compounds. *Antimicrobial Agents and Chemotherapy* 42 (7):1587–1591.

Wang, B., Y. P. Timilsena, E. Blanch, and B. Adhikari. 2017a. Mild thermal treatment and in-vitro digestion of three forms of bovine lactoferrin: Effects on functional properties. *International Dairy Journal* 64:22–30. doi:10.1016/j.idairyj.2016.09.001.

Wang, B., Y. P. Timilsena, E. Blanch, and B. Adhikari. 2017b. Characteristics of bovine lactoferrin powders produced through spray and freeze drying processes. *International Journal of Biological Macromolecules* 95:985–994. doi:10.1016/j.ijbiomac.2016.10.087.

Wang, B., Y. P. Timilsena, E. Blanch, and B. Adhikari. 2017c. Drying and denaturation characteristics of three forms of bovine lactoferrin. *Drying Technology* 5:606–615. doi:10.1080/07373937.2016.1196699.

Wang, W. Y., J. H. Wong, D. T. M. Ip, D. C. C. Wan, R. C. Cheung, and T. B. Ng. 2016. Bovine Lactoferrampin, Human Lactoferricin, and Lactoferrin 1–11 Inhibit Nuclear Translocation of HIV Integrase. *Applied Biochemistry and Biotechnology* 179 (7):1202–1212. doi:10.1007/s12010-016-2059-y.

Wei, Z., T. Nishimura, and S. Yoshida. 2000. Presence of a glycan at a potential N-glycosylation site, Asn-281, of bovine lactoferrin. *Journal of Dairy Science* 83 (4):683–689. doi:10.3168/jds.S0022-0302(00)74929-0.

Wiesner, J., and A. Vilcinskas. 2010. Antimicrobial peptides: the ancient arm of the human immune system. *Virulence* 1 (5):440–464. doi:10.4161/viru.1.5.12983.

Wolf, J. S., G. Li, A. Varadhachary, K. Petrak, M. Schneyer, D. Li, et al. 2007. Oral lactoferrin results in T cell–dependent tumor inhibition of head and neck squamous cell carcinoma in vivo. *Clinical Cancer Research* 13 (5):1601–1610. doi:10.1158/1078-0432.CCR-06-2008.

Yamano, E., M. Miyauchi, H. Furusyo, A. Kawazoe, A. Ishikado, T. Makino, et al. 2010. Inhibitory effects of orally administrated liposomal bovine lactoferrin on the LPS-induced osteoclastogenesis. *Laboratory Investigation* 90 (8):1236–1246. doi:10.1038/labinvest.2010.80.

Yao, X., C. Bunt, J. Cornish, S. Y. Quek, and J. Wen. 2013. Oral delivery of lactoferrin: a review. *International Journal of Peptide Research and Therapeutics* 19 (2):125–134. doi:10.1007/s10989-012-9326-8.

Yao, X., C. Bunt, J. Cornish, S. Y. Quek, and J. Wen. 2014. Stability of bovine lactoferrin in luminal extracts and mucosal homogenates from rat intestine: a prelude to oral absorption. *Chemical Biology & Drug Design* 84 (6):676–684. doi:10.1111/cbdd.12360.

Yao, X., C. Bunt, J. Cornish, S. Y. Quek, and J. Wen. 2015. Oral Delivery of Bovine Lactoferrin Using Pectin−and Chitosan−Modified Liposomes and Solid Lipid Particles: Improvement of Stability of Lactoferrin. *Chemical Biology & Drug Design* 86 (4):466–475. doi:10.1111/cbdd.12509.

Yeo, Y., E. Bellas, W. Firestone, R. Langer, and D. S. Kohane. 2005. Complex coacervates for thermally sensitive controlled release of flavor compounds. *Journal of Agricultural and Food Chemistry* 53 (19):7518–7525. doi:10.1021/jf0507947.

Yoshida, S., Z. Wei, Y. Shinmura, and N. Fukunaga. 2000. Separation of lactoferrin-a and-b from bovine colostrum. *Journal of Dairy Science* 83 (10):2211–2215. doi:10.3168/jds.S0022-0302(00)75104-6.

Yount, N. Y., M. T. Andrés, J. F. Fierro, and M. R. Yeaman. 2007. The γ-core motif correlates with antimicrobial activity in cysteine-containing kaliocin-1 originating from transferrins. *Biochimica et Biophysica Acta (BBA)-Biomembranes* 1768 (11):2862–2872. doi:10.1016/j.bbamem.2007.07.024.

Zarember, K. A., J. A. Sugui, Y. C. Chang, K. J. Kwon-Chung, and J. I. Gallin. 2007. Human polymorphonuclear leukocytes inhibit Aspergillus fumigatus conidial growth by lactoferrin-mediated iron depletion. *The Journal of Immunology* 178 (10):6367–6373. doi:10.4049/jimmunol.178.10.6367.

Zhang, Y., X. Wang, Y. Qiu, J. Cornish, A. J. Carr, and Z. Xia. 2014. Effect of indomethacin and lactoferrin on human tenocyte proliferation and collagen formation in vitro. *Biochemical and Biophysical Research Communications* 454 (2):301–307. doi:10.1016/j.bbrc.2014.10.061.

CHAPTER 3

Drying and Denaturation Characteristics of Lactoferrin

Published in *Drying Technology*, 2017, 35(5), 606-615

DRYING TECHNOLOGY
2017, VOL. 35, NO. 5, 606–615
http://dx.doi.org/10.1080/07373937.2016.1196699

Taylor & Francis
Taylor & Francis Group

Drying and denaturation characteristics of three forms of bovine lactoferrin

Bo Wang[a], Yakindra Prasad Timilsena[a,b], Ewan Blanch[a], and Benu Adhikari[a,b]

[a]School of Applied Sciences, RMIT University, Melbourne, Victoria, Australia; [b]CSIRO Manufacturing Flagship, Clayton South, Victoria, Australia

ABSTRACT

The drying and denaturation characteristics of native, iron-depleted (apo-), and iron-saturated (holo-)lactoferrin (LF) were studied in convective air-drying (CD) process using single droplet drying. The extent of loss of LF due to denaturation and changes in the secondary structures during CD and isothermal water heating (IHT) were measured. The holo-LF was found to be most stable among these three forms both at 70 and 95°C. The apo-LF was the least stable compared to other two. The secondary structural features of LF were altered to significantly higher extent when subjected to IHT than to CD both at 70 and 95°C. Holo-LF should be preferred when producing LF powder through a convective drying process.

KEYWORDS

Bovine lactoferrin; denaturation; drying kinetics; iron binding; secondary structure

Introduction

Lactoferrin (LF) is a single polypeptide chain protein commonly found in milk, tear, saliva, peripheral fluid, and the like. It consists of ~ 700 amino acids and the molecular weight of LF is about 80 kDa.[1] The polypeptide chain is folded into two symmetrical lobes (the N-lobe and C-lobe). Each lobe can bind one metal ion (e.g., iron, copper, zinc, or manganese). Because of its ability to reversibly bind Fe^{3+}, LF can exist in three different forms in terms of iron saturation. One molecule of LF can bind two molecules of iron; thus, the fully iron-saturated LF or holo LF (holo-LF) contains one iron molecule in each lobe. A LF molecule containing only one iron molecule in its structures is monoferric LF. The LF molecule not containing iron in its structure is called apo LF (apo-LF). The native form of LF (native-LF) is a mixture of these three different forms.[2–4] In general, native form of LF extracted from bovine milk is salmon pink in color with 15–20% iron saturation.[5] Apo-LF can be found in breast milk with less than 5% iron saturation,[5] whereas the iron-saturated holo-LF is rare and not commercially available yet.

Besides its well-known metal-binding abilities, LF possesses antibacterial, anticancer, immunomodulatory, and anti-inflammatory properties which are highly dependent on its unique structure.[6–8] The iron-binding property of LF helps in promoting intestinal absorption of iron from the food. The LF obtained from human, bovine, and caprine milk is very similar in characteristics.[9,10] So far, bovine LF is the only LF widely available commercially.[11]

Lactoferrin in liquid form has a very short storage life of the order of 4 weeks.[12] One of the most preferred methods of extending the shelf life of LF is to convert it into powder which can be achieved by freeze and spray drying. Although spray drying is commonly used industrial method of producing food proteins,[13] it has not been used, except in limited cases, to produce LF powders in commercial scale.

Thermal, interfacial, and rapid evaporation-related stresses encountered by proteins during spray drying can alter secondary and higher structural conformation and ultimately affect the functional attributes of the protein powders. Several researchers have studied thermally induced denaturation of LF, in liquid form, using differential scanning calorimetry.[14,15] It has been reported that native form of bovine LF has two denaturation temperatures: One around 60°C and the other around 90°C, corresponding to apo and holo forms, respectively.[14,15] The higher denaturation temperature of holo-LF is attributed to its more compact conformation formed due to binding with iron.[14,15] It was also reported that the binding of iron by LF only affects the tertiary structure but keeps the secondary structure unchanged.[15] The effects of convective drying processes such as spray drying on structure and function of LF are not researched and the extent and nature of changes in its structural configuration, that is, denaturation, are not adequately reported. The quantification of nature and extent of denaturation of LF in convective drying environment are expected to provide further insights into the effect of these changes on its biofunctionality.

CONTACT Benu Adhikari benu.adhikari@rmit.edu.au School of Applied Sciences, RMIT University, Melbourne, VIC 3083, Australia.

Owing to the difficulty of measuring drying kinetics in situ in the spray drying process, single droplet drying (SDD) is frequently used to simulate the spray drying process. SDD allows measurement of denaturation and drying kinetics and morphological changes fairly and conveniently.[16–19] In SDD, a single droplet is dried under controlled air conditions (air velocity, relative humidity) mimicking spray drying environment to the extent it is practically possible extent.[18] Although it has not been possible to date to measure the drying kinetics of a droplet in size range prevailing in spray drying operation; however, SDD does offer a practical and direct way of measuring the rate of drying and morphological changes that occur at droplet/particle level within the practical limitation. The drying kinetics data and morphological features obtained from SDD studies are used as a basis for validation of mathematical models and provide understanding of heat and mass transfer processes in droplets subjected to spray drying. The changes in the secondary and tertiary structure of proteins have been studied using spectroscopic methods such as Fourier-transform infrared spectroscopy (FTIR) and circular dichroism (CD).[20–22]

In this manuscript, we aimed to study the drying and denaturation characteristics of three different forms of LF (native-, apo-, and holo-LF) in convective air-drying environments. We also compared the denaturation of these three LF forms in air-drying and isothermal solution heating at the same medium temperature. CD spectroscopic method was used to quantify and explain the alteration in the secondary structure of these three forms of LF. The findings of this study will pave way for successful conversion of LF into powder form using industrial spray drying. As spray drying is cheaper option than the industrial freeze drying, it will help make LF more commonly available for food and pharmaceutical applications.

Materials and methods

Materials

Bovine LF was donated by Tatura Milk Industries Ltd. (Subsidiary of Bega Cheese, Victora, Australia). All the chemicals including nitrilotriacetic acid (≥99% purity), ferric nitrate nanohydrate (≥98% purity), sodium phosphate (≥96% purity), ethylenediaminetetraacetic acid (≥99% purity), trifluoroacetic acid (TFA; Purris p.a., for high performance liquid chromatography [HPLC], ≥99% purity) were purchased from Sigma-Aldrich (NSW, Australia). Pierce™ BCA protein assay kit was obtained from Thermo Scientific (Victoria, Australia). All the chemicals used were of analytical grade and were used as received.

Preparation of apo and holo forms of LF

Holo-LF was prepared from native-LF according to the method described by Bokkhim et al.[15] For this, 20 mg/ml native-LF was dissolved in citrate/phosphate buffer (pH 7.4). It was then mixed with freshly prepared ferric nitrilotriacetic acid (FeNTA) solution prepared by mixing 9.9 mM ferric nitrate and 8.5 mM nitrilotriacetic acid in Milli-Q water. The pH of this solution was adjusted to 7.4 with sodium bicarbonate. The LF and FeNTA solutions were mixed to achieve an iron-to-LF molar ratio of 2:1 to fully saturated LF with iron. This LF–FeNTA blend was incubated at ambient temperature for 1 h. It was then dialyzed using a cellulose membrane against Milli-Q water for 48 h under constant stirring with frequent changes of water. Apo-LF was prepared according to the method given by Mazurier and Spik.[23] For this, 20 mg/ml native-LF was dissolved in phosphate buffer containing 40 mM ethylenediaminetetraacetic acid (EDTA) and 0.2 M sodium phosphate at pH 4.0. This solution was equilibrated overnight and then dialyzed for 2 days against Mili-Q water with frequent changes of water. Both apo-LF and holo-LF samples were converted to powder using a laboratory-scale freeze-dryer (Advantage Pro, Scitek, NSW, Australia). The samples were prefrozen at −30°C for 24 h followed by primary drying at 0°C for 12 h and secondary drying at 20°C for 6 h. The collector temperature of −50°C and a vacuum of 16 Pa were maintained in the drying chamber. The samples were dried until the sample temperature reached the shelf temperature (20°C). To compare the effect of freeze drying on the structure and functionality, the native liquid LF was also freeze dried using the same protocol. The yields of holo-LF and apo-LF were 91% (w/w) and 93% (w/w) of the initial mass of native-LF, respectively.

The amount of iron was estimated by the ratios of absorbance at 280 and 466 nm (A_{280}/A_{466}) using UV–Vis spectrophotometer (Cary 60, Agilent Technology, Australia) according to the previously reported method.[24] The protein content was determined by BCA protein assay method. The moisture content was determined using AOAC standard method 925.10. The molecular weight patterns of these three forms of LF were determined using sodium dodecyl polyacrylamide gel electrophoresis.

Isothermal heat treatment

Hundred milligrams each of three forms of LF were dissolved in 2 ml Milli-Q water and 1 ml of this solution was taken in two 2-ml centrifuge tubes. These tubes were then heated for 10 min in water baths maintained

at 70 and 95°C. Microthermocouples were inserted into an additional tube containing the same amount of solution to record the temperature history. After completion of the heating process, the tubes were taken out and were immediately cooled down to an ambient temperature.

Measurement of denaturation and degradation temperatures

The thermal denaturation properties of native-, apo-, and holo-LF were studied using a differential scanning calorimeter (Micro DSC VII SETARAM, Caluire, France), following Iafisco's method.[25] About 600 µL sample solution (5%, w/v) was weighed in a stainless steel cell and equal amount of distilled water was loaded in the reference cell. Both cells were hermetically sealed and heated from 20 to 98°C at a scanning rate of 2°C/min under nitrogen flow of 20 ml/s. Samples were cooled at 2°C/min from 98 to 20°C and reheated to 90°C at the same scanning rate to check renaturation of the proteins.

The thermal degradation of all the three forms of LF was determined using thermogravimetric analyzer (TGA 7, PerkinElmer Inc., USA). For this, 1–2 mg sample was loaded in an open platinum pan. The mass loss was recorded as a function of temperature from 30 to 850°C. The temperature was increased at a rate of 5°C/min. Nitrogen was used as heating medium at a flow rate of 20 ml/s.

Determination of the drying characteristics

Drying kinetics (moisture and temperature histories) of different forms of LF were determined using SDD experiment. Details of the SDD instrument and its working procedure are provided elsewhere.[26,27] For the purpose of determining drying kinetics, 50 mg/ml LF was dissolved in Milli-Q water. Then, two droplets of 7.0 ± 0.1 µl each, in volume, were suspended on either tip of a glass filament with 0.64 ± 0.13 mm diameter. The suspending glass filament was supported by a cylindrical Teflon droplet suspension system. The droplets were allowed to dry by passing clean and heated air. The droplets were dried at two different air temperatures (70 and 95°C) at a constant air velocity of 0.5 m/s. These air temperatures in convective drying were chosen to cover the thermal denaturation temperatures of iron-free LF (at 70°C) and iron-saturated LF (at 95°C) obtained from the measurements. These two temperatures also fall within the outlet temperatures used to spray dry protein solutions.[27] The relative humidity of the drying air was calculated using psychrometric equations using dry bulb and wet bulb temperatures and it was found to be $6.8 \pm 0.1\%$. The wet bulb temperatures corresponding to air temperatures of 70 and 95°C were 31 and 33°C, respectively. The droplets were dried to a final moisture content of less than 5% (wet basis). Images of the droplets during drying were captured every minute by a digital camera (EOS 60D, Canon, NSW, Australia) at 40 × to 50 × magnification while the increase in temperature and loss in mass of droplets were recorded using the proprietary software. All the drying experiments were performed in triplicates and the average values of three measurements of moisture loss and droplet temperature were used to generate moisture and droplet history plots.

Determination of the denaturation characteristics

The denaturation kinetics of LF were determined according to Haque et al.[27] who determined the denaturation kinetics of whey protein isolate. For this, droplets of LF dried at 120-s intervals were collected and diluted to a concentration of 200 µg/ml with Milli-Q water. This solution was centrifuged at 10,000× *g* for 10 min. Then, the supernatant was collected and injected onto the reversed-phase column. The injection volume was 50 µl. The signal absorbance was detected at 210 nm wavelength.

The denatured LF was separated using reversed phase high performance liquid chromatography (RP-HPLC) following the method given by Yao et al.[28] Separation was performed on a C_{18} HPLC column (Jupiter 5µ C_{18} 300 R, 250 × 4.6 mm, 5 µm, Phenomenex, NSW, Australia). In this case, 0.1% TFA and acetonitrile with a ratio of 95:5 were used as mobile phase A, 0.1% TFA and acetonitrile with a ratio of 5:95 was used as mobile phase B. Elution started with 35% mobile phase B for 1 min and increased linearly to 60% mobile phase B for 19 min. It was then equilibrated for 10 min. The flow rate of solvent was fixed to 0.5 ml/min and the column temperature was maintained at 37°C. The degree of denaturation of LF was calculated by comparing the peak area of treated samples with peak area of control or untreated LF sample using Eq. (1):

$$\text{Denatured lactoferrin } (\%) = \left[\frac{(1 - \sum A_{\text{treat}})}{\sum A_0}\right] \times 100, \quad (1)$$

where ΣA_{treat} is the sum of peak areas of the dried LF samples and ΣA_0 is the sum of peak areas of the LF without drying treatment.

Quantify secondary structure changes

Far-UV CD spectra of apo-, native-, and holo-LF dried using SDD and heated using isothermal heat treatment (IHT) were obtained using JASCO J-810 spectropolarimeter (Jasco International Co., Ltd., Tokyo, Japan). For this, 60 µl of each LF sample (0.1%, w/v) was loaded to a 0.1-cm cylindrical quartz cell with optical path length of 0.1 cm, and the results were average values of 10 readings. The CD spectra were analyzed using CDPro software to determine the contents of each secondary structural feature according to the method outlined previously.[22]

Statistical analysis

Statistical analysis was performed using IBM's statistical software (SPSS®, version 21, IBM Corp.). All experimental measurements were conducted at least in triplicate, and data were expressed as the mean ±standard deviation where feasible. To determine the significant level of difference between treatments, analysis of variance(ANOVA) was performed at 95% confidence level ($P < 0.05$). Significantly different groups were classified using Duncan's multiple range test.

Results and discussion

Proximate composition

The protein, iron, and moisture contents of apo, native, and holo forms of LF were determined. The protein content of native, apo, and holo forms of LF was found to be 97.0 ± 1.6, 91.0 ± 2.1, and 100.0 ± 3.1%, respectively. Likewise, the iron saturation level of native, apo, and holo forms of LF was found to be 12.6 ± 1.1, 1.4 ± 0.5, and 100.0 ± 0.3%, respectively. The moisture content of all samples was less than 2.2% (w/w). The protein patterns of all the three forms of LF are shown in Fig. 1. These patterns suggest that they have approximately same molecular weight of about 75 kDa as demonstrated by a single intense band at this molecular weight range.

Effect of iron saturation level on thermal characteristics

The DSC thermograms of native-, apo-, and holo-LF in solutions at pH 7.0 are shown in Fig. 2a. The denaturation temperature range (T_{onset}–T_{endset}), peak denaturation temperature (T_{max}), and enthalpy of denaturation (ΔH) determined from these thermograms are presented in Table 1. Endothermic transitions were observed in the temperature range (T_{onset}–T_{endset}) of 60.5–74.5 and 76.3–98.4°C, respectively, in case of

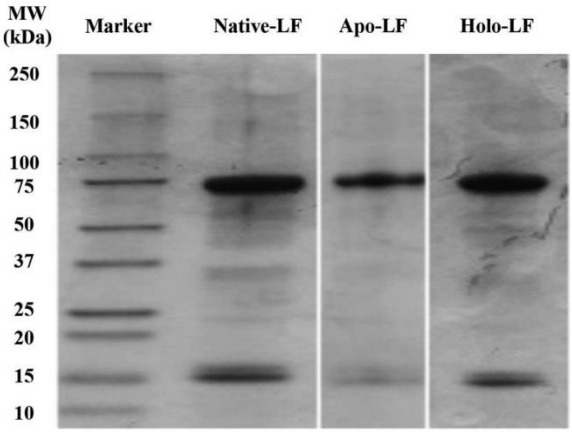

Figure 1. Sodium dodecyl sulfate-polyacrylamide gel electrophoresis profile of three forms of LF.

apo- and holo-LF. Similarly, two denaturation peaks (major peak at 61.4°C and minor peak at 89.3°C) were observed in the case of native-LF. Since native-LF is a mixture of two or more forms, it is expected for it to show multiple denaturation peaks. The first peak corresponds to the denaturation of iron-depleted apo-LF, whereas the second peak corresponds to the denaturation of iron-saturated holo-LF. These peaks' denaturation temperatures are in accordance with the previous studies.[13,15,29] Further, the denaturation enthalpy (ΔH) of the holo-LF is much ($P < 0.05$) higher than that of the native- and apo-LF. It can be inferred from these observations that holo form of LF is more resistant to thermal stresses than the native and apo forms. This kind of higher resistance to thermal denaturation of holo-LF might be due to its more compact structure resulting from the iron binding in both lobes. The slightly higher denaturation temperature of apo-LF (65.8°C) than that of native-LF (61.7°C) might be due to differences in the ionic strength of the solution resulting from the adjustment of pH and this fact was also reported previously.[15,29–31]

The mass loss patterns revealed by the thermogravimetric analysis of three forms of LF are presented in Fig. 2b. In all cases, it can be observed that very small percentage (~2%, w/w) of mass loss was detected during heating until the temperature reached 200°C due to the moisture loss. The mass of all the three forms of LF stared to drop dramatically at temperatures >200°C, which indicated to the degradation of the polypeptide structure. This trend showed that the saturation of LF will not provide higher resistance against thermal degradation. The similar extent of mass loss in apo- and native-LF in 200–400°C range indicates that the primary pyrolysis products of these two LF samples would be

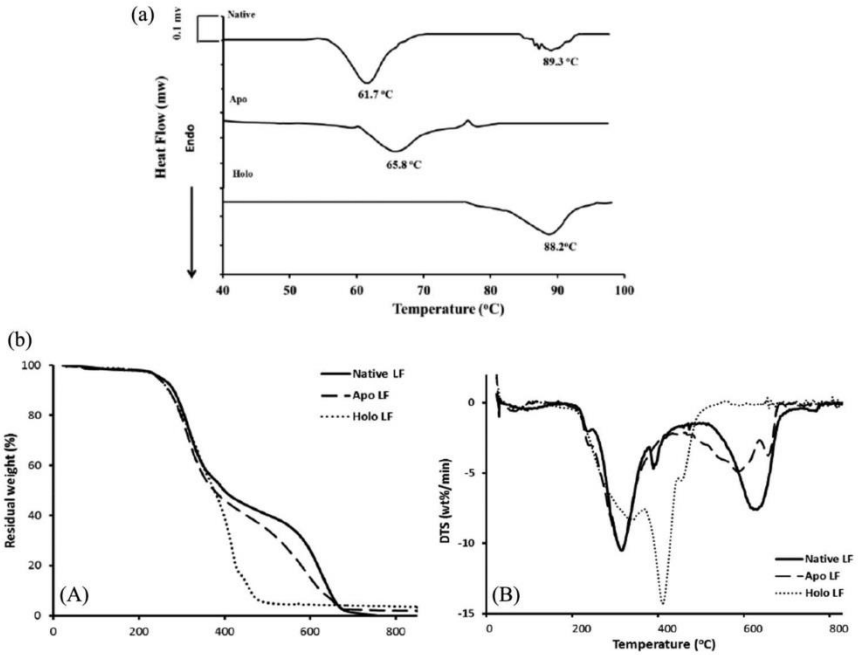

Figure 2. (a) DSC thermograms of different forms of LF. (b) Mass loss of Apo, Holo, and Native-LF powders as a function of furnace temperature (A), the DTG curves (B) showing the mass loss events.

similar. The secondary degradation of apo- and native-LF (indicated by distinct rate of mass loss) occurred at around 530–680°C. The degradation of holo-LF started at the same temperature as other two forms; however, significant ($P < 0.05$) mass loss (39.9%) was observed at much higher temperature (360–440°C) and no second stage of degradation was observed in the case of holo-LF. This observation indicated that iron-saturated LF is more resistant to thermal compared to two other forms at higher temperatures (Fig. 2b). The higher resistance of holo-LF is unlikely to be resulted from the compact conformation of holo-LF as its structure already destroyed during the peptide degradation stage. It appears the presence of free iron prevents the pyrolysis reaction.[32] At this stage, the mechanism with which the free iron prevents the secondary pyrolysis of LF is not clear and needs to be studied further. At temperature >750°C, all forms of LF were degraded or combusted and 2–3% of initial mass (ash or inorganic compounds) was left behind.

Table 1. Denaturation temperature range (ΔT_d), denaturation temperature (T_d), and enthalpy of denaturation (ΔH) of three forms of LF determined using DSC.

Material	T_{onset} (°C)	$T_{endfset}$(°C)	T_{max}(°C)	ΔH (J/g)
Native-LF	52.5 ± 1.9	70.6 ± 7.2	61.7 ± 2.9	14.9 ± 2.1
	82.8 ± 2.3	92.4 ± 1.2	89.3 ± 1.2	4.94 ± 1.1
Apo-LF	60.5 ± 1.1	74.5 ± 2.2	65.8 ± 0.9	15.6 ± 0.4
Holo-LF	76.3 ± 4.7	98.4 ± 1.9	88.8 ± 1.4	22.0 ± 3.0

LF concentration 5% (w/v), pH 7.0 ($n = 3$).
DSC, differential scanning calorimeter; LF, lactoferrin.

Drying kinetics of three forms of LF

The drying kinetics (moisture content and temperature profiles) of apo-LF, native-LF, and holo-LF dried at 70 and 95°C are shown in Fig. 3a and b, respectively. It is seen from Fig. 3a that when dried at 70°C, the rate of moisture loss in these three forms of LF is significantly ($P < 0.05$) different. Holo-LF reached its lowest moisture level at 435 s of commencement of drying, whereas the native-LF achieved the same in 540 s. The drying time required for apo-LF to reach its lowest moisture content was between those of native- and holo-LF. At 95°C, the dewatering process for holo-LF was the shortest (330 s) and for native-LF was the longest (372 s), that of apo-LF remained in between the former two. The fastest rate of moisture loss was observed in the case of holo-LF and slowest rate of moisture loss was observed in the case of native-LF at both drying temperatures. At 70°C, the droplet temperature profiles of all three forms of LF almost overlapped one another during the first 250 s of drying, after which the temperature profiles were different. The droplet temperature of native-LF increased faster than the other two forms. This might be due to the soluble

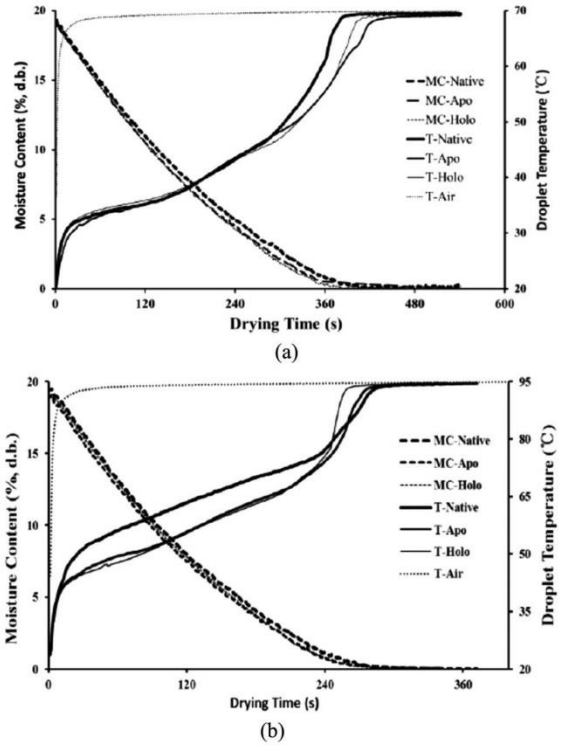

Figure 3. Drying kinetics of different forms of LF at (a) 70°C and (b) 95°C in convective air-drying system where MC means moisture content and *T* represents droplet temperature.

complex formed between the apo form and holo form present in native-LF because they have opposite charges and might interact electrostatically during drying process.[31] To better understand this, we determined the drying rate (d*X*/d*t*) from the experimental moisture loss versus time data (Fig. 4) and plotted the drying rate curve against moisture content (on dry basis) as suggested in the literature.[27] A polynomial model equation was fitted with the experimental moisture ratio and the model constants are shown in Table 2. From Fig. 4, it can be seen that the drying rate of native-LF at 70°C (0.0807 kg water/kg dry solid/s) was lower than those of apo and holo forms LF (0.0846 kg water/kg dry solid/s) at the beginning of convictive drying process. When dried at 95°C (Fig. 3b), it was observed that the droplet temperature of native-LF was higher than those of apo and holo forms up to 250 s after which both the apo and holo forms showed sudden increase in temperature. Mass and energy transfer theories explain that the temperature of slower drying droplet is higher due to higher resistance to outward moisture diffusion[27] As expected, the drying rates of three forms of LF at 95°C are higher than those at 70°C (Fig. 4). These differences in drying rates in these three forms of LF also

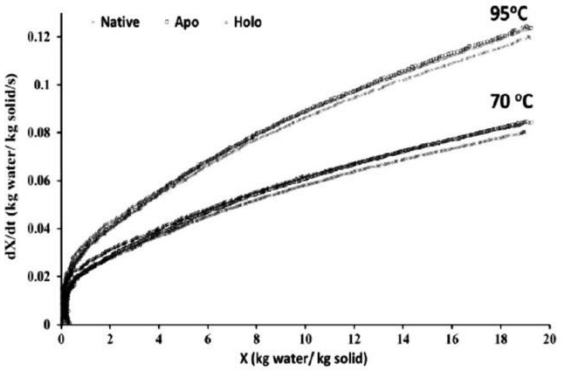

Figure 4. Drying rates of different forms of LF at 70 and 95°C in convective air-drying system.

might be due to the iron content and the way it is bound with the protein.

Changes in droplet morphology

The droplets of apo-, native- and holo-LF solutions developed different morphological features when dried at both drying temperatures (Fig. 5). The droplets of apo-LF were colorless whereas the droplets of native-LF and holo-LF were light yellow and cherry red, respectively.

It can be observed that all droplets folded and wrinkled to some extent at the end of drying. Apo- and holo-LF showed similar morphological features when dried at 70°C. They started deviating from spherical shape at about 120 s and developed wrinkled shape at the end of 600 s. The droplet of native-LF also deviated from spherical shape after 120 s and produced a buckled particle at the end of the experiment. In all cases, a precipitated mass of LF was observed at the bottom of the droplet toward the end of the drying process. Drying at 95°C showed that apo-LF was less capable of resisting the deformation of droplet/particle surface during drying. The droplet of apo-LF lost its spherical shape after 240 s. On the other hand, native-LF

Table 2. Modeling constant of drying rate.

Polynomial model equation: $MR = \frac{X_t - X_\infty}{X_0 - X_\infty} = At^2 + Bt + C$

Samples	Constant *A*	*B*	*C*	R^2
		70°C		
Native-LF	$8.30e^{-5}$	−0.081	19.463	0.99
Apo-LF	$9.26e^{-05}$	−0.085	19.343	0.99
Holo-LF	$8.99e^{-5}$	−0.085	19.371	0.99
		95°C		
Native-LF	$1.95e^{-4}$	$-1.25e^{-1}$	19.739	0.99
Apo-LF	$2.00e^{-4}$	$-1.25e^{-1}$	19.531	0.99
Holo-LF	$1.85e^{-4}$	$-1.21e^{-1}$	19.619	0.99

MR is the experimental moisture ratio.

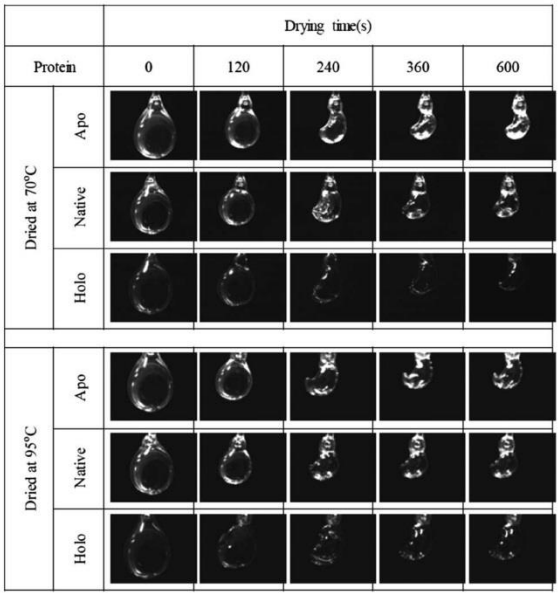

Figure 5. Morphological features of three different forms of LF during the convective drying process at 70 and 95°C.

maintained its spherical shape for longer time; however, most of the aggregated proteins appeared at the wrinkled part of the droplet. A thin and fragile skin was formed on the surface of the droplet during drying and it cracked at the end of drying process. This sometimes produced drying curves with significant fluctuation in mass after 400 and 290 s during drying at 70 and 95°C, respectively. The denaturation of LF mainly occurred at the air–liquid interface of droplets. During the drying process, the concentration of unfolded (denatured) protein was increased and aggregated, which lead to the formation of "fragile skin" on the surface of droplets. This skin made the air–liquid interface more rigid, provided resistance to the outward diffusion of vapor due to which vapor was trapped inside. When the skin was pierced due to increased internal pressure, the evaporation rate was increased instantaneously. Because holo-LF was more resistant to thermal denaturation, the "skin" formed on the surface due to denaturation was less than that in other forms. This observation also explained why the drying rate of holo-LF was the highest.

Denaturation characteristics of LF and its relationship with drying kinetics

The denaturation profiles of three forms of LF are shown in Fig. 6. At drying temperature of 70°C, all forms of LF showed similar extent of denaturation before 240 s. It suggests that the iron binding states

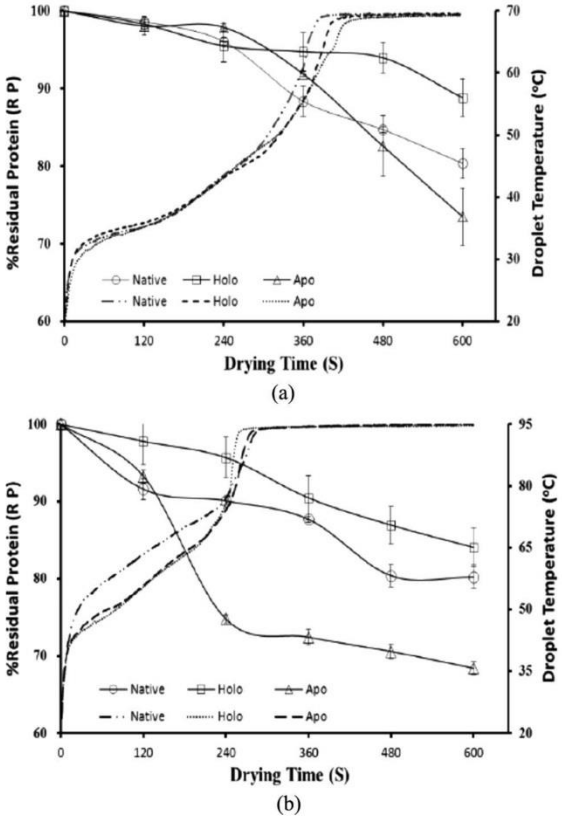

Figure 6. Denaturation profiles of three forms of LF at 70°C (a) and 95°C (b) convective drying temperature ($n = 3$).

of LF did not affect its thermal stability when the air temperature was below 40°C. However, once the air temperature reached 60°C after 360 s of the start of the drying process, apo- and native-LF began to lose the protein conformation demonstrating an increased extent of denaturation of up to 9 and 11%, respectively. As the droplet temperature increased, more and more protein got denatured, and at the end of the drying process (i.e., 600 s), the denaturation of apo, native, and holo forms of LF reached 26.5, 19.7, and 11.2%, respectively. When LF was dried at 95°C, the convective drying caused greater extent of protein denaturation (31.6, 19.8, and 16.0% for apo, native, and holo forms of LF, respectively). Interestingly, because of the droplet temperature increased to 60°C at the very beginning of the drying process, significant amount of protein (2–8%) was denatured even at 120 s of commencement of drying process. The extent of denaturation increased by 10 and 5% for apo- and holo-LF at the next 120 s, respectively, and slowed down when the evaporation process was completed (372 s), indicating that protein–water interaction is essential aspect in the protein denaturation.[33–36] Holo-LF showed quite different

denaturation history compared to other two forms of LF irrespective of the drying temperature used. This fact was also reflected in the morphological changes as well. The more compact conformation of holo-LF as described before apparently protected it from thermal and air interfacial stresses and reduced the extent of denaturation. The denaturation kinetics, drying kinetics, and the morphological developments indicate that the formation of the rigid skin on the surface of droplets is due to denaturation of proteins, and this rigid skin is responsible for slower evaporation.[27,35] When the extent of denaturation of protein was lower, the droplet dried faster and the dewatering process became shorter. This is the reason why the holo-LF was more stable during drying process and also dried faster than other two forms.

Changes of secondary structure of LF during drying

The changes in the LF's molecular structure during convective drying and isothermal heat treatment were determined using CD analysis. The CD spectra of three forms of LF subjected to convective drying and IHT at 95°C for 10 min are presented in Fig. 7. The change in the ellipticity indicates to the extent of conformational changes in LF due to drying or solution heating. The shape of CD spectra of LF samples subjected to convective drying was similar to that of control samples. However, small changes at 208 and 222 nm were observed in the CD spectra of convectively dried LF due to the decrease in helix structure. On the other hand, a sharp decrease in ellipticity was observed at 190 and 222 nm in the CD spectra of LF sample subjected to isothermal heat treatment. This observation suggests yet again that IHT causes higher loss of α-helix than the convective drying.

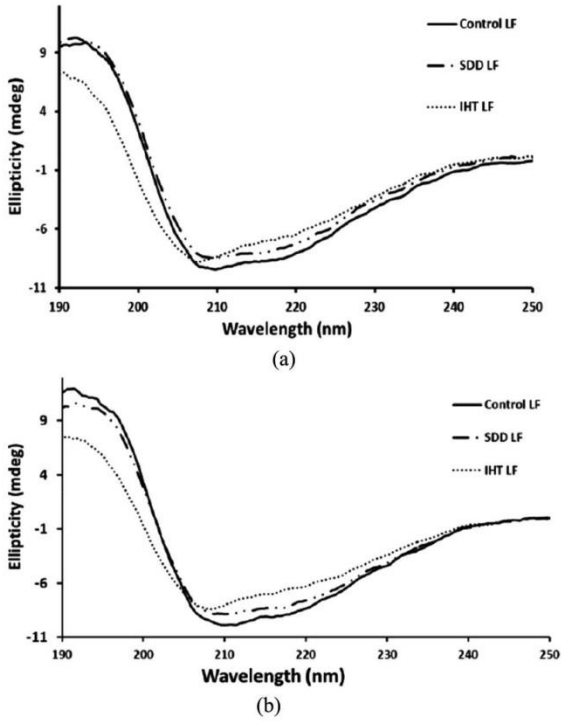

Figure 7. Far-UV CD spectra of LF where black, green, and red color indicate control sample, single droplet dried samples, and isothermal heated samples, respectively. (a) The profile of native-LF, (b) apo-LF, and (c) holo-LF.

The percentage of the helices, turns, sheets, and unordered structures of LFs subjected to convective drying and IHT at 95°C and 10 min are given in Table 3. It shows that, before any kind of heat treatment, three forms of LF share the similar secondary structures which also consist with the Moora et al.'s results[37] obtained through X-ray diffraction. For native-LF, the convective drying under experimental condition caused 5.8% decrease in α-helix content and 4.7% increase in β-sheets. In the case of IHT, the helix content decreased by 9.9%, whereas the content of sheets and unordered structures (random coils) increased by 4.4 and 2.5%, respectively. In the case of holo-LF, although the change in the secondary structure due to IHT was similar to that in other forms of LF, the convective dying caused less damage to its conformation with 3.6% decrease in α-helix content and 3.3% increase in β-sheets. This result further confirms that convective drying process, which involves simultaneous heating and evaporation causes less alteration to the native structure of LF compared to IHT where heating is not accompanied by evaporation or evaporative cooling,[26] and that the holo-LF is more resistant to thermally induced conformation changes.

Table 3. Percentage of secondary structural features of lactoferrin determined using CD ($n = 3$).

	%			
Sample	Helices	Sheets	Turns	Unordered
Native-LF				
Control	30.4 ± 1.9^a	22.3 ± 2.1^a	19.8 ± 2.1^a	27.2 ± 1.6^a
SDD	24.6 ± 0.6^b	27.0 ± 1.0^b	20.6 ± 0.2^a	27.8 ± 1.2^a
IHT	20.5 ± 1.3^c	26.7 ± 1.6^b	21.7 ± 0.6^a	29.7 ± 1.9^a
Apo-LF				
Control	31.4 ± 2.3^a	20.9 ± 2.0^a	19.9 ± 1.8^a	27.8 ± 0.9^a
SDD	27.8 ± 1.7^a	$23.9 \pm 1.9^{a,b}$	20.6 ± 0.6^a	27.6 ± 0.9^a
IHT	21.4 ± 1.3^b	27.6 ± 2.7^b	21.3 ± 0.3^a	29.0 ± 1.8^a
Holo-LF				
Control	31.1 ± 2.1^a	21.7 ± 1.6^a	19.1 ± 2.1^a	28.0 ± 0.8^a
SDD	27.5 ± 3.3^a	25.0 ± 2.9^a	18.7 ± 2.3^a	$28.3 \pm 0.3^{a,b}$
IHT	21.3 ± 1.1^b	25.6 ± 0.9^a	21.8 ± 0.3^a	30.2 ± 1.5^b

The different letters correspond to significant difference ($P < 0.05$) for each form of LF in the same column.

CD, circular diachroism; SDD, single droplet drying; IHT, isothermal heat treatment; LF, lactoferrin.

Conclusion

The degree of iron saturation had significant effect on the extent of denaturation of LF when dried at 70 and 95°C. The thermal stability of the iron-saturated holo form was the highest, that of apo-from was the lowest, and that of native form remained in between these two at both drying air temperatures. The holo-LF had higher denaturation and degradation temperatures which further corroborated that the iron binding makes LF more thermally stable. The alteration of secondary structural features (α-helix, β-sheet, β-turn, and random coil) of all the three forms of LF was significantly higher in IHT conditions than in convective drying conditions in both medium temperatures (70 and 95°C) and exposure time (10 min). The iron-saturated holo form will be more suitable than the native and apo forms to produce LF powder using convective drying process.

References

[1] González-Chavez, S.A.; Arevalo-Gallegos, S.; Rascon-Cruz, Q. Lactoferrin: Structure, function and applications. *International Journal of Antimicrobial Agents* **2009**, *33*(4), 301.e1–301.e8.

[2] Garcia-Montoya, I.A.; Cendon, T.S.; Arevalo-Gallegos, S.; Rascon-Cruz, Q. Lactoferrin a multiple bioactive protein: An overview. *Biochimica et Biophysica Acta* **2012**, *1820*(3), 36–226.

[3] Brisson, G.; Britten, M.; Pouliot, Y. Heat-induced aggregation of bovine lactoferrin at neutral pH: Effect of iron saturation. *International Dairy Journal* **2007**, *17*(6), 617–624.

[4] Kanyshkova, T.; Buneva, V.; Nevinsky, G. Lactoferrin and Its biological functions. *Biochemistry (Moscow)* **2001**, *66*(1), 1–7.

[5] Steijins, J.M.; van Hooijdonk, A.C. Occurrence, structure, biochemical properties and technological characteristics of lactoferrin. *British Journal of Nutrition* **2000**, *84*(1), 11–17.

[6] Levay, P.F.; Viljoen, M. Lactoferrin: A general review. *Haematologica* **1995**, *80*(3), 252–267.

[7] Baynes, R.D.; Bezwoda, W.R. Lactoferrin and the inflammatory response. *Advances in Experimental Medicine and Biology* **1994**, *357*, 133–141.

[8] Bradley E.B.; Jonathan, S.S.; Myron, S.C. The role of lactoferrin as an anti-inflammatory molecule. *Advances in Experimental Medicine and Biology* **1994**, *357*, 143–156.

[9] Sreedhara, A.; Flengsrud, R.; Langsurd, T.; Kaul, P.; Prakash, V.; Vegarud, G.S. Structural characteristic, pH and thermal stabilities of apo and holo forms of caprine and bovine lactoferrins. *An International Journal on the Role of Metal Ions in Biology, Biochemistry and Medicine* **2010**, *23*(6), 1159–1170.

[10] Schanbacher, F.L.; Goodman, R.E.; Talhouk, R.S. Bovine mammary lactoferrin: Implications from messenger ribonucleic acid (mRNA) sequence and regulation contrary to other milk proteins. *Journal of Dairy Science* **1993**, *76*(12), 3812.

[11] Tomita, M.; Wakabayashi, H.; Shin, K.; Yamauchi, K.; Yaeshima, T.; Iwatsuki, K. Twenty-five years of research on bovine lactoferrin applications. *Biochimie* **2009**, *91*(1), 7–52.

[12] Cao, L.; Maas, H.; Holding, B.V. Heat-stable, aqueous lactoferrin composition and its preparation and use. U.S. Patent 2015, 8999923.

[13] Sánchez, L.; Peiro, J.M.; Castillo, H.; Perez, M.D.; Ena, J.M.; Calvo, M. Kinetic parameters for denaturation of bovine milk lactoferrin. *Journal of Food Science* **1992**, *57*(4), 873–879.

[14] Stanciuc, N.; Aprodu, I. Analysis of the thermally induced structural changes of bovine lactoferrin. *Journal of Agricultural and Food Chemistry* **2013**, *61*(9), 2234–2243.

[15] Bokkhim, H.; Bansal, N.; Bhandari, B. Physico-chemical properties of different forms of bovine lactoferrin. *Food Chemistry* **2013**, *141*(3), 3007–3013.

[16] Mezhericher, M.; Levy, A.; Borde.I. Theoretical drying model of single droplets containing insoluble or dissolved solids. *Drying Technology* **2007**, *25*(6), 1025–1032.

[17] Che, L.; Li, D.; Chen, X.D. Convective drying kinetics of single droplets of aqueous glucose. *Drying Technology* **2012**, *30*(10), 1029–1036.

[18] Fu, N.; Woo, M.W.; Chen, X.D. Single droplet drying technique to study drying kinetics measurement and particle functionality: A review. *Drying Technology* **2012**, *30*(15), 1771–1785.

[19] Lin, R.; Woo, M.W.; Fu, N.; Selomulya, C.; Chen, X.D. In situ observation of taurine crystallization via single droplet drying. *Drying Technology* **2013**, *31*(13–14), 1553–1561.

[20] Byler D.M.; Susi, H. Examination of the secondary structure of proteins by deconvolved FTIR spectra. *Biopolymers* **1986**, *25*, 469–487.

[21] Hadden, J.M.; Bloemendal, M.; Haris, P.I.; Srai, S.K.S.; Chapman, D. Fourier transform infrared spectroscopy and differential scanning calorimetry of transferrins: Human serum transferrin, rabbit serum transferrin and human lactoferrin. *Biochimica et Biophysica Acta/ Protein Structure and Molecular Enzymology* **1994**, *1205*(1), 59–67.

[22] Wen, P.; Guo, H.; Zhang, H.; Gan, B.; Ding, Q.; Ren, F. Effect of glucose on the lactoferrin's conformation and its effect on MC 3T3-E1 cell proliferation. *The Protein Journal* **2012**, *31*(4), 300–305.

[23] Mazurier, J.; Spik, G. Comparative study of the iron-binding properties of human transferrins: I. Complete and sequential iron saturation and desaturation of the lactotransferrin. *Biochimica et Biophysica Acta – General Subjects* **1980**, *629*(2), 399–408.

[24] Majka, G.; Spiewak, K.; Kurpiewska, K.; Heczko, P.; Stochel, G.; Strus, M.; Brindell, M. A high-throughput method for the quantification of iron saturation in lactoferrin preparations. *Analytical Bioanalytical Chemistry* **2013**, *405*(15), 5191–5200.

[25] Iafisco, M.; Foltran, I.; Foggia, D.I.; Bonora, S.; Roveri, N. Calorimetric and Raman investigation of cow's milk lactoferrin. *An International Forum for Thermal Studies* **2011**, *103*(1), 41–47.

[26] Adhikari, B.; Howes, T.; Bhandari, B.R. Use of solute fixed coordinate system and method of lines for

prediction of drying kinetics and surface stickiness of single droplet during convective drying. *Chemical Engineering and Processing: Process Intensification* **2007**, *46*(5), 405–419.

[27] Haque, M.A.; Putranto, A.; Aldred, P.; Chen, J.; Adhikari, B. Drying and denaturation kinetics of whey protein isolate (WPI) during convective air drying process. *Drying Technology* **2013**, *31*(13–14), 1532–1544.

[28] Yao, X.D.; Bunt, C.; Cornish, J.; Quek, S.; Wen, J.Y. Improved RP-HPLC method for determination of bovine lactoferrin and its proteolytic degradation in simulated gastrointestinal fluids. *Biomedical Chromatography* **2013**, *27*(2), 197–202.

[29] Mata, L.; Sanchez, L.; Headon, D.R.; Calvo, M. Thermal denaturation of human lactoferrin and its effect on the ability to bind iron. *Journal of Agricultural and Food Chemistry* **1998**, *46*(10), 3964–3970.

[30] Steijns, J.M.; Hooijdonk, A.C.M. Occurrence, structure, biochemical properties and technological characteristics of lactoferrin. *British Journal of Nutrition* **2000**, *84*(S1), 11–17.

[31] Bovetto, L.; Breuille, D.; Donato, L.; Panchaud, A.; Pouteau, E.; Schmitt, C. Wipo. Lactoferrin based complex coacervates and their uses. U.S. Patent 2012, 045801.

[32] Richard, G.N.; Zheng, G. Influence of metal ions and of salts on products from pyrolysis of wood: Applications to thermochemical processing of newsprint and biomass. *Journal of Analytical and Applied Pyrolysis* **1991**, *21*(1–2), 133–146.

[33] Mallamace, F.; Corsaro, C; Mallamace, D.; Baglioni, P.; Stanley, H.E.; Chen, S.H. A possible role of water in the protein folding process. *The Journal of Physical Chemistry B* **2011**, *115*(48), 14280–14294.

[34] Robinson, G.W.; Cho, C.H. Role of hydration water in protein unfolding. *Biophysical Journal* **1999**, *77*(6), 3311–3318.

[35] Fitter, J. The temperature dependence of internal molecular motions in hydrated and dry a-amylase: The role of hydration water in the dynamical transition of proteins. *Biophysical Journal* **1999**, *76*(2), 1034–1042.

[36] Chen, X.D. The basics of a reaction engineering approach to modeling air-drying of small droplets or thin-layer materials. *Drying Technology* **2008**, *26*(6), 627–639.

[37] Moora, S.A.; Anderson, B.F.; Groom, C.R.; Haridas, M.; Baker, E.N. Structure of diferric bovine lactoferrin at 2.8 angstroms resolution. *Journal of Molecular Biology* **1997**, *274*(2), 222–236.

CHAPTER 4

Powder Production and Characterisation of Lactoferrin

Published in *International Journal of Biological Macromolecules*, 2017, 95, 985-994

International Journal of Biological Macromolecules 95 (2017) 985–994

Contents lists available at ScienceDirect

International Journal of Biological Macromolecules

journal homepage: www.elsevier.com/locate/ijbiomac

Characteristics of bovine lactoferrin powders produced through spray and freeze drying processes

Bo Wang[a], Yakindra Prasad Timilsena[a,b], Ewan Blanch[a], Benu Adhikari[a,b,*]

[a] School of Science, RMIT University, Melbourne, VIC 3083, Australia
[b] CSIRO Manufacturing Flagship, Clayton South, VIC 3169, Australia

ARTICLE INFO

Article history:
Received 26 September 2016
Received in revised form 23 October 2016
Accepted 24 October 2016
Available online 29 October 2016

Keywords:
Lactoferrin
Spray drying
Freeze drying
Denaturation
Antioxidant activity

ABSTRACT

Bovine lactoferrin (LF_b) powders were produced using spray drying and freeze drying. Industrially obtained fresh liquid-LF_b was used as starting material. The antioxidant capacity, solubility in water, moisture sorption behaviour, the extent of denaturation and changes in the secondary structural features of spray-dried ($SDLF_b$) and freeze-dried bovine lactoferrin ($FDLF_b$) powders were determined. The residual moisture content, water activity, particle size and amorphous/crystalline nature of the $SDLF_b$ and $FDLF_b$ were also measured. Results showed that both $SDLF_b$ and $FDLF_b$ powders had negligible denaturation and conformation changes compared to the liquid-LF_b. Both $SDLF_b$ and $FDLF_b$ showed type II sorption behaviour with almost identical monolayer moisture content. The $SDLF_b$ powders were amorphous in nature with >98% solubility in water. The antioxidant activity of $SDLF_b$ was similar to that of the liquid-LF_b while it was ~6% less in $FDLF_b$. Based on the residual moisture content, water activity, solubility and preservation of secondary structure of LF_b in resultant powders, a spray drying process with 180 °C inlet and 95 °C outlet temperature was found to produce similar or better quality LF_b powders compared to the ones produced through a freeze drying process.

1. Introduction

Lactoferrin (LF) is a multifunctional glycoprotein found in relatively higher concentration in bovine (0.02–0.2 g L^{-1}) and human milk (2.00–7.00 g L^{-1}) [1]. It is also present, in lower concentration, in other exocrine secretions such as tears, saliva, synovial fluid and blood [1–3]. Interestingly, the LFs obtained from bovine (LF_b) and human (LF_h) milk have quite similar chemical composition and functional characteristics [4,5]. A number of previous studies undertaken on LF_b revealed that it possesses anti-bacterial, anti-oxidant and anti-carcinogenic properties and acts as an iron transfer agent in human body [3,6,7]. Due to these reasons, LF_b is used in a variety of commercial products including functional foods, therapeutic drinks, fermented milks, chewing gums, cosmetics and tooth paste [8].

LF_b in liquid state or in solution form is very sensitive to chemical or microbial degradation and starts to lose its functional properties when it is stored at ambient temperature for more than four weeks [9]. Therefore, it is converted into dry powder form particularly using freeze drying in order to extend its shelf-life and to preserve its bio-functional properties. Spray drying is industrially preferred method to produce food protein powders. This is because spray drying requires lower capital cost (<8 times) as well as operational cost (<5 times) in comparison to freeze drying [10]. However, it is not commonly adopted by industry to produce LF_b powders mainly because of limited information on denaturation and other physicochemical characteristics of the spray-dried LF_b powders. The process parameters involved in extraction and drying of proteins induce certain degree of changes in the protein structure and ultimately affect their functional properties and nutritional value. The knowledge of the factors affecting the above functional properties of LF_b is important to adopt less astringent process parameters to produce LF_b powder with better functional characteristics. Hence, it is of practical significance to investigate the spray drying process of LF_b and comparatively evaluate it with freeze drying in terms of powder characteristics such as water sorption, solubility, extent of denaturation and antioxidant capacity.

During spray drying process, LF_b molecules are subjected to relatively higher thermal and interfacial stresses compared to that in freeze drying. Therefore, it can be hypothesized that these stresses can alter the structural features of LF_b (specially the secondary and higher order structures) and hence negatively impact the properties of the resultant powders [11–13]. However, if the spray drying

* Corresponding author at: School of Science, RMIT University, Melbourne, VIC 3083, Australia.
E-mail address: benu.adhikari@rmit.edu.au (B. Adhikari).

http://dx.doi.org/10.1016/j.ijbiomac.2016.10.087
0141-8130/

parameters such as inlet/outlet temperature, feed flow rate and LF_b concentration can be optimized such a way that their impacts on LF_b's secondary and higher order structures are minimised, functionally high quality powders can be produced. In our previous work, we have determined the denaturation temperature and other denaturation related characteristics of LF_b [14]. It was found that native form of LF_b (12% iron saturation) denatured at ~60 °C, whereas holo form of LF_b (100% iron saturation) denatured at much higher temperature (~90 °C). This could be due to the fact that when LF_b binds with iron, the conformation of LF_b becomes more compact which can help improve its resistance to thermal stress. Native-LF_b is a mixture of apo (devoid of iron) and holo (saturated with iron) forms and usually contains 15–20% holo- and 80–85% apo-LF_b [15]. We also reported in our previous work that 10–30% of native-LF_b were denatured during 10 min-long convective air drying trials carried out at 70 °C and 95 °C [14]. On the other hand, freeze drying is usually preferred to convert heat sensitive materials into powder form and is expected to better preserve its native conformation. However, long processing time, low production throughput, batch mode of production and possible chill injury associated with freezing are considerable disadvantages of this process [16]. Although there are publications [11,17,18] dealing with the functional properties of spray-dried and freeze-dried protein powders, to the best of our knowledge, comparison of the extent of denaturation and functional properties of spray-dried ($SDLF_b$) and freeze-dried LF_b ($FDLF_b$) is not available in the literature. As LF_b is a very important protein due to its unique iron binding and transferring properties, a systematic study on the drying process of LF_b would be of practical importance. Furthermore, if LF_b powders can be produced, in industrial scale, using spray drying without compromising its physicochemical and functional characteristics, the cost of production can also be substantially reduced. Therefore, this study was undertaken in order to determine the effects of spray drying and freeze drying processes on the secondary structural features and functional properties of resultant native LF_b powders. Liquid LF_b produced through membrane filtration process and supplied directly by an industry was to produce powders through spray and freeze drying. The extent of protein denaturation, amorphous/crystalline nature, water activity, moisture sorption profile and conformation changes of these LF_b powders were measured and compared. Effect of drying on the antioxidant capacity of LF_b was also determined and explained.

2. Experimental

2.1. Materials

Fresh LF_b solution (16–18%, w/v) was obtained by courtesy of Tatura Milk Industries Ltd. (Subsidiary of Bega Cheese, Victora, Australia). Pierce™ BCA protein assay kit was acquired from Thermo Scientific (Victoria, Australia). Mini-PROTEAN® TGX™ gels, WesternC™ blotting standards (Catalogue no: 1610376), Laemmli sample buffer, Tris/Glycine/SDS buffer, β-mercaptoethanol and Coomassie Brilliant Blue R-250 solution were purchased from Bio-Rad (Victoria, Australia). Lysozyme from chicken egg white (Catalogue no: 12650883) and 2, 2-Diphenyl-1-picrylhydrazyl (DPPH) was bought from Sigma Aldrich (NSW, Australia). All the chemicals listed above were of analytical grade and were used as received.

2.2. Preparation of spray-dried and freeze-dried LF_b powders

$SDLF_b$ powders were produced using a laboratory scale spray dryer (Spray dryer FT30 MKII, Armfield, UK). Briefly, Aqueous LF_b solution (16–18%, w/v) obtained from membrane filtration and provided by Tatura Milk Industries Ltd was used as feed without any further treatment. The inlet temperature was maintained at 180 °C. In order to investigate the extent of denaturation of the spray-dried powders, two outlet temperatures (70 °C and 95 °C) were chosen. These temperatures were chosen because 70 °C is above the denaturation temperature of apo-LF and 95 °C is above the denaturation of both LFs. The selected air inlet and outlet temperatures were within the recommended inlet (180–220 °C) and outlet (90–110 °C) temperature ranges used for spray drying of heat sensitive products at normal atmospheric pressure [19]. These two inlet and outlet temperature ranges are also commonly used in the industrial production of protein powders through spray drying [20,21]. The feed flow rate during the spray drying process was adjusted between 1000 and 1200 mL h^{-1} to maintain the set outlet temperatures. Powders collected from the cyclone were used for further tests and the powders remained in the chambers were discarded. The $FDLF_b$ were prepared in our laboratory using a laboratory scale freeze dryer (FreeZone™, Labconco Inc, USA). The liquid LF_b mentioned above was pre-frozen at −30 °C for 24 h. The temperature was increased, at the rate of 0.05 °C min^{-1}, to 0 °C and it was held for 12 h at this temperature for primary drying. The temperature was then raised to 20 °C at the same ramping rate and this temperature was maintained for 6 h for secondary drying. The collector temperature was −80 °C and a vacuum of 16 Pa was maintained in the drying chamber. The $FDLF_b$ produced in this way was collected and pulverized to pass through a 200 μm sieve. Both $FDLF_b$ and $SDLF_b$ powders were sealed hermetically and were kept at 4 °C until further tests.

2.3. Measurement of moisture content, water activity and colour parameters

The moisture content of both $FDLF_b$ and $SDLF_b$ powders was measured using an infrared moisture meter (Moisture Analyser – IC-MB45, OHaus, Switzerland). Water activity values of the powders were determined using a water activity meter (ms1 Set AMS, Novasina, Switzerland). The colour parameters of LF_b powders obtained from both spray and freeze drying methods were measured using a chromameter (CR-300, Konica Minolta Sensing Inc., Japan). The colour parameters were recorded in CIELab coordinates (L^*, a^*, b^*), which indicate the extent of black/white, red/green, yellow/blue, respectively. Calibration was done using the supplied standard reference plate (L^* = 96.90, a^* = 0.21, b^* = 1.93).

2.4. Determination of particle size and bulk density

The particle size distribution of $SDLF_b$ was determined by using Mastersizer™ 3000 (Malvern Instruments, Malvern, UK). Briefly, the $SDLF_b$ powders were sifted and then loaded into an Aero S dry cell. A refractive index value of 1.45 was used in these tests and volume mean diameter ($D_{[4,3]}$) values were measured. The bulk density was measured according to the method described by Joshi et al., [20]. For this, $FDLF_b$ and $SDLF_b$ powders were transferred to a 5 mL measuring cylinder with a lid. The cylinder was tapped for 50 times during the filling until the volume of the powders became stable. The density of the samples was calculated and expressed as kg/m^3.

2.5. Determination of amorphous/crystalline nature

The amorphous/crystalline nature of the powders was measured in terms of crystallinity using an X-ray diffractometer (Siemens D4, Endeavor, Bruker AXS GmbH, Karlsruhe, Germany) with Co-Kα radiation. X-ray (wide angle) diffractograms were taken at a range of 5° to 55° (2θ) with the rate of 1° min^{-1} (2θ). The step size was fixed to 0.05° (2θ). All measurements were carried

out at room temperature (25 °C). The crystallinity was measured by using software (DIFFRACplus Evaluation (Eva), version 10.0) available with the machine.

2.6. Monitoring and observation of surface morphology

The surface morphology of $FDLF_b$ and $SDLF_b$ powders was captured using a scanning electron microscope (SEM) (FEI Quanta 200 ESEM, Japan). The $FDLF_b$ and $SDLF_b$ powders were deposited on aluminium stubs using double-sided adhesive carbon tape and observed under SEM without gold coating. The accelerating voltage of 15 kV was used during these measurements.

2.7. Measurement of molecular weight and polypeptide profile of LF_b powders

The molecular weights of LF_b in liquid LF_b, $FDLF_b$ and $SDLF_b$ were examined using sodium dodecyl sulphate polyacrylamide gel electrophoresis (SDS-PAGE). The experiment was performed with a 4–15% precast polyacrylamide gel under both reducing and non-reducing conditions. For this purpose, the $FDLF_b$ and $SDLF_b$ and liquid LF_b were mixed with Milli-Q water and diluted to achieve the final protein concentration of 2 mg mL^{-1}. Then, 100 μL of these diluted solutions were mixed with equal volume of SDS-loading buffer (95% of laemmlie buffer and 5% of β-mercaptoethanol). These solutions were heated at 95 °C for 5 min. Ten microliter of the heated samples were loaded onto the pre-cast gels. Same volume (10 μL) of WesternC™ blotting protein standard was also loaded onto each gel as a molecular weight marker. The Mini-PROTEAN Tetra system used in this measurement was equilibrated at 100 V for 10 min before sample loading. The experiment was further run at 15 V for 10 min with standards and samples followed by running at 100 V for 75 min. The precast gel was removed and dyed with 0.1% (w/v) Coomassie Brilliant Blue R-250 solution on a shaker (40 rpm) for 2 h at ambient temperature (25 °C). It was then de-stained using de-staining solution containing 10% (v/v) acetic acid and 40% (v/v) methanol for another 2 h. Multiple washing was carried out with frequent changes of the de-staining solution. The image of the washed gel was captured by using a digital camera.

2.8. Determination of the extent of denaturation

The extent of denaturation of LF_b in powders was measured according to Anandharamakrishnan et al., [22] by using a micro DSC (Micro DSC VII SETARAM, Caluire, France). For this purpose, about 600 mg sample solution (10%, w/v) was weighed in a stainless steel cell and equal amount of Milli-Q water was loaded in the reference cell. Both cells were hermetically sealed and heated from 20 to 98 °C at a scanning rate of 2 °C min^{-1} under nitrogen flow of 20 mL s^{-1}. The extent of denaturation was determined using decrease in the enthalpy of denaturation (ΔH) values. The ΔH values were calculated from the area under a line extending from 50 to 75 °C and the values were normalized using the sample mass to give ΔH per gram of protein.

2.9. Determination of protein content and solubility

The protein content of the LF_b solutions and powders was determined using bicinchoninic acid (BCA) assay method [23]. This method is based on the reaction between BCA and Cu^+, which forms a purple-colored complex that strongly absorbs light at 562 nm. As the peptide bonds in protein reduce Cu^{2+} ions in BCA solution to Cu^+, the resulting amount of Cu^+ is liner to the protein concentration [23]. Therefore, the protein content of unknown sample can be determined spectrophotometrically by comparison with known protein standards.

For the purpose of determination of protein solubility, both $SDLF_b$ and $FDLF_b$ were dissolved in Milli-Q water to a concentration of 0.5 mg mL^{-1} (pH 7.0, 25 °C). These mixtures were stirred at 400 rpm for 30 min. These dissolved samples were centrifuged at 17500 × *g* for 30 min at 4 °C and the supernatant was recovered. This supernatant was used for determination of protein content using BCA protein assay method described above. Solubility was calculated from the ratio of quantity of LF_b remained dissolved in supernatant and the one used to make solution.

2.10. Monitoring the changes in secondary structural features

The nature and degree of changes in the secondary structural features of LF_b obtained from spray and freeze drying methods were determined by using Far-UV circular dichroism (CD) spectra (Jasco International Co., Ltd., Tokyo, Japan). For this, 60 μL of each LF_b sample (0.1% w/v) was loaded to a cylindrical quartz cell with optical path length of 0.1 mm. Five measurements were taken for each sample and the data was averaged. The CD spectra were analysed by using DicroWeb to determine the contents of each secondary structural features according to previously reported method [24,25].

The composition and structure changes of liquid LF_b, $SDLF_b$ and $FDLF_b$ powders were also compared by Fourier transform infrared spectroscopy (FTIR) coupled with an ATR accessory (Spectrum 100, Perkin Elmer, USA). All spectra were average of 64 scans from 4000 cm^{-1} to 650 cm^{-1} at a resolution of 4 cm^{-1}.

2.11. Measurement of antioxidant activity

The antioxidant activity of $FDLF_b$ and $SDLF_b$ powders was measured by using 2, 2-diphenyl-1-picrylhydrazyl radical (DPPH) method, which is commonly used to measure the radical scavenging activity [26]. For this purpose, 200 μL of the liquid LF_b, $FDLF_b$ and $SDLF_b$ were added to 2.65 mL citrate/phosphate buffer (0.1 M, pH 3.0) containing 1% (v/v) polysorbate-20 (Tween 20™). The concentrations of LF_b samples were varied from 0.2 mg mL^{-1} to 6.4 mg mL^{-1}. The radical scavenging reaction was initiated by adding 150 μL of 2 mM freshly prepared methanolic DPPH solution to the above mixtures to achieve a final DPPH concentration of 0.1 mM. The citrate/phosphate buffer without LF_b (pH 3.0) was used as control. Lysozyme has been reported to have very limited antioxidant activity [26] and it was used for comparison. The absorbance values were taken at 517 nm using Milli-Q water as the blank. All samples were gently mixed and stored in dark at ambient temperature (25 °C) and the absorbance of each solution was measured once again after 120 min. The radical scavenging activity was calculated by the percentage loss of absorbance at 517 nm wavelength using Eq. (1).

$$I\% = \left[\frac{A_{so} - A_{s1}}{A_{so}} - \frac{A_{c0} - A_{c1}}{A_{c0}}\right] \times 100\% \quad (1)$$

Where, As_0 and Ac_0 are the absorbance of LF_b sample and the buffer, respectively at the beginning of the incubation (2 min). As_1 and Ac_1 are the absorbance values of samples and buffer, respectively after storing them in dark for 120 min.

2.12. Measurement of moisture sorption isotherm

The moisture sorption isotherm profiles of $FDLF_b$ and $SDLF_b$ were measured using a standardised static gravimetric method [27–29]. For this purpose, seven saturated salt solutions were prepared in air tight desiccators, where LiCl, $KC_2H_3O_2$, K_2CO_3, $Mg(NO_3)_2$, KI, NaCl and KCl were used to maintain headspace equilibrium water activity (a_w) values of 0.11-0.85. Approximately 1 g of $FDLF_b$ and $SDLF_b$ samples were taken in clean and dry Petri dishes.

The Petri dished loaded with samples were transferred to the desiccators and kept into an incubator maintained at 25.0 ± 0.5 °C. All the samples were weighed in the interval of five days until the weight of samples reached an equilibrium state (< 0.02% change in mass). Then, the moisture contents of the equilibrated samples were measured and fitted against a_w using Guggenheim-Anderson-de Boer (GAB) model using Eq. (2).

$$\frac{m}{M_0} = \frac{CKa_w}{(1 - Ka_w)[1 - Ka_w + CKa_w]} \quad (2)$$

M_0 is the monolayer moisture content (kg water/kg solid). C and K are the GAB equation constants related to the moisture sorption enthalpies of monolayer and multilayer [30]. Similarly, m is the moisture content (kg water/kg solid) of sample and a_w is the water activity value corresponding to the moisture content (m).

2.13. Statistical analysis

Statistical analysis was performed using IBM's statistical software (SPSS®, version 21, IBM Corp.). All experimental data was obtained from triplicate runs and the data was expressed as the mean ± standard deviation where feasible. To detect any significant effects of treatments, data for each experiment was separately tested using analysis of variance (ANOVA). Significantly different groups were classified after post hoc comparison tests (Duncan's Multiple Range Test, DMRT) at 95% confidence level ($p = 0.05$).

3. Results and discussion

3.1. Physicochemical properties

The protein and residual moisture contents, water activity, solubility, mean particle size and colour parameters of both $SDLF_b$ and $FDLF_b$ are presented in Table 1. The protein content of both powders was higher than 90% with no significant difference ($p > 0.05$). The moisture content and water activity of $FDLF_b$ were about half of $SDLF_b$ dried at 95 °C outlet temperature ($SDLF_{b95}$) and quarter of $SDLF_b$ dried at 70 °C outlet temperature ($SDLF_{b70}$). This indicated that these two spray drying conditions retained more water from LF_b solutions. The residual moisture content of $SDLF_{b95}$ was within the moisture range reported in most spray-dried protein powders while that of $SDLF_{b70}$ was slightly higher [31,32]. $FDLF_b$ had higher bulk density than that of $SDLF_b$. The lower bulk density of $SDLF_b$ is due to the hollow structured particles and also due to higher percentage of voids surrounding each particle.

The $SDLF_b$ powder was light-red (pink) as indicated by the colour parameters given in Table 1. $FDLF_b$ powder had much darker red colour than $SDLF_b$ powder. No significant difference ($p > 0.05$) was observed in the colour of LF_b powders obtained by spray drying at these two outlet temperatures. The difference in the colour of $SDLF_b$ and $FDLF_b$ most probably due to difference in their bulk densities as the light reflected from $SDLF_b$ powders is expected to be affected by higher percentage of void in them. According to Mie's light scattering theory, a smaller particle scatters light less intensely and at wide angle while a larger particle scatters light more intensely and at narrow angle [33]. Since the mean particle size of the spray dried particles was ¼ of that of the freeze dried ones and hence it is natural for the spray dried powders to appear fainter. Furthermore, it has also been shown that smaller and internally hollow particles scatter light much less intensely [33]. The internally hollow $SDLF_b$ particles allowed greater penetration of light to the hollow interior and its greater absorption by the solid shells. This fact also explains that why the $SDLF_b$ particles appeared less dark red than the $FDLF_b$ particles.

The solubility values of $FDLF_b$, $SDLF_{b70}$ and $SDLF_{b95}$ are given in Table 1. It can be seen that solubility of $FDLF_b$ was lower than those of spray-dried ones. Given that the extent of denaturation of $FDLF_b$ is very close to the $SDLF_b$, this extent of lower solubility was not expected. Thus, the decrease of solubility of $FDLF_b$ powders might be due to the larger particle size which reduced the surface area/energy of solute particles. It has been reported in the literature that freeze-dried soy proteins and pea protein isolate also had lower solubility compared to their spray-dried counterparts [34,35].

3.2. Surface morphology of spray-dried and freeze-dried LF_b powders

The SEM micrographs of $FDLF_b$ and $SDLF_b$ are shown in Fig. 1. The micrographs indicate that both $FDLF_b$ and $SDLF_b$ particles had smooth surface. $SDLF_b$ particles mostly appeared spherical in shape and the volume mean size of these particles varied between 2 and 20 μm. $SDLF_b$ particles mostly appeared to be hollow inside which underpins the low bulk density in $SDLF_b$ powders (Table 1). The buckled shape and hollow interior in $SDLF_b$ may be due to formation of glassy skin in the early stage of drying of LF_b droplets in the particle formation process [12,36]. These authors explained that the low moisture diffusivity in glassy skin of polymeric materials results into internal vaporisation and periodic escape of water which results into blow-holes. Wrinkled surface in particles of spray-dried polymeric materials is commonly observed in proteins, protein-rich formulations [37] and also in maltodextrins [38]. The presence of blow holes also affects the bulk density and solubility of powders as articulated in preceding section.

3.3. Molecular weight profiles of spray-dried and freeze-dried LF_b powders

The molecular weight profiles of the liquid LF_b, $FDLF_b$ and $SDLF_b$ obtained from reducing and non-reducing SDS-PAGE experiments are presented in Fig. 2. The main band of all the LF_b samples appeared at ~75 kDa with a small portion of peptides appearing at ~15 kDa, which might be the residual α-lactalbumin [39]. The molecular weight profile is consistent with previous findings [40–42]. The bands seen in reducing and non-reducing lanes had no observable difference, which indicated that these two drying process did not affect the molecular weight or polypeptide make up of LF_b. As LF_b is a single polypeptide protein with two symmetric domains [43,44], the similar bands observed in reducing and non-reducing PAGE experiments indicated that the reduction of disulphide bonds did not lead to the breakdown of the LF_b peptide, which would otherwise show decrease in molecular weight in the reducing condition.

3.4. Amorphous/crystalline nature of spray-dried and freeze-dried LF_b powders

The X-ray diffractograms of $FDLF_b$, $SDLF_{b70}$ and $SDLF_{b95}$ powders are shown in Fig. 3. All of these powders exhibited three characteristic peaks at 9°, 19° and 44° (2θ). The extent of crystallization was calculated from 30–55° (2θ). The $FDLF_b$ and $SDLF_b$ were primarily amorphous in nature with highest crystallinity being 2.1%. There was no significant difference ($p > 0.05$) in crystallinity among these spray and freeze-dried powders.

3.5. The extent of denaturation of LF_b in spray-dried and freeze-dried powders

The extent of denaturation of LF_b in spray-dried and freeze-dried powders was measured by using DSC and the thermograms are presented in Fig. 4. Two denaturation peaks, major peak at 59 °C and minor peak at 88 °C, can be observed for liquid LF_b, which is in accordance with the denaturation peaks observed in

Table 1
Physicochemical properties of LF_b powders obtained from freeze and spray drying methods. FD = Freeze-dried LF_b, SD_{70} = Spray-dried LF_b at 70 °C outlet temperature, SD_{95} = Spray-dried LF_b at 95 °C outlet temperature.

Samples	Protein content (%)	Moisture content (%)	Water activity (a_w)	Solubility (%)	Bulk density (kg/m^3)	Particle size (μm)	Colour		
							L^*	a^*	b^*
FD	90.0 ± 2.3^a	2.7 ± 0.5^a	0.1 ± 0.0^a	94.3 ± 0.8^a	681.9 ± 15.5^a	48.0 ± 0.7^a	71.2 ± 1.6^a	8.8 ± 0.6^s	15.7 ± 0.9^a
SD_{70}	92.2 ± 2.2^a	8.6 ± 0.3^b	0.4 ± 0.0^b	99.3 ± 0.8^b	382.7 ± 7.5^b	12.9 ± 0.2^b	82.7 ± 1.0^b	4.4 ± 0.5^b	9.5 ± 0.4^b
SD_{95}	94.0 ± 2.6^a	5.2 ± 0.8^c	0.2 ± 0.0^c	98.4 ± 2.1^b	289.0 ± 13.1^c	12.8 ± 0.1^b	82.6 ± 0.9^b	4.4 ± 0.3^b	9.2 ± 0.2^b

All the data are expressed as mean ± SD and are the mean of triplicates.
Mean values with different lower case letters in superscript at the same column are significantly different ($p < 0.05$).

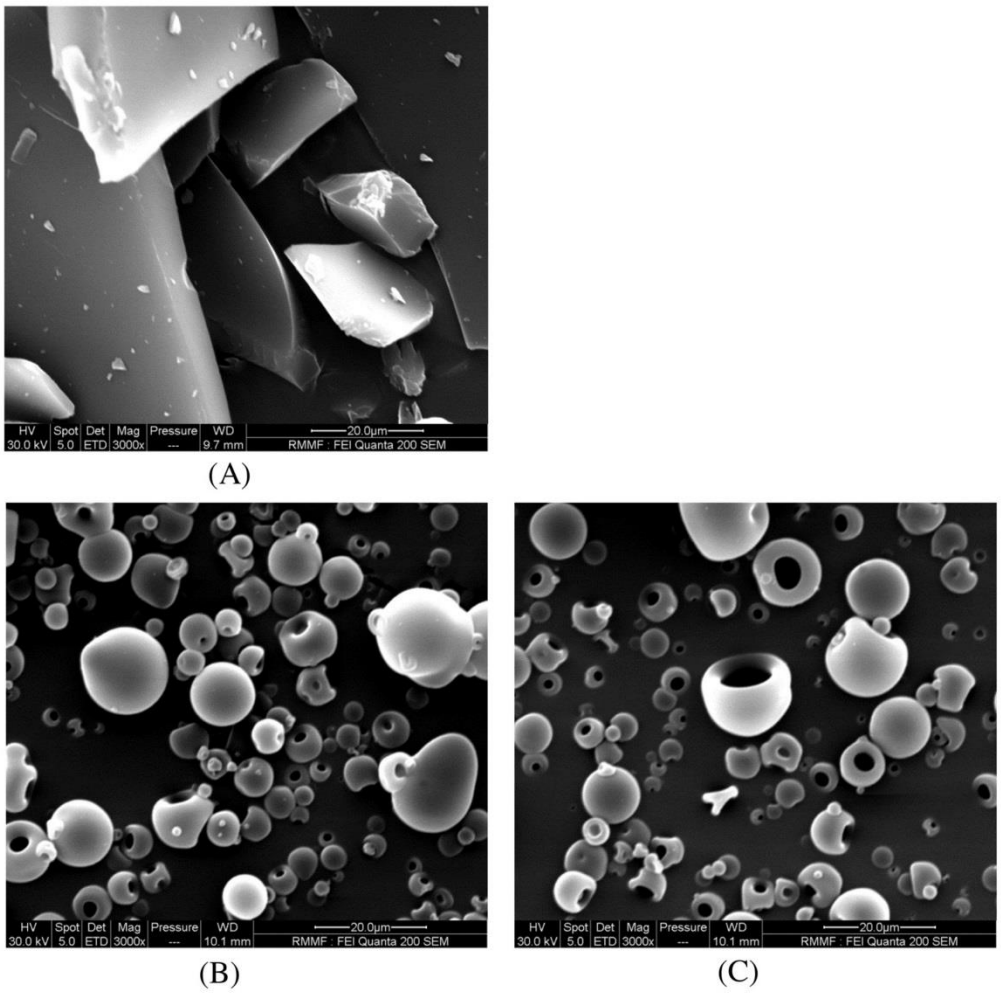

Fig. 1. Scanning electron micrographs (SEM) of spray-dried and freeze-dried LF_b powders. (A) $FDLF_b$: freeze-dried LF_b powder (B) $SDLF_{b70}$: spray-dried LF_b powder at outlet temperature of 70 °C and (C) $SDLF_{b95}$: spray-dried LF_b powder at outlet temperature of 95 °C.

Table 2
The composition of secondary structural features (α-helix, β-sheets, β-turns and random coil) and the extent of denaturation of liquid, spray-dried and freeze-dried LF_b. FD = Freeze-dried LF_b, SD_{70} = Spray-dried LF_b at 70 °C outlet temperature, SD_{95} = Spray-dried LF_b at 95 °C outlet temperature.

Samples	α-helix (%)	β-sheets (%)	β-turns (%)	Random coil (%)	Denaturation (%)
Liquid	21.0 ± 1.2^a	30.9 ± 2.7^a	12.3 ± 0.2^a	35.8 ± 1.6^a	–
FD	21.2 ± 1.2^a	31.4 ± 3.3^a	12.0 ± 0.3^a	35.3 ± 1.9^a	0.9 ± 1.0^a
SD_{70}	21.2 ± 1.5^a	32.7 ± 5.2^a	12.1 ± 0.5^a	34.0 ± 3.2^a	2.0 ± 1.3^a
SD_{95}	20.0 ± 0.6^a	32.2 ± 1.9^a	12.1 ± 0.2^a	35.7 ± 1.6^a	1.2 ± 0.6^a

All the data are expressed as mean ± SD and are the mean of triplicates.
Mean values with different lower case letters in superscript at the same column are significantly different ($p < 0.05$).

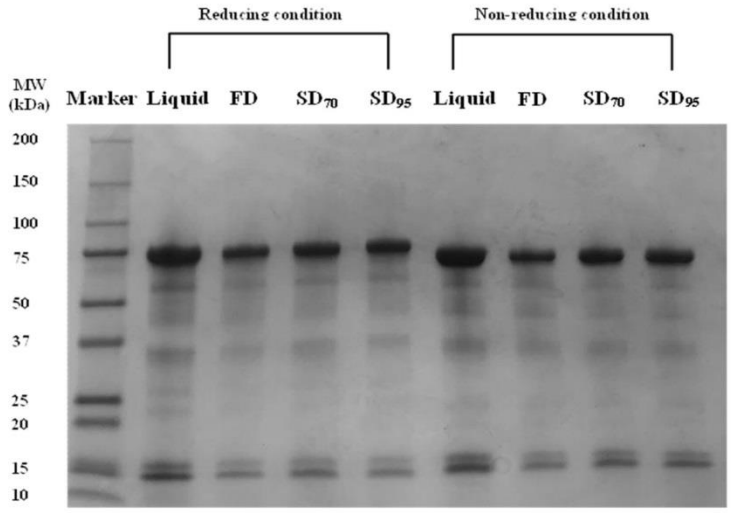

Fig. 2. Protein molecular weight patterns of liquid, freeze-dried and spray-dried LF_b. SD_{70} represents spray-dried LF_b powder at outlet temperature of 70 °C and SD_{95} represents spray-dried LF_b powder at outlet temperature of 95 °C.

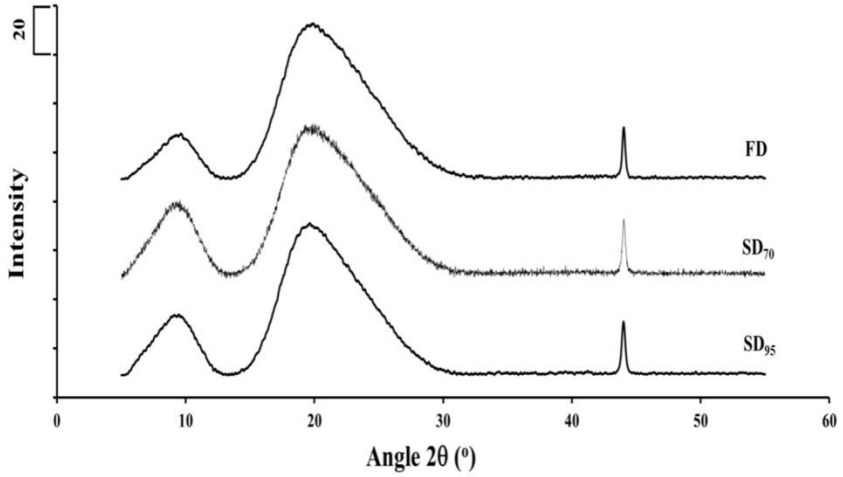

Fig. 3. X-ray diffraction profiles of spray-dried and freeze-dried LF_b powders. FD represents the freeze dried LF_b powder, SD_{70} represents spray-dried LF_b powder at outlet temperature of 70 °C and SD_{95} represents spray-dried LF_b powder at outlet temperature of 95 °C.

native-LF_b [14]. $FDLF_b$ and $SDLF_b$ also exhibited two denaturation peaks at the same temperatures. The denaturation enthalpy (ΔH) values of liquid LF_b, $FDLF_b$, $SDLF_{b70}$ and $SDLF_{b95}$ were 1.35, 1.34, 1.32 and 1.33 J/g, respectively which are not significantly different ($p > 0.05$). Thus, both spray drying and freeze drying methods did not appear to denature LF_b within the process parameters used in this study. These results suggest that low temperature used in freeze drying and very short residence time during spray drying help preserve the native molecular configuration of LF_b and that these processes do not cause significant structural modification. Although, the inlet temperature in the spray drying was 180 °C, due to very high evaporative cooling and high moisture evaporation flux, the actual particle temperature towards the end of the drying process were expected to be close to the outlet temperatures of 70 °C and 95 °C. As the particles reach these temperatures after complete formation of solid structure, the kinetic motion of LF_b molecules is severely limited. These severe limitations in availability of water and molecular motion of LF molecules meant that unfolding of LF_b molecules and subsequent aggregation of unfolded molecules (which are precondition for denaturation during drying) were not favoured. The combination of the cooling effect (fast drying rate) and the short residence time are major factors which help LF_b to retain its native molecular configuration during spray drying. We have shown, in our previous work that about 20% of LF_b can be denatured when LF_b droplet is convectively dried at 95 °C for 10 min [14]. In this case, the single droplet dying experiment used much larger droplet (2.41 mm in diameter) and it was exposed to elevated temperature for much longer time (10 min). Longer exposure at higher temperature together with the presence of abundant water provided favourable conditions for unfolding of LF_b molecules and subsequent aggregation of unfolded molecules which led to denaturation. These findings suggest that the time of exposure and availability of water are much more critical factors than drying temperature in denaturing LF_b. The data presented

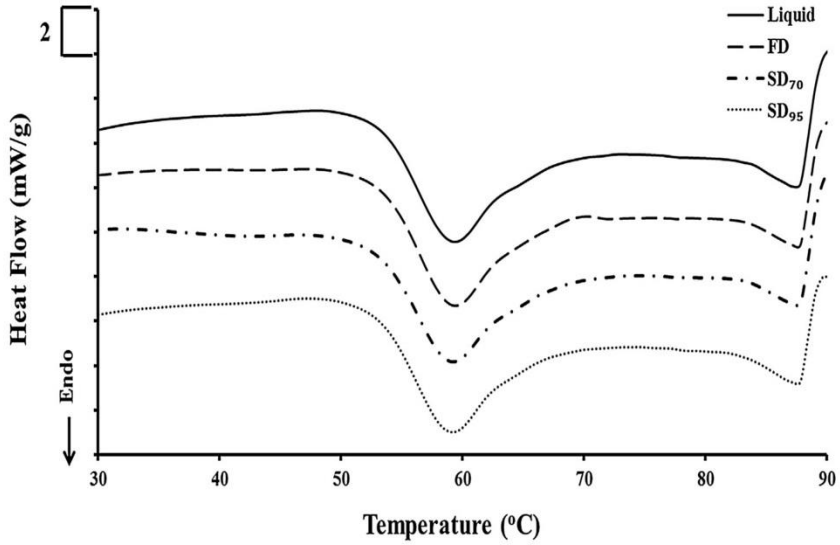

Fig. 4. Differential scanning calorimetric (DSC) thermograms of liquid, spray-dried (SD) and freeze-dried (FD) LF_b powders. SD_{70} = spray-dried LF_b powder at outlet temperature of 70 °C, SD_{95} = spray-dried LF_b powder at outlet temperature of 95 °C.

in Table 2 show that the degree of denaturation of LF_b even at relatively high outlet temperature (95 °C) was similar to that in freeze-dried powders. This indicates that spray drying can be confidently used as an alternative to freeze drying as the former is much more economical.

3.6. Conformation changes in spray-dried and freeze-dried LF_b powders

Far-UV circular dichroism (CD) spectra of liquid LF_b, $FDLF_b$, $SDLF_{b70}$ and $SDLF_{b95}$ are presented in Fig. 5(A). The change in the ellipticity indicates the extent of conformational changes in LF_b caused by the drying process. The spectral curves of liquid LF_b, $SDLF_b$ and $FDLF_b$ showed the highest negative peaks at 210 nm, which correspond to α-helix structure (208 and 222 nm). Similarly, the positive peaks at 195 nm of all LF_b samples correspond to the β-sheet structure (195 and 212 nm). From the CD spectral data, the percentage of helices, turns, sheets and unordered structures of the LF_b samples were calculated by using Dichroweb on-line analysis software and the results are presented in Table 2. The native-LF_b used in this study consisted of 21% α-helix, 31% β-sheets, 12% β-turns and 36% random coil. This observation agrees well with the proportion of its secondary structural features reported in the literature [41]. The proportion of the secondary structural features of $FDLF_b$, $SDLF_{b70}$ and $SDLF_{b95}$ did not have any significant difference ($p > 0.05$) with that of native form in the solution. It indicates that the secondary structural features of $FDLF_b$ and $SDLF_b$ were all preserved during the drying process.

FTIR spectra of liquid LF_b, $SDLF_b$ and $FDLF_b$ powders were recorded in order to complement the findings of CD analysis and to determine the presence of different functional groups. The FTIR spectra of liquid LF_b, $SDLF_{b70}$ and $SDLF_{b95}$ are shown in Fig. 5(B). It can be seen that liquid LF_b had a strong water absorbance peak at 3298 cm^{-1}. For the dried LF_b powders, the intensity of this band is substantially lower than that of the liquid LF_b indicating that large quantity of water is lost during drying process. Lower intensity of this peak in the case of $FDLF_b$ than that of $SDLF_{b70}$ and $SDLF_{b95}$ suggests that $FDLF_b$ had lower moisture content than $SDLF_b$ which corroborated to the moisture content data of these samples (Table 1). Other characteristic IR absorption peaks for liquid LF_b are found at 1645 cm^{-1} (amide-I, C=O and C—N stretching), 1541 cm^{-1} (amide-II, C—N stretching and N—H bending) and 1250 cm^{-1} (amide III, C—N stretching and N—H bending) [45,46]. The dried samples have similar peaks at amide I and amide III, whereas the amide II peaks have shifted either to the left or the right side to that of liquid LF_b depending on the drying method and drying conditions. This shift occurred at 1527 cm^{-1} in the case of $FDLF_b$, at 1553 cm^{-1} in the case of $SDLF_{b70}$ and at 1532 cm^{-1} in the case of $SDLF_{b95}$. The shift of amide II bind is more complex and has not been used as an indicator of the changes in the secondary structure of proteins [47].

3.7. Effect of drying on the antioxidant capacity of LF_b

The antioxidant capacity of LF_b was measured in terms of DPPH radical scavenging capacity and corresponding data for liquid LF_b, $FDLF_b$ and $SDLF_b$ are shown in Fig. 6. The antioxidant capacity of both $SDLF_{b70}$ and $SDLF_{b95}$ were found to be similar to that of the liquid LF_b, i.e. ~52% DPPH inhibition at 6.4 mg mL^{-1} LF_b concentration. On the other hand, the antioxidant capacity of $FDLF_b$ was found to be slightly lower (46% DPPH inhibition at 6.4 mg mL^{-1} LF) compared to that of liquid LF_b. The Lysozyme used in this research for comparison showed less than 22% DPPH inhibition at the same concentration (6.4 mg mL^{-1}). Since all the dried powders had identical conformation and denaturation profiles, the decrease of the antioxidant capacity of $FDLF_b$ could be due to its lower solubility (Table 1) which indicates lower probability of interaction between LF_b and free radical. This reduced scavenging capacity can also be attributed to the reduction of Fe^{3+} in LF_b by oxygen during the long (>18 h) drying process [48].

3.8. Moisture sorption behaviours of spray-dried and freeze-dried LF_b powders

The moisture sorption profiles of $FDLF_b$ and $SDLF_b$ are presented in Fig. 7. These profiles show that both $FDLF_b$ and $SDLF_b$ possessed similar moisture absorption behaviours. The sorption values of these powders were well fitted to GAB model ($R^2 > 0.99$) and the GAB parameters obtained from data fitting are shown in Table 3.

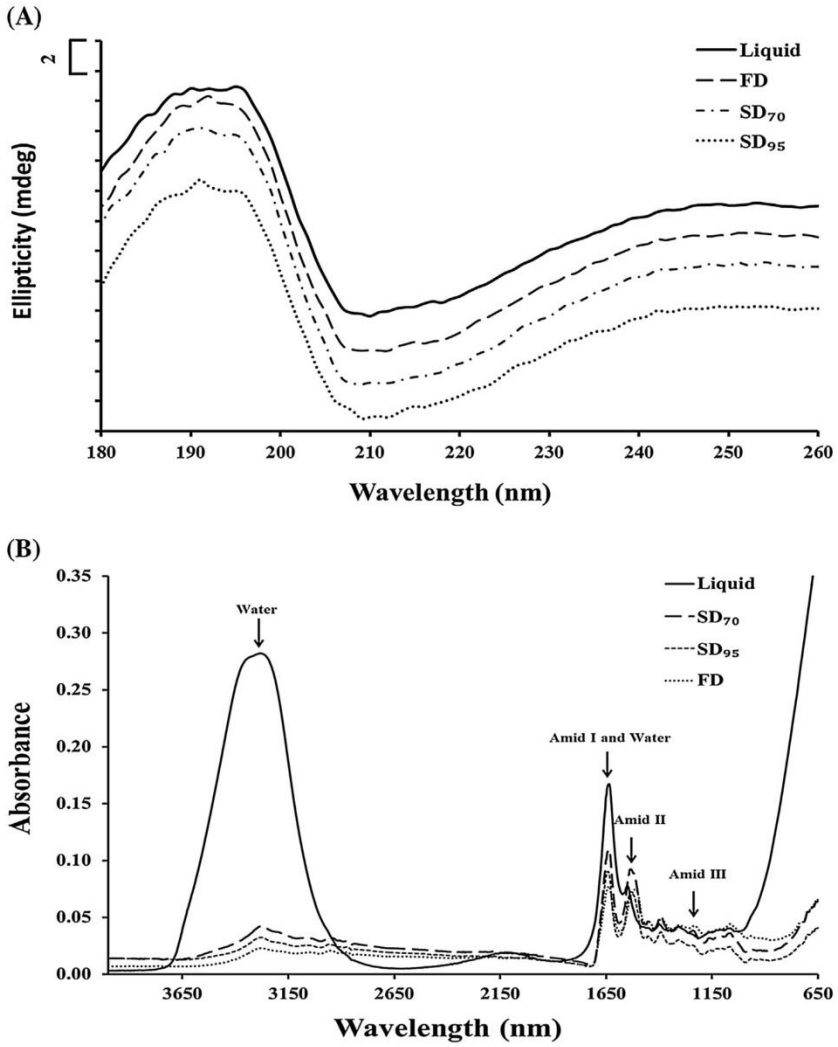

Fig. 5. (A). Circular dichroism (CD) spectra and (B) FTIR spectra of liquid, freeze-dried (FD) and spray-dried (SD) LF_b. SD_{70} = spray-dried LF_b powder at outlet temperature of 70 °C, SD_{95} = spray-dried LF_b powder at outlet temperature of 95 °C.

Table 3
GAB model constants for LF_b powders. FD = Freeze-dried LF_b, SD_{70} = Spray-dried LF_b at 70 °C outlet temperature, SD_{95} = Spray-dried LF_b at 95 °C outlet temperature.

GAB model Equation: $\frac{m}{M_0} = \frac{CKa_W}{(1-Ka_W)[1-Ka_W+CKa_W]}$

Samples	Constant			
	M_0	C	K	R^2
FD	0.072	16.107	0.793	0.998
SD_{70}	0.073	24.029	0.790	0.998
SD_{95}	0.074	22.223	0.780	0.997

The M_0 parameter corresponds to the monolayer moisture content which is strongly adsorbed to the molecules [30]. C indicates the difference in free enthalpy of the water molecules between monolayer and multi-layer. K represents the energetic interactions between water molecules across multi-layers and the bulk liquid phase [49]. Typically, if C values are higher than 2, it is considered to be type II isotherms [49]. The M_0 and K values of $FDLF_b$ and $SDLF_b$ are very close to each other, while the C value of the samples shows a variation from 16.107 ($FDLF_b$) to 24.029 ($SDLF_{b70}$). Therefore, both $FDLF_b$ and $SDLF_b$ exhibit type II moisture sorption isotherms. They shared similar water binding affinity on the monolayer, but different affinity at the multi-layers. The hollow structures of $SDLF_b$ (Fig. 1) may affect the vapor pressure when it holds water inside and change the enthalpy of water molecules thus showing lower affinity towards bulk water.

4. Conclusions

LF_b powders were produced through spray drying and freeze drying processes using freshly obtained industrial sample of liquid LF_b as starting material. The spray drying process with inlet temperature of 180 °C and outlet temperature of 95 °C produced $SDLF_b$ powders with 5.2% (w/w) moisture content while the moisture content of the $FDLF_b$ was much lower (2.7%, w/w). The solubility of both $SDLF_b$ and $FDLF_b$ in water was >94% indicating negligible

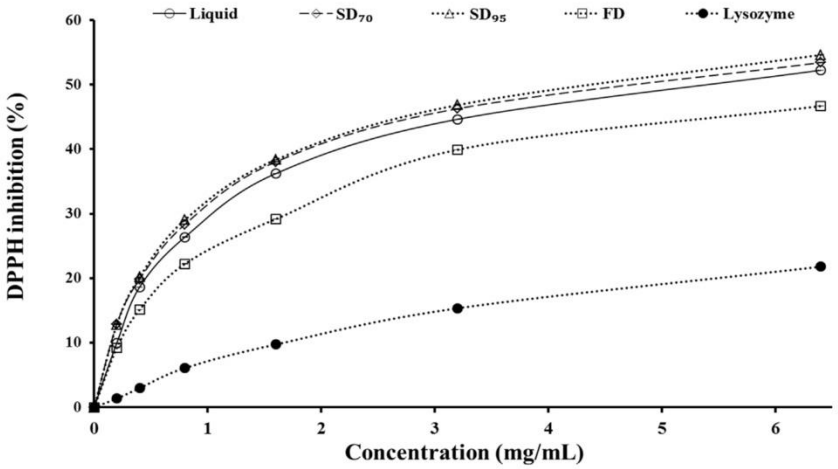

Fig. 6. Radical scavenging capacity of liquid, freeze-dried (FD) and spray-dried (SD) LF_b. SD_{70} = spray-dried LF_b powder at outlet temperature of 70 °C, SD_{95} = spray-dried LF_b powder at outlet temperature of 95 °C.

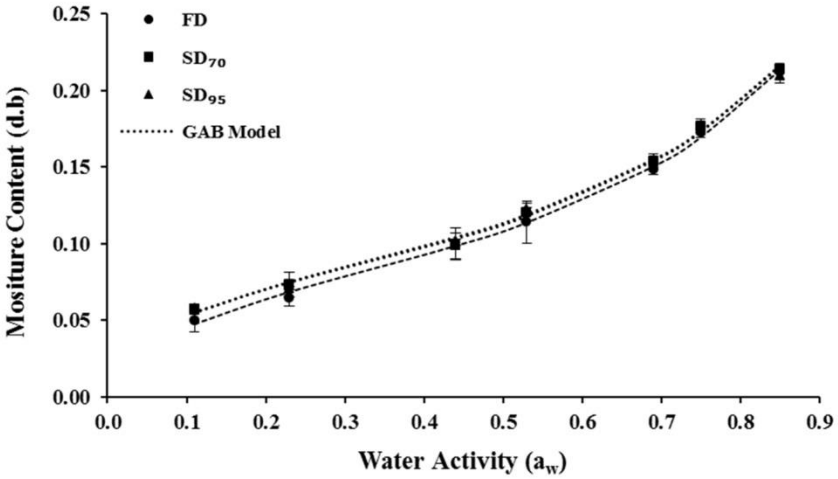

Fig. 7. Change of sorption isotherm of LF_b powders. FD = Freeze-dried LF_b, SD_{70} = Spray-dried LF_b at 70 °C outlet temperature, SD_{95} = Spray-dried LF_b at 95 °C outlet temperature.

denaturation induced insolubility in powders. The fact that the LF_b did not denature during spray and freeze drying processes was further corroborated by absence of observable changes in the secondary structural features and observation of identical denaturation enthalpy values of $SDLF_b$ and $FDLF_b$ and liquid LF_b. The moisture sorption properties of $SDLF_b$ and $FDLF_b$ were similar to each other, sharing an identical type II sorption behaviour. The antioxidant activity of $SDLF_b$ was close to that of fresh liquid LF_b while it was ~6% less in the case of $FDLF_b$. This work shows that spray drying can be confidently used to produce amorphous LF_b powders with intact molecular configuration and high antioxidant capacities.

Acknowledgment

The authors gratefully acknowledge Tatura Milk Industries Ltd. (Subsidiary of Bega Cheese, Australia) for kindly donating freshly produced native bovine lactoferrin for this study.

References

[1] P.L. Masson, J.F. Heremans, Lactoferrin in milk from different species, Comp. Biochem. Physiol. Part B: Comp. Biochem. 39 (1) (1971), 119–IN13.
[2] Y. Hirai, N. Kawakata, K. Satoh, Y. Ikeda, S. Hisayasu, H. Orimo, Y. Yoshino, Concentrations of lactoferrin and iron in human milk at different stages of lactation, J. Nutr. Sci. Vitaminol. (Tokyo) 36 (6) (1990) 531–544.
[3] B. Lönnerdal, S. Iyer, Lactoferrin: molecular structure and biological function, Annu. Rev. Nutr. 15 (1) (1995) 93–110.
[4] F.L. Schanbacher, R.E. Goodman, R.S. Talhouk, Bovine mammary lactoferrin: implications from messenger ribonucleic acid (mRNA) sequence and regulation contrary to other milk proteins, J. Dairy Sci. 76 (12) (1993) 3812–3831.
[5] A. Sreedhara, R. Flengsrud, T. Langsrud, P. Kaul, V. Prakash, G.E. Vegarud, Structural characteristic, pH and thermal stabilities of apo and holo forms of caprine and bovine lactoferrins, Biometals 23 (6) (2010) 1159–1170.
[6] J. Artym, M. Zimecki, The role of lactoferrin in the proper development of newborns, Adv. Hyg. Exp. Med. 59 (2005) 421–432.
[7] M.M. El-Loly, M.B. Mahfouz, Lactoferrin in relation to biological functions and applications: a review, Int. J. Dairy Sci. 6 (2) (2011) 79–111.
[8] M. Tomita, H. Wakabayashi, K. Shin, K. Yamauchi, T. Yaeshima, K. Iwatsuki, Twenty-five years of research on bovine lactoferrin applications, Biochimie 91 (1) (2009) 52–57.
[9] L. Cao, H. Maas, Heat-stable, aqueous lactoferrin composition and its preparation and use. U.S. Patent No. 8, 999, 923, 7th April 2015.

[10] C. Ratti, Freeze drying process design, in: S. Rahman, J. Ahmed (Eds.), Handbook of Food Process Design, John Wiley & Sons, New York, 2012, pp. 621–647.
[11] C. Chen, Y.J. Chi, W. Xu, Comparisons on the functional properties and antioxidant activity of spray-dried and freeze-dried egg white protein hydrolysate, Food Bioprocess Technol. 5 (6) (2012) 2342–2352.
[12] M.A. Haque, P. Aldred, J. Chen, C. Barrow, B. Adhikari, Drying and denaturation characteristics of α-lactalbumin, β-lactoglobulin, and bovine serum albumin in a convective drying process, J. Agric. Food Chem. 62 (20) (2014) 4695–4706.
[13] A. Ghodsvali, M.H. Khodaparast, M. Vosoughi, L.L. Diosady, Preparation of canola protein materials using membrane technology and evaluation of meals functional properties, Food Res. Int. 38 (2) (2005) 223–231.
[14] B. Wang, Y.P. Timilsena, E. Blanch, B. Adhikari, Drying and denaturation characteristics of three forms of bovine lactoferrin, Drying Technol. (2016), http://dx.doi.org/10.1080/07373937.2016.1196699, Article in press.
[15] J.M. Steijns, A.C.M. Van Hooijdonk, Occurrence, structure, biochemical properties and technological characteristics of lactoferrin, Br. J. Nutr. 84 (S1) (2000) 11–17.
[16] M.A. Haque, B. Adhikari, Drying and denaturation of proteins in spray drying process, in: A. Mujumdar (Ed.), Handbook of Industrial Drying, CRC Press, Florida, 2015, pp. 971–981.
[17] E. Cepeda, M.C. Villaran, N. Aranguiz, Functional properties of faba bean (*Vicia faba*) protein flour dried by spray drying and freeze drying, J. Food Eng. 36 (3) (1998) 303–310.
[18] A. Millqvist-Fureby, M. Malmsten, B. Bergenståhl, Spray-drying of trypsin—surface characterisation and activity preservation, Int. J. Pharm. 188 (2) (1999) 243–253.
[19] I. Filkova, L.X. Huang, A.S. Mujumdar, Industrial spray drying systems, in: A. Mujumdar (Ed.), Handbook of Industrial Drying, CRC Press, Florida, 2015, pp. 191–225.
[20] M. Joshi, B. Adhikari, P. Aldred, J.F. Panozzo, S. Kasapis, Physicochemical and functional properties of lentil protein isolates prepared by different drying methods, Food Chem. 129 (4) (2011) 1513–1522.
[21] G. Chegini, M. Taheri, Whey powder: process technology and physical properties: a review, Middle-East J. Sci. Res. 13 (10) (2013) 1377–1387.
[22] C. Anandharamakrishnan, C.D. Rielly, A.G.F. Stapley, Effects of process variables on the denaturation of whey proteins during spray drying, Drying Technol. 25 (5) (2007) 799–807.
[23] P. Smith, R.I. Krohn, G.T. Hermanson, A.K. Mallia, F.H. Gartner, M. Provenzano, et al., Measurement of protein using bicinchoninic acid, Anal. Biochem. 150 (1) (1985) 76–85.
[24] J.G. Lees, A.J. Miles, F. Wien, B.A. Wallace, A reference database for circular dichroism spectroscopy covering fold and secondary structure space, Bioinformatics 22 (16) (2006) 1955–1962.
[25] L. Whitmore, B.A. Wallace, Protein secondary structure analyses from circular dichroism spectroscopy: methods and reference databases, Biopolymers 89 (5) (2008) 392–400.
[26] S.C. Nicklisch, J.H. Waite, Optimized DPPH assay in a detergent-based buffer system for measuring antioxidant activity of proteins, MethodsX 1 (2014) 233–238.
[27] M.A. Haque, B. Adhikari, A. Putranto, Predictions of drying kinetics of aqueous droplets containing WPI-lactose and WPI-trehalose by application of composite reaction engineering approach (REA), J. Food Eng. 189 (2016) 29–36.
[28] W.E.L. Spiess, W. Wolf, Critical evaluation of methods to determine moisture sorption isotherms, in: L.B. Rockland, L.R. Beuchat (Eds.), Water Activity: Theory and Applications to Food, Marcel Dekker, Inc, New York, 1987, pp. 215–233.
[29] W. Wolf, W.E.L. Spiess, G. Jung, Standardization of isotherm measurements (Cost-Project 90 and 90 BIS), in: D. Simatos, J.L. Multon (Eds.), Properties of Water in Foods, Martinus Nijhoff Publishers, Boston, 1985, pp. 661–681.
[30] T.A. Comunian, E.S. Monterrey-Quintero, M. Thomazini, J.C. Balieiro, P. Piccone, P. Pittia, C.S. Favaro-Trindade, Assessment of production efficiency, physicochemical properties and storage stability of spray-dried chlorophyllide, a natural food colourant, using gum Arabic, maltodextrin and soy protein isolate based carrier systems, Int. J. Food Sci. Technol. 46 (6) (2011) 1259–1265.
[31] F. Guyomarc'h, F. Warin, D.D. Muir, J. Leaver, Lactosylation of milk proteins during the manufacture and storage of skim milk powders, Int. Dairy J. 10 (12) (2000) 863–872.
[32] Y.F. Maa, P.A. Nguyen, J.D. Andya, N. Dasovich, T.D. Sweeney, S.J. Shire, C.C. Hsu, Effect of spray drying and subsequent processing conditions on residual moisture content and physical/biochemical stability of protein inhalation powders, Pharm. Res. 15 (5) (1998) 768–775.
[33] W. Suthabanditpong, C. Takai, M. Fuji, R. Buntem, T. Shirai, Improved optical properties of silica/UV-cured polymer composite films made of hollow silica nanoparticles with a hierarchical structure for light diffuser film applications, Phys. Chem. Chem. Phys. 18 (24) (2016) 16293–16301.
[34] X. Hu, Y. Cheng, J. Fan, Z. Lu, K. Yamaki, L. Li, Effects of drying methods on physicochemical and functional properties of soy protein isolates, J. Food Process. Preserv. 34 (2010) 520–540.
[35] A.K. Sumner, M.A. Nielsen, C.G. Youngs, Production and evaluation of pea protein isolate, J. Food Sci. 46 (1981) 364–372.
[36] B. Adhikari, T. Howes, A.K. Shrestha, B.R. Bhandari, Development of stickiness of whey protein isolate and lactose droplets during convective drying, Chem. Eng. Process. Process Intensif. 46 (5) (2007) 420–428.
[37] N. Fu, M.W. Woo, X.D. Chen, Colloidal transport phenomena of milk components during convective droplet drying, Colloids Surf. B: Biointerfaces 87 (2) (2011) 255–266.
[38] B. Adhikari, T. Howes, B.R. Bhandari, V. Troung, Effect of addition of maltodextrin on drying kinetics and stickiness of sugar and acid-rich foods during convective drying: experiments and modelling, J. Food Eng. 62 (1) (2004) 53–68.
[39] F.F. Costa, M.A.V.P. Brito, M.A.M. Furtado, M.F. Martins, M.A.L. de Oliveira, P.M. de Castro Barra, et al., Microfluidic chip electrophoresis investigation of major milk proteins: study of buffer effects and quantitative approaching, Anal. Methods 6 (6) (2014) 1666–1673.
[40] H. Bokkhim, N. Bansal, L. Grøndahl, B. Bhandari, *In-vitro* digestion of different forms of bovine lactoferrin encapsulated in alginate micro-gel particles, Food Hydrocoll. 52 (2016) 231–242.
[41] T. David-Birman, A. Mackie, U. Lesmes, Impact of dietary fibers on the properties and proteolytic digestibility of lactoferrin nano-particles, Food Hydrocoll. 31 (1) (2013) 33–41.
[42] B. Wang, Y.P. Timilsena, E. Blanch, B. Adhikari, Mild thermal treatment and *in-vitro* digestion of three forms of bovine lactoferrin: effects on functional properties, Int. Dairy J. 64 (2017) 22–30.
[43] D. Legrand, A. Pierce, E. Elass, M. Carpentier, C. Mariller, J. Mazurier, Lactoferrin structure and functions, in: Z. Bosze (Ed.), Bioactive Components of Milk, Springer, New York, 2008, pp. 163–194.
[44] A.K. Sharma, T.P. Singh, Lactoferrin–metal interactions: first crystal structure of a complex of lactoferrin with a lanthanide ion (Sm^{3+}) at 3.4 Å resolution, Acta Crystallogr. Sect D: Biol. Crystallogr. 55 (11) (1999) 1799–1804.
[45] J. Kong, S. Yu, Fourier transform infrared spectroscopic analysis of protein secondary structures, Acta Biochim. Biophys. Sin. 39 (8) (2007) 549–559.
[46] Y.P. Timilsena, R. Adhikari, C.J. Barrow, B. Adhikari, Physicochemical and functional properties of protein isolate produced from Australian chia seeds, Food Chem. 212 (2016) 648–656.
[47] W. Gallagher, FTIR Analysis of Protein Structure, Course Manual Chem 2009 [Online], 2009, Available from http://download.bioon.com.cn/view/upload/201110/10233820_7954.pdf. (accessed 23.10.16).
[48] K.L. Fong, P.B. McCay, J.L. Poyer, H.P. Misra, B.B. Keele, Evidence for superoxide-dependent reduction of Fe^{3+} and its role in enzyme-generated hydroxyl radical formation, Chem. Biol. Interact. 15 (1) (1976) 77–89.
[49] A.M. Ceballos Peñaloza, G.I. Giraldo Gómez, C.E. Orrego Alzate, J. Telis-Romero, Sorption thermodynamics of soursop powders obtained by different dehydration technologies, Revista Facultad Nacional de Agronomña, Medellñn 66 (2) (2013) 7107–7116.

CHAPTER 5

In-vitro Digestion Study of Lactoferrin

Published in *International Dairy Journal*, 2017, 64, 22-30

International Dairy Journal 64 (2017) 22–30

Contents lists available at ScienceDirect

International Dairy Journal

journal homepage: www.elsevier.com/locate/idairyj

Mild thermal treatment and in-vitro digestion of three forms of bovine lactoferrin: Effects on functional properties

Bo Wang [a], Yakindra Prasad Timilsena [a, b], Ewan Blanch [a], Benu Adhikari [a, b, *]

[a] School of Science, RMIT University, Melbourne, VIC 3083, Australia
[b] CSIRO Manufacturing Flagship, Clayton South, VIC 3169, Australia

ARTICLE INFO

Article history:
Received 15 June 2016
Received in revised form
30 August 2016
Accepted 7 September 2016
Available online 16 September 2016

ABSTRACT

In-vitro digestion behaviour of iron saturated (holo)-, native- and iron depleted (apo)- bovine lactoferrin (LF) was studied in simulated oral, gastric and intestinal digestion conditions. All LFs were hydrolysed to <10 kDa peptides; 93% of iron was released from holo-LF within 2 h of gastric digestion. Iron binding ability of all the three LFs was decreased by 80–90% during gastric digestion, while antioxidant activities at the end of gastric digestion were 3–8 times higher than those at the end of oral and intestinal digestion. Antioxidant activity of apo-LF was higher than that of holo-LF after gastric and intestinal digestion. Gastric and intestinal digestion of all the three forms of LF produced negatively charged peptides or amino acids. There were only minor differences among the three forms of LF in terms surface charge, hydrolysis patterns and iron binding/release characteristics between heated and unheated LF samples after gastric digestion.

1. Introduction

Lactoferrin (LF) is an iron-binding protein present in bovine and human milk in a concentration range of 0.02–0.2 mg mL^{-1} and 2.0–7.0 mg mL^{-1}, respectively (Masson & Heremans, 1971). As a member of the transferrin family, LF helps transfer iron and facilitates the absorption of sugars (Artym & Zimecki, 2005; Uchida, Oda, Sato, & Kawakami, 2006). It also performs many other biological functions such as providing defence against infection and inflammation (Britigan, Serody, & Cohen, 1994; El-Loly & Mahfouz, 2011; Ripolles et al., 2015; Wakabayashi, Yamauchi, & Takase, 2006), modulating cell growth and inhibiting the formation of several toxic compounds, namely lipopolysaccharide and glycosamino-glycan (Baveye, Elass, Mazurier, Spik, & Legrand, 1999). Because these important functions, LF is generally added to functional foods, therapeutic drinks, and other food supplements as well as being used in cosmetics.

The functional properties of LF, especially iron binding ability, are highly dependent on its unique structure. LF consists of two homologous globular lobes (N-lobe and C-lobe), and each lobe can bind an iron atom (Fe^{2+} or Fe^{3+}) in synergy with the binding of one carbonate ion (Baker & Baker, 2004). Due to the presence of carbonate, the bond between LF and iron remains intact even at pH values as low as 4.0, but below this pH it tends to break down (Baker & Baker, 2004; Sreedhara et al., 2010). Based on its iron-saturation level, LF exists in three different forms: iron depleted (apo-LF), iron saturated (holo-LF) and partially iron associated (mono-LF) (García-Montoya, Cendón, Arévalo-Gallegos, & Rascón-Cruz, 2012; Levay & Viljoen, 1995). Information available in the literature shows that holo-LF possesses a more compact structure and is more resistant to thermal stress, whereas apo-LF has the least stability to thermal stress (Bokkhim, Bansal, Grøndahl, & Bhandari, 2013; Iafisco, Foltran, Di Foggia, Bonora, & Roveri, 2010; Yao, Bunt, Cornish, Quek, & Wen, 2013).

The demand for LF has increased in the past few decades due to the fact that consumers are becoming aware of its several beneficial functions. Due to this increased interest, lactoferrin is isolated from bovine, human and goat milks; however, currently available commercial LF mainly comes from bovine sources. For this reason, bovine LF is widely utilised as a high value food protein and also as a therapeutic agent in food and medical industries (Tomita et al., 2009). Interestingly, lactoferrin finds better application in pharmaceutical field than in food.

Available literature indicates that contemporary research on lactoferrin is largely focused on developing processes to improve its

* Corresponding author. Tel.: +61 3 992 59940.
E-mail address: benu.adhikari@rmit.edu.au (B. Adhikari).

http://dx.doi.org/10.1016/j.idairyj.2016.09.001
0958-6946/

yield and quality. One such research endeavour reported that the pasteurisation of LF at 72 °C for 15 s did not result in a loss of immunoreactivity (Navarro, Harouna, Calvo, Pérez, & Sánchez, 2015). In another study, it was reported that LF was thermally stable at pH 4.0 even when it was subjected to 90 °C and it did not suffer any significant loss in its physicochemical properties (Cao & Maas, 2015; Saito, Takase, Tamura, Shimamura, & Tomita, 1994). However, damage may occur through inappropriate heat treatment. The molecular modelling study of native- and heat treated LF (80 °C, 10 min) showed that the elements of regular secondary structure decreased with increased temperature (Stănciuc et al., 2013). Consequently, 15–30% iron binding capacity of bovine native-LF was lost after heating at 90 °C for 4 min (Kawakami, Tanaka, Tatsumi, & Dosako, 1992). Similarly, a 50% loss of iron binding ability of human native-LF was observed after heating at 85 °C for 20 min (Mata, Sánchez, Headon, & Calvo, 1998).

These studies revealed that LF is very sensitive to heat treatment. Interestingly, when LF is saturated with iron, its denaturation temperature increased from ~60 °C to ~90 °C (Bokkhim et al., 2013; Wang, Timilsena, Blanch, & Adhikari, 2016). These observations suggest that the increase in iron saturation level can improve the thermal stability of LF. However, there is very limited information in the literature regarding the loss of anti-oxidant activity and iron-binding properties during digestion processes.

Previously reported in vivo and in vitro digestion studies suggested that up to 40% of apo-LF is degraded under gastric conditions, whereas holo-LF is more stable and is degraded only up to 20% under similar conditions (Bokkhim, Bansal, Grøndahl, & Bhandari, 2016; Troost, Steijns, Saris, & Brummer, 2001). Publications available in the literature have also report that the native-LF is completely degraded under gastric digestion. However, there is no study that compares the fate of all the three forms of LF at different phases (oral, gastric and intestinal) of digestion (David-Birman, Mackie, & Lesmes, 2013; Furlund et al., 2013). Therefore, further research is needed to better understand the digestion pattern of all the three forms of lactoferrin in the human gastro-intestinal environment.

Iron is an essential element for growth and survival of all living organisms because it is required as a cofactor for essential enzymes that are involved in many basic cellular functions and metabolic pathways. However, the ferric form of iron (Fe^{3+}) is insoluble in aqueous medium and at physiological pH and thus unavailable at the site of action. In addition, free iron catalyses reactions that produce free oxygen radicals that are highly toxic to cells. These oxygen radicals cause denaturation of proteins, breaking down of DNA and peroxidation of lipids. Therefore, the iron bound to specific proteins, such as blood serotransferrin, lactoferrin and ferritin is beneficial to living organisms (Schaible & Kaufmann, 2004). If intact LF is delivered to the proximal pyloric portion of the small intestine, it can bind with free oxygen radicals and help protect the human body from their detrimental effects (Pan, Rowney, Guo, & Hobman, 2007). For this reason it is essential that LF reaches the targeted portion of human gastrointestinal tract in a structurally intact and biologically active condition (Lönnerdal & Kelleher, 2009). If LF is denatured due to thermal processing and is further degraded by gastric fluids, the functional domains of LF can be destroyed. In this case it is likely that the LF loses its bio-functional properties such as transporting iron and combating free oxygen radicals.

Among the three different forms of lactoferrin, holo-LF has the most compact structural conformation, which is believed to make it the most heat resistant of the three forms. The highest degree of thermal resistance of holo-LF is corroborated by its highest denaturation temperature (Bokkhim et al., 2013). The compact molecular conformation and the highest denaturation temperature make the holo-LF more stable and more capable to protect its bio-functionality during digestion (Bokkhim et al., 2016). It has also been reported that the native or undenatured form of LF possesses moderate antioxidant activity in gastrointestinal environment (Medina, Tombo, Satué, German, & Frankel, 2002). However, the anti-oxidant activity of apo- and holo-LFs and the effects of thermal stress and gastrointestinal digestion environment on this property are not available in the literature.

In this research, we investigated the effect of isothermal heat treatment (IHT) on the digestion and functional activities of three forms of LF. The choice of temperature for IHT used in this study was based on our previous study (Wang et al., 2016). It was found that 26.5%, 19.7% and 11.2% of apo-, native- and holo-LF, respectively, were denatured in convective air drying carried out at 70 °C for 10 min. In addition, holo-LF tends to lose iron and hence form iron-hydroxide precipitate when heated at temperatures higher than 80 °C (Bates & Schlabach, 1973; Kawakami et al., 1992). The in vitro digestion system used in this study simulated the adult gastro-intestinal environment including oral, gastric and intestinal stages. The extent and the nature of degradation of lactoferrin during the in vitro digestion was monitored using sodium dodecyl polyacrylamide gel electrophoresis (SDS-PAGE). The changes in the zeta potential (electrostatic charge) and secondary structural features were measured at oral, gastric and intestinal digestion stages to gain a better insight into the effects of these stages on the structure and property of lactoferrin. The changes in the iron release/binding ability and anti-oxidant activity of all three forms of LF in these three digestion stages were also studied.

2. Materials and methods

2.1. Materials and sample preparation

Bovine lactoferrin was received by courtesy of Tatura Milk Industries Ltd. (a subsidiary of Bega Cheese, Australia). α-Amylase, mucin, pepsin (1891 U mg^{-1}), bile salts and 2,2-diphenyl-1-picrylhydrazyl were purchased from Sigma–Aldrich (NSW, Australia). Pancreatin (Catalogue no. 02102557) was purchased from MP Bio-medicals (Welland, Australia). Mini-PROTEAN® TGX™ gels, WesternC blotting protein standards (Catalogue no. 1610376), Laemmli sample buffer, Tris/Glycine/SDS buffer, β-mercaptoethanol and Coomassie Brilliant Blue R-250 solution were purchased from Bio-Rad (Victoria, Australia). All chemicals used in this work were of analytical grade and were used as received.

The apo and holo forms of LF were prepared according to literature with some modifications (Feng, Van Der Does, & Bantjes, 1995; Van Berkel et al., 1995). Briefly, apo-LF was prepared by dissolving 20 mg mL^{-1} native-LF in 0.2 M sodium phosphate buffer, pH 4.0. This solution was equilibrated overnight and then dialysed for 2 days against Milli-Q water with frequent changes of water. Holo-LF was prepared by dissolving 20 mg mL^{-1} native-LF in 0.1 M citrate/phosphate buffer (pH 7.4). It was then mixed with freshly prepared ferric nitrilotriacetic acid (FeNTA) solution to achieve an iron-to-LF molar ratio of 2:1. This LF-FeNTA blend was incubated at ambient temperature for 1 h. It was then dialysed using a cellulose membrane against Milli-Q water for 48 h under constant stirring with frequent changes of water. The native bovine lactoferrin as received from the supplying company was used as a control sample without any further treatment or modification. The protein content of apo, native and holo forms of LF used in this study was measured by bicinchoninic acid (BCA) assay method and found to be 97.0 ± 1.6%, 91.0 ± 2.1% and 100.0 ± 3.1%, respectively.

The iron saturation levels of apo-, native- and holo-lactoferrin were determined by the ratios of absorbance at 280 and 466 nm using an UV–Vis spectrophotometer (Cary 60, Agilent Technology,

Australia) according to a previously reported method (Majka et al., 2013) and were found to be 4.5 ± 1.4%, 9.5 ± 0.6% and 83.6 ± 4.1%, respectively. We used native lactoferrin commercially produced in Australia. The often reported values of iron saturation in native LF vary from 10 to 20%. Both apo-LF and holo-LF samples were converted to powder using a laboratory scale freeze-dryer (Advantage Pro, Scitek, NSW, Australia). The moisture content of all the three forms of LF powders was measured using an IR-based moisture meter (Moisture Analyser - IC-MB45, OHaus, Switzerland) and was found to be 2.0–2.2% (on wet basis).

2.2. Isothermal heat treatment

For isothermal heat treatment (IHT), all the three types of LF powders were individually dissolved in Milli-Q water to make a final concentration of 16% (w/v). The sample solution was transferred to a sample vial and the vial was lowered into a water bath maintained at 70 °C. It was ensured that the water level at the outer surface of vial was always higher than the level of LF solution inside the vial. The temperature of the sample solution was brought to 70 °C and then maintained at this temperature for 10 min. Microthermocouples were inserted into an additional vial containing the same amount of solution to record the temperature history. After the completion of the heating process, the sample solutions were immediately cooled down to room temperature (25 °C) by lowering the vials in another water bath which contained chilled water.

2.3. In vitro digestion of LF

The in vitro digestion experiment consisted of 20 mL Falcon tubes mounted in a digitally controlled shaking water bath (MaXturdy 30, Daihan Scientific, South Korea). The temperature of the water bath and the agitation rate were maintained at 37 °C and 95 rpm, respectively.

2.3.1. Preparation of simulated oral fluid and oral digestion

The simulated oral fluid (SOF) was prepared according to a previously reported method (Minekus et al., 2014). For this purpose, specified quantities of salts (521 mg $NaHCO_3$, 137 mg $K_2HPO_4 \cdot 3H_2O$, 88 mg NaCl, 48 mg KCl, 41 mg $CaCl_2$) were dissolved in 100 mL Milli-Q water. Then, 216 mg mucin and 20,000 U α-amylase were added to the solution and the pH was adjusted to 7.0 using 1.0 M HCl or 1.0 M NaOH. The digestion, under these simulated oral conditions, was carried out by addition of 750 μL pre-warmed SOF to 750 μL LF solutions and incubating at 37 °C for 2 min in the above mentioned shaking water bath. After 2 min digestion, a portion of the digesta was separated for immediate analysis and the remainder was stored in −20 °C to arrest further α-amylase–substrate reaction.

2.3.2. Preparation of simulated gastric fluid and gastric digestion

Simulated gastric fluid (SGF) was prepared by mixing 200 mg NaCl and 106 mg pepsin in 100 mL Milli-Q water to maintain the final concentration of pepsin at 2000 U mL^{-1}. The final pH was adjusted to 2.0 using 1.0 M HCl. To initiate gastric digestion, 1.5 mL of pre-warmed SGF (37 °C) solution was added to 1.5 mL of oral digesta of LF to achieve a pepsin-to-lactoferrin ratio of 1:80 (w/w). The mixture was incubated at 37 °C using a water bath for 2 h after adjusting the pH to 2.0 using 1.0 M HCl or 1.0 M NaOH. The pH was monitored continuously and adjusted to 2.0 by drop-wise addition of 1.0 M HCl or 1.0 M NaOH during incubation period. After completion of the gastric digestion, a portion of the sample was taken for immediate analysis and the remaining portion of the sample frozen at −20 °C to stop pepsin-substrate reaction.

2.3.3. Preparation of simulated intestinal fluid and intestinal digestion

Simulated intestinal fluid (SIF) was prepared as reported by Minekus et al. (2014). For this purpose, 680 mg monobasic potassium phosphate, 876 mg sodium chloride, 500 mg bile salts and 640 mg pancreatin (1 U mg^{-1}) were dissolved in 100 mL Milli-Q water and the final pH was adjusted to 7.0. The intestinal digestion was initiated by the addition of 3 mL of pre-warmed SIF (37 °C). The pH was adjusted to 7.0 initially and also during the incubation period of 2 h by intermittently adding 1.0 M NaOH or 1.0 M HCl. After completion of the intestinal digestion, a portion of the sample was taken for immediate analysis and the part of the sample was stored at −20 °C to terminate the pancreatin-substrate reaction.

2.4. Acquiring degradation patterns of the LF fragments

The degradation patterns and the change in molecular mass of all three forms of LF subjected to and not subjected to (control) IHT were examined using sodium SDS-PAGE. The experiment was performed with a 4–15% precast polyacrylamide gel under reducing conditions. For this purpose, the digesta from oral digestion (SOF), gastric digestion (SOF + SGF) and intestinal digestion (SOF + SGF + SIF) were diluted to 2 mg mL^{-1} by addition of Milli-Q water. Then, 100 μL of this diluted solution was mixed with an equal volume of SDS-loading buffer (95% 2 × Laemmli buffer and 5% β-mercaptoethanol). These mixtures were heated at 95 °C for 5 min. Five microlitres of the heated samples were loaded onto the precast gels. Ten microlitres of WesternC™ blotting protein standard was also loaded onto each gel as a molecular mass marker. The Mini-Protean Tetra Cell was equilibrated at 100 V for 10 min before sample loading. The experiment was further run at 15 V for 10 min with standards and samples. Then, the voltage was raised to 100 V and maintained at this level for 75 min. The precast gel was removed and dyed with 0.1% (w/v) Coomassie Brilliant Blue R-250 solution on a shaker (40 rpm) overnight at ambient temperature. It was then de-stained using de-staining solution containing 10% (w/v) acetic acid and 40% (w/v) methanol for 2 h. Multiple washing was carried out with frequent changes of de-staining solution. The image of the washed gel was captured by using a digital camera.

2.5. Determination of zeta potential

The zeta potential values of three forms of LF with and without subjecting to IHT and subjected to oral, gastric and intestinal digestion condition were acquired using a Malvern NanoZS (Malvern Instruments Ltd., Malvern, Worcestershire, UK). The samples were diluted to 2 mg mL^{-1} with Milli-Q water. Likewise, the fluids and digesta obtained from each phase of digestion were diluted to 2 mg mL^{-1} solids. The pH of the digesta obtained from the oral and the intestinal digestion was adjusted to 7.0. Similarly, the pH of digesta obtained from the gastric digestion was adjusted to 2.0. We also measured zeta potential values of SOF, SOF + SGF, SOF + SGF + SIF without adding LF samples at the same solid concentration as that of LF samples. All of the above samples were vortexed for 30 s and then filtered through a 0.45 μm membrane to remove insoluble parts. Each experiment was carried out in triplicate.

2.6. Monitoring of the change in conformation

Far-UV circular dichroism (CD) spectra of digested and undigested samples without (control) and with IHT treatment were obtained by using a JASCO J-810 spectropolarimeter (Jasco International Co., Ltd., Tokyo, Japan). For this, 60 μL of each LF sample (0.1%, w/v) was loaded to a cylindrical quartz cell with an optical

path length of 0.1 mm. Five measurements were taken for each sample and the data was averaged. The CD spectra were analysed using an online analysis software (DicroWeb) to determine secondary structural features according to previously reported methods (Lees, Miles, Wien, & Wallace, 2006; Whitmore & Wallace, 2008).

2.7. Measurement of iron release and iron binding ability

The iron release profile of all the three forms of LF was measured according to the method reported by Feng et al. (1995) and Majka et al. (2013). Each sample was diluted to 1.0 mg mL^{-1} and then centrifuged at 10,000 × *g* for 10 min at ambient temperature (25 °C). The supernatant was withdrawn and the extent of decrease in absorbance at 466 nm was used to measure the release of iron previously bound to LF. Milli-Q water was used as the blank. The iron binding ability was measured by mixing the supernatant with freshly prepared FeNTA solution (9.9 mM ferric nitrate and 8.5 mM nitrilotriacetic acid in Milli-Q water) at iron to LF molar ratio of 2:1. The mixture was incubated at ambient temperature for 1 h and then dialysed against Milli-Q water for 48 h with three changes of water. The absorbance value measured at 466 nm was used to measure the iron binding ability.

2.8. Measurement of anti-oxidant activities

The antioxidant activity of various forms of LF subjected to the treatments described above was measured using the 2,2-diphenyl-1-picrylhydrazyl radical (DPPH) method, which is commonly used to measure the radical scavenging activity (Nicklisch & Waite, 2014). The LF digesta obtained after each phase of digestion were diluted to 20 mg mL^{-1}. Then, 2 mL of each of the diluted digesta samples was taken and the pH was adjusted to either 7.0 or 2.0. This pH adjusted samples were mixed with 850 μL citrate/phosphate buffer (0.1 M, pH 7.0) containing 1% (v/v) polysorbate-20 (Tween 20). The reaction was initiated by addition of 150 μL of 2 mM freshly prepared methanolic DPPH solution to the above mixture to achieve a final DPPH concentration of 0.1 mM. The simulated digestion fluids without LF were also used as controls. The absorbance values were taken at 515 nm using Milli-Q water as the blank.

All samples were gently mixed and stored in the dark at ambient temperature (25 °C) and the absorbance of each solution was re-measured after 30 min. The radical scavenging activity was calculated by the percentage loss of absorbance at 515 nm wavelength using Eq. (1):

$$I\% = \left(\frac{A_{s0} - A_{s1}}{A_{s0}} - \frac{A_{c0} - A_{c1}}{A_{c0}}\right) \times 100 \quad (1)$$

where A_{s0} and A_{c0} are the absorbance of digested LF and the corresponding simulated fluid at the beginning of the incubation (2 min) and A_{s1} and A_{c1} are the absorbance values of samples after storage in the dark for 30 min.

2.9. Statistical analysis

Statistical analysis was performed using IBM statistical software (SPSS®, version 21, IBM Corp.). All experimental data were obtained from triplicate runs and the data were expressed as the mean ± standard deviation where feasible. To detect any significant effects of our treatments, data for each experiment were separately tested using analysis of variance (ANOVA, $P < 0.05$). Significantly different groups were classified after post hoc comparison tests (Duncan's Multiple Range Test, DMRT, $P = 0.05$).

3. Results and discussion

3.1. Digestion of LF in simulated oral, gastric and intestinal environments

The changes in the molecular mass of apo-, native- and holo-LF before and after IHT treatment and molecular mass profiles of their peptide fragments obtained from in vitro oral, gastric and intestinal digestion phases are presented in Fig. 1. Before digestion, the major bands of all forms of LF correspond to the molecular mass of

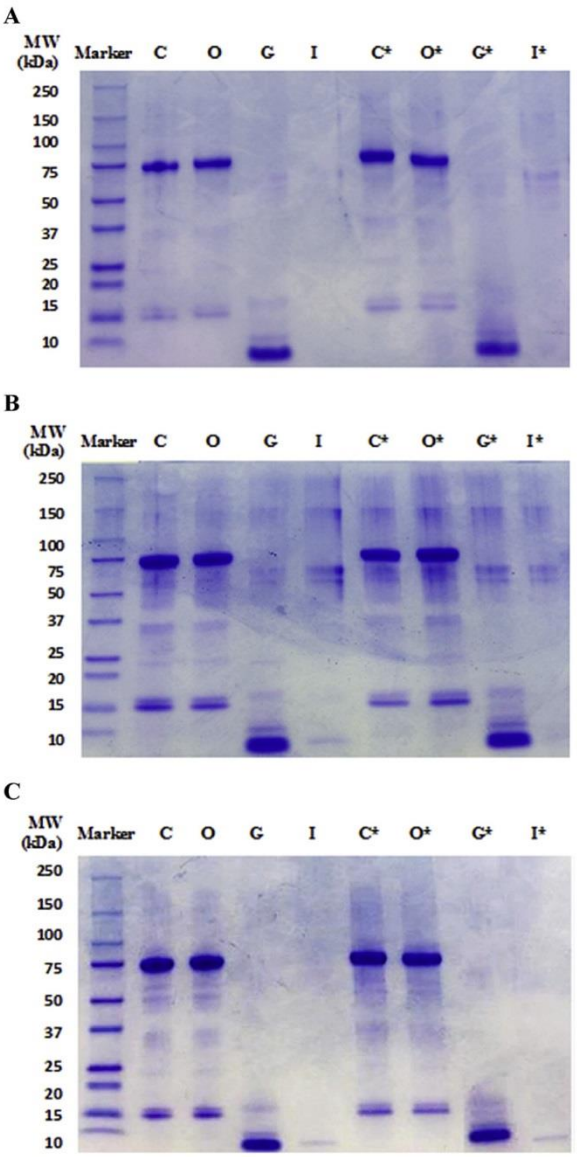

Fig. 1. SDS-PAGE profile of (A) apo-, (B) native- and (C) holo-lactoferrin before and after in vitro digestion: C and C*, control samples; O and O*, samples after oral digestion; G and G*, samples after successive oral + gastric digestion; I and I*, samples after oral + gastric + intestinal digestion. The asterisk indicates samples subjected to isothermal heat treatment prior to digestion.

75 kDa; however, there are some minor bands at around 15 kDa, which might be due to the residual α-lactalbumin (Costa et al., 2014). Subjecting LF to IHT (70 °C, 10 min) did not cause noticeable changes in the intensity of the major protein band, which suggested that no molecular degradation of LF occurred due to this degree of thermal treatment. As shown by this figure, oral digestion also did not cause noticeable proteolysis as demonstrated by the SDS-PAGE. However, when LF was subjected to simulated gastric digestion, it was hydrolysed into <10 kDa fragments. This observation indicates that LF is unable to resist pepsin proteolysis, which agrees well with the earlier study of David-Birman et al. (2013). During intestinal digestion, all three forms of LF were further hydrolysed by trypsin and other proteases present in the pancreatin enzyme mixture. The hydrolysis of LF during intestinal digestion occurred to such an extent that the peptide fragments were below the scale of the SDS-PAGE marker used (<10 kDa). This observation indicates that both thermally treated and the untreated LF were hydrolysed into small peptides in gastric environment. The peptides of LF produced during gastric digestion were further degraded (hydrolysed) into smaller peptide fragments due to proteolysis in intestinal environment prevailing in the small intestine. Although literature indicates that thermal treatment increases the digestion or hydrolysis rates of proteins (Bougrier, Delgenes, & Carrere, 2007), we found no observable difference between the thermally treated and untreated (control) LF in simulated gastric environment. It appears that LF must be encapsulated to withstand the gastric environment (pepsinolysis) if it has to reach the intestinal phase with intact iron binding and antioxidant capacities, and other biofunctionalities.

3.2. Variation of zeta potential during in vitro digestion

The zeta potential values of control (not heated and not digested) apo-, native-, and holo-LF samples are provided in Fig. 2A. The zeta potential values of all the three forms of LF before and after oral, gastric and intestinal digestion are shown in Fig. 2B. Fig. 2A shows the variation of zeta potential of the control LF sample as a function of pH. As can be seen, pI values of apo-, native- and hold-LF are 5.3, 8.3 and 8.0, which fall within the pI range of these three forms as reported in the literature. Bokkhim et al. (2013) and Gulão,

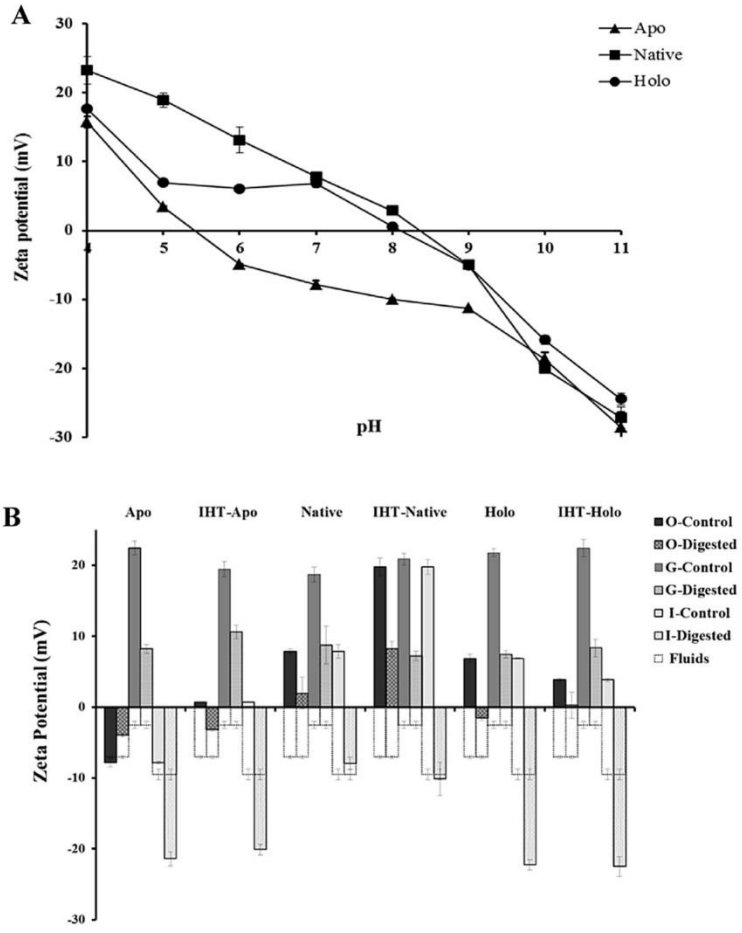

Fig. 2. Zeta potential values of 0.2% (w/v) lactoferrin (LF) as (A) a function of pH (▲, apo-LF; ■, native-LF; ●, holo-LF) and (B) before and after oral (O-Digested), gastric (G-Digested), and intestinal digestion (I-Digested); O-Control, G-Control and I-Control represent control samples at oral, gastric and intestinal digestion pH conditions, respectively. The oral, oral + gastric and oral + gastric + intestinal fluids at the same solid concentration (0.2%, w/v) were presented in dashed columns. IHT, isothermal heat treatment at 70 °C for 10 min (n = 3).

de Souza, da Silva, Coimbra, and Garcia-Rojas (2014) reported that the pI of apo-LF ranges between 5.5 and 6.5 and pI values of native- and holo-LF range between 7.0 and 9.5. The variation of zeta potential with pH of our samples and those reported in the literature does not follow a trend in their iron saturation levels.

Fig. 2B shows that, prior to any treatment, all the three forms of LF were positively charged at pH 2.0 (pH maintained at gastric condition but no enzyme added). This is because dominance of positively charged amino acids or due to their excess (compared with negatively charged ones) exposure to the surface. However, at the oral and intestinal pH of 7.0 (pH maintained at these two conditions but no enzyme added) the zeta potential values varied significantly. In the case of apo-LF the zeta potential was −7.8 mV while it was 7.8 mV for native-LF and 6.9 mV for holo-LF. This may be due to different isoelectric point of these three forms of LF.

During oral digestion, the surface charge of all forms of LF decreased substantially. Native-LF demonstrated the most dramatic changes as the positive surface charge of this LF interacted with negatively charged fluids. Similar trend is observed for the LF subjected to gastric and intestinal digestions. Interestingly, the zeta potential of the intestinal digesta is close to or even lower than that of the simulated intestinal fluids for all the three forms of LF. The increase in the magnitude of the negative charge after intestinal digestion could be attributed to the exposure or release of negatively charged amino acid groups such as glutamate and aspartate (11% in lactoferrin structure), or the folding of positively charged amino acids such as lysine, histidine and asparagine (13% in lactoferrin structure; Mead & Tweedie, 1990). Since the iron binding site of LF in each lobe involves aspartate, tyrosine and histidine (Baker & Baker, 2004), the change of surface charge during digestion also indicates the release of iron and breakdown of these iron containing domains. Furthermore, the exposed amino acids and covalently bound glycans at the proteins/peptides surface play an important role on recognition of and interaction with the intestinal cells. Investigation of zeta potential is valuable and could indicate to the changes in protein functional properties including their interfacial characteristics (Zhang, Zhang, Zhang, Decker, & McClements, 2015). The knowledge of surface charge of protein is important in many other protein processing systems such as membrane separation, isoelectric precipitation, surface adsorption (Bowen, Hall, Pan, Sharif, & Williams, 1998). IHT at 70 °C for 10 min (pH 7.0) caused an increase of magnitude of positive zeta potential values in general except for the holo-LF whose zeta potential value decreased slightly. This increase in the magnitude of positive charge of apo- and native-LF might be due to some degree of unfolding and exposure of positively charged amino acids. As this temperature is below the denaturation temperature of holo-LF such unfolding was unexpected. There was no statistically significant difference ($P > 0.05$) in zeta potential values between the heated (IHT-LF) and control (unheated) LF after gastric digestion, which indicated that the molecular structure of both heated and unheated LF was destroyed at this stage. This observation is corroborated by CD data that will be discussed in following section.

3.3. Changes in the structure of heat treated and untreated LF during in-vitro digestion

The changes in the molecular structure of LF's subjected to IHT and that of the untreated one at different digestion stages, as measured by the CD spectra, are presented in Fig. 3. The change in the ellipticity indicates the extent of conformational changes in LF due to the thermal stress, enzymatic hydrolysis and pH variation. The shapes of CD spectra of all the three forms of control (without any treatment) LF are similar, which indicated that the level of iron in LF did not affect its secondary structural features to any

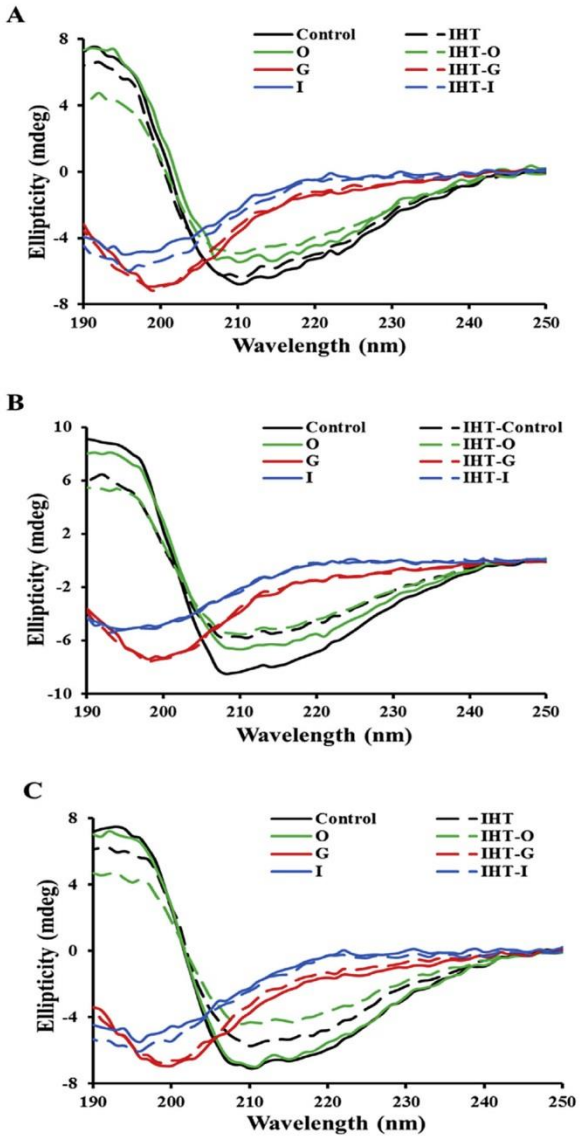

Fig. 3. Far-UV circular dichroism spectra of (A) apo- (B) native-, and (C) holo-lactoferrin: black, green, red and blue indicate control, oral digested (O), gastric digested (G) and intestinal digested (I) samples (solid line), respectively. The isothermal heat treated (IHT)-samples are presented by dashed lines. (For interpretation of the references to colour in this figure legend, the reader is referred to the web version of this article.)

significant extent. It is evident that there is a small decrease in the ellipticity at 208 nm and 222 nm (α-helix) in oral digesta as indicated by the unaltered peak position and shape. However, after gastric digestion, the ellipticity curve of all forms of LF changed substantially with the peak shifting from 210 nm to about 200 nm. This shift can be attributed to the breakdown of LF into smaller polypeptides. The change in the pH (from 7.0 to 2.0) also has been reported as a cause of this kind of conformational change (Sreedhara et al., 2010). The intestinal digestion caused an even higher degree of alteration in the structure of LF. In this case, the

sample subjected to IHT at 70 °C for 10 min did not show a significantly different ($P > 0.05$) breakdown pattern in molecular structure of LF compared with the unheated one. These observations further indicated that the molecular structure of LF was primarily degraded at the gastric digestion stage. The above observation suggested that the level of iron saturation or IHT did not alter the breakdown pattern of molecular structure of LF during digestion.

The percentage of helices, turns, sheets and unordered structures of both unheated and IHT treated LF samples subjected to oral, gastric and intestinal digestion are presented in Table 1. The compiled data show that, in the absence of any treatment, these three forms of lactoferrin shared similar secondary structures, which agrees with previously reports (David-Birman et al., 2013). After gastric digestion, the secondary structure of LF was dominated by random coil which comprised 51.8%, 51.8% and 48.1% in apo, native and holo forms, respectively. At the same time, the α-helix structure decreased to 5.8%, 6.1% and 6.5%, respectively, in apo, native and holo forms. Interestingly, the β-sheet and β-turn structures of various forms of LF remained comparatively stable during the digestion process. As both lobes of LF contain substantial proportion of α-helices (García-Montoya et al., 2012), the decrease in their content can be attributed to the unfolding of iron binding domains during digestion. The reduction in α-helices results into a reduction in LF's iron binding ability which will be discussed further below.

3.4. Iron release and iron binding properties

The iron release profiles of the three forms of LF are presented in Fig. 4A. The holo-LF released ~93% of its iron content during gastric digestion. The residual iron content of holo-LF was similar to that in other forms after gastric and intestinal digestion. This means that the iron content of both holo- and native-LF is released completely before it reaches the intestinal digestion phase. This observation leads to an important conclusion that unless the structure of the LF is preserved during gastric digestion phase by means of encapsulation or other methods there is no advantage to a higher degree of iron saturation in LF (i.e., holo-LF) as a vehicle of delivering bound iron to small intestine. It has been reported that the electrostatic interaction between LF and ferric ions tend to decrease when the pH is lower than 4.0 (Baker & Baker, 2004; Hu et al., 2008; Sreedhara et al., 2010). Carbonate ion (CO_3^{2-}) is essential for binding of iron by LF and this balance is disturbed due to the decrease in pH. In addition, the pepsinolysis in the stomach is another factor in the release of iron from its iron binding lobes. The highly acidic environment of the stomach (pH ~2.0) alters the conformation of LF as shown by the CD analysis (Fig. 3). Due to this alteration in conformation coupled with hydrolysis of LF into peptides, the effectiveness of LF as an iron transferring protein is almost completely lost. When the structure of LF is broken down, it is unable to carry iron. Regarding the effect of thermal treatment, it was found that IHT did not have much effect on the iron release properties as they were all below 10% after gastric or intestinal digestion.

The iron binding abilities of digested LF samples is presented in Fig. 4B. All the three forms of control samples of LF had an iron saturation level of more than 80% (data not shown). During in vitro digestion, the iron binding ability of all three forms of LF showed a similar trend as was observed in the case of iron release. Only about 10–20% of original LF iron binding capacity was retained after

Table 1
Percentage of secondary structural features of lactoferrin after oral, gastric and intestinal digestion.[a]

Samples	Percentage (%)			
	Helices	Sheets	Turns	Unordered
Apo-LF				
Control	18.0 ± 0.4^{a}	31.0 ± 0.1^{a,b}	16.4 ± 5.5^{a}	34.5 ± 5.3^{a}
Oral	15.4 ± 0.7^{a}	34.6 ± 0.7^{b}	15.1 ± 4.7^{a}	34.9 ± 4.0^{a}
Gastric	5.8 ± 2.5^{b}	28.5 ± 5.4^{a}	13.9 ± 3.0^{a}	51.8 ± 3.5^{d}
Intestinal	4.4 ± 2.4^{b}	33.7 ± 3.3^{a,b}	15.0 ± 1.8^{a}	47.0 ± 4.0^{c,d}
IHT	17.1 ± 1.2^{a}	31.2 ± 0.9^{a,b}	15.4 ± 4.7^{a}	36.2 ± 2.8^{a}
IHT-Oral	11.3 ± 4.1^{c}	34.7 ± 3.7^{b}	16.1 ± 3.6^{a}	37.8 ± 1.9^{a,b}
IHT-Gastric	5.9 ± 2.7^{b}	32.6 ± 4.4^{a}	14.1 ± 0.4^{a}	47.9 ± 6.4^{c,d}
IHT-Intestinal	6.6 ± 0.1^{b}	36.5 ± 0.5^{b}	13.9 ± 0.1^{a}	43.5 ± 1.7^{b,c}
Native-LF				
Control	23.0 ± 0.1^{a}	28.0 ± 0.6^{a}	16.8 ± 5.4^{a}	31.8 ± 5.9^{a}
Oral	19.0 ± 0.5^{b}	32.0 ± 0.4^{a,b}	16.5 ± 5.5^{a}	32.8 ± 5.6^{a}
Gastric	6.1 ± 2.9^{d}	30.6 ± 5.8^{a,b}	12.8 ± 1.8^{a}	51.8 ± 6.5^{b}
Intestinal	5.0 ± 2.3^{d}	33.9 ± 3.3^{b}	15.0 ± 2.1^{a}	46.9 ± 4.0^{b}
IHT	15.8 ± 0.9^{c}	32.9 ± 1.0^{a,b}	16.8 ± 5.5^{a}	35.0 ± 4.0^{a}
IHT-Oral	15.1 ± 1.3^{c}	32.3 ± 0.1^{a,b}	16.5 ± 5.4^{a}	36.1 ± 3.5^{a}
IHT-Gastric	6.1 ± 2.7^{d}	31.1 ± 5.1^{a,b}	13.7 ± 0.7^{a}	49.1 ± 7.9^{b}
IHT-Intestinal	4.9 ± 2.4^{d}	34.8 ± 3.3^{b}	14.5 ± 1.6^{a}	45.7 ± 4.1^{b}
Holo-LF				
Control	19.4 ± 0.4^{a}	30.9 ± 1.1^{a}	15.3 ± 4.7^{a}	34.3 ± 5.3^{a}
Oral	19.1 ± 0.4^{a,b}	31.0 ± 0.9^{a}	15.3 ± 4.5^{a}	34.5 ± 5.0^{a}
Gastric	6.5 ± 3.2^{c,d}	32.0 ± 4.6^{a,b}	13.4 ± 1.6^{a}	48.1 ± 7.1^{b}
Intestinal	4.9 ± 2.2^{d}	35.2 ± 3.8^{a,b}	14.5 ± 1.6^{a}	45.4 ± 4.5^{b}
IHT	15.4 ± 0.9^{b}	34.0 ± 0.6^{a,b}	15.2 ± 4.8^{a}	35.4 ± 4.1^{a}
IHT-Oral	10.1 ± 2.9^{c}	37.5 ± 1.9^{b}	19.1 ± 6.0^{a}	33.3 ± 5.0^{a}
IHT-Gastric	5.9 ± 2.6^{d}	32.3 ± 4.6^{a,b}	13.9 ± 0.4^{a}	47.8 ± 7.0^{b}
IHT-Intestinal	4.9 ± 2.3^{d}	33.7 ± 4.1^{a,b}	14.3 ± 0.9^{a}	47.1 ± 5.6^{b}

[a] Abbreviations are: LF, lactoferrin; IHT, isothermal heat treatment. Different superscript letters indicate significant differences ($P < 0.05$) for each form of LF in the same column, n = 3.

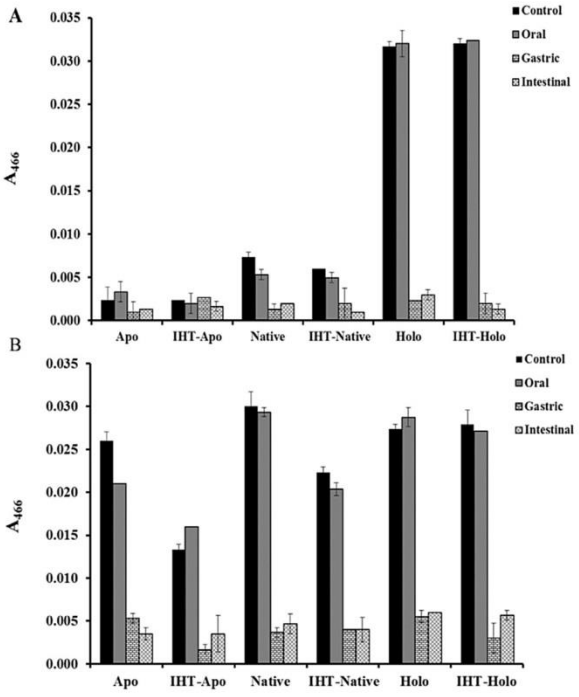

Fig. 4. Iron release (A) and iron binding (B) profiles of apo-, native- and holo-lactoferrin at different digestion stages. Isothermal heat treatment (IHT) was carried out at 70 °C for 10 min.

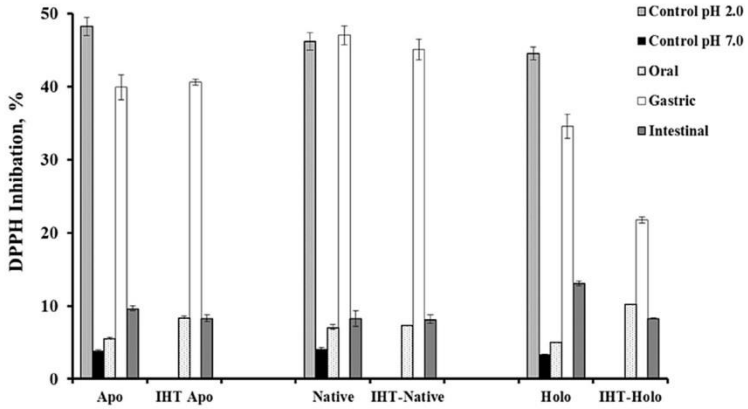

Fig. 5. Antioxidant capacity of apo-, native- and holo-lactoferrin after different digestion stages. The control samples were lactoferrin at pH 7.0 and at pH 2.0. IHT, isothermal heat treatment.

gastric digestion. The intestinal digestion showed similar results to that of the gastric digestion, with the LF retaining 13–22% iron binding ability compared with the control LF. One of the possible reasons for this observation is that both the N and C iron-binding lobes were irreversibly damaged during digestion in the majority of the LF molecules during gastric digestion. Interestingly, the iron saturated form of LF showed a lower degree of loss in iron-binding ability compared with other forms. Three types of amino acids in LF structure are directly involved in the interaction with iron: two tyrosine residues (Y), one aspartic acid (D) and one histidine (H) (Baker & Baker, 2004). From the primary sequence of bovine LF, it is possible that digested LF could also form peptides that have certain degree of iron binding ability.

The IHT carried out at 70 °C for 10 min decreased the iron binding ability in apo- and native-LF; however, there was no significant ($P > 0.05$) effect on that in holo-LF. The higher stability of IHT treated holo-LF during digestion can be attributed to its higher denaturation temperature (~90 °C), which enables it to retain its intact structure and thus contributes in retaining its iron binding ability. On the other hand, the denaturation temperatures of the apo and native forms of LF are lower than the temperature maintained in IHT which resulted into unfolding of its iron binding domains and hence reduced the amount of iron bound to LF.

3.5. Anti-oxidant activities of three forms of LF during in vitro digestion

The antioxidant activity profiles of the three forms of LF subjected to in vitro digestion are shown in Fig. 5. All the three forms of LF demonstrated much higher antioxidant capacity (45–48% DPPH inhibition) in acidic conditions (gastric environment) than at neutral pH (3–4% DPPH inhibition) prevailing in the oral and intestinal environment. This figure also shows that the antioxidant capacity decreased with the increase in the level of iron saturation as shown by the higher anti-oxidant capacity of apo-LF (48% DPPH inhibition) than that of holo-LF (45% DPPH inhibition). The anti-oxidant activity of proteins is related to the prevailing hydrogen ion concentration of the medium as it alters the mechanism of scavenging process of DPPH. The decrease in pH means that the proton coupled electron transfer (PC-ET) mechanism (Pękal & Pyrzynska, 2015) dominates the antioxidant behaviour. The lower anti-oxidant effect of holo-LF as shown by DPPH assay might be due to the higher proportion of iron. This observation closely agrees with that reported by Pękal and Pyrzynska (2015) in which they found that the presence of aluminium slowed down the DPPH reaction in case of tea. It appears that the antioxidant property of lactoferrin is a function pH. All the three forms of LF possessed the highest level of antioxidant activity in the gastric pH before digestion. After gastric digestion too, these digesta had higher antioxidant activity compared with the digesta obtained from oral and intestinal conditions. In the case of intestinal digestion, the antioxidant activity of digesta of all three forms of LF was higher than that of the undigested samples at same pH. This could be attributed to the released amino acids such as methionine and cysteine. These amino acids possess higher antioxidant activity than the protein itself (Levine, Moskovitz, & Stadtman, 2000).

4. Conclusions

The in vitro digestion revealed that hydrolysis of bovine lactoferrin occurred during the gastric digestion stage. LF was almost completely hydrolysed into <10 kDa fractions during gastric digestion and it was degraded further during intestinal digestion. The holo-LF did not show a higher resistance to proteolysis at the end of the gastric digestion and the molecular conformation of the holo-LF was affected in a fashion similar to that of other forms of LF during digestion. More than 90% of the iron was released from holo-LF during gastric digestion and its iron binding ability was irreversibly destroyed. The residual iron binding ability of the holo-LF at the end of the intestinal digestion was slightly higher than those of native- and apo-LF. The extent of positively charged peptides/amino acids decreased (more negatively charged peptides and amino acids were released) during gastric and intestinal digestion. The exposure of negatively charged domains indicated to the breakdown of iron binding domains. Antioxidant activity of gastric digesta of all the three forms of LF was 3–7 times higher than that of intestinal digesta, which is primarily due to the lower pH in gastric condition. The molecular mass and iron release patterns and zeta potential values of all the three forms of LF subjected to IHT at 70 °C for 10 min were almost identical to those of the untreated counterparts. The iron-binding ability and antioxidant activity of LFs subjected to IHT was slightly lower than those of untreated counterparts at the end of intestinal digestion.

Acknowledgement

The authors gratefully acknowledge Tatura Milk Industries Ltd. (a subsidiary of Bega Cheese, Australia) for kindly donating freshly produced native lactoferrin for this study.

References

Artym, J., & Zimecki, M. (2005). The role of lactoferrin in the proper development of newborns. *Advances in Hygiene and Experimental Medicine, 59*, 421–432.
Baker, H. M., & Baker, E. N. (2004). Lactoferrin and iron: Structural and dynamic aspects of binding and release. *Biometals, 17*, 209–216.
Bates, G. W., & Schlabach, M. R. (1973). The reaction of ferric salts with transferrin. *Journal of Biological Chemistry, 248*, 3228–3232.
Baveye, S., Elass, E., Mazurier, J., Spik, G., & Legrand, D. (1999). Lactoferrin: A multifunctional glycoprotein involved in the modulation of the inflammatory process. *Clinical Chemistry and Laboratory Medicine, 37*, 281–286.
Bokkhim, H., Bansal, N., Grøndahl, L., & Bhandari, B. (2013). Physico-chemical properties of different forms of bovine lactoferrin. *Food Chemistry, 141*, 3007–3013.
Bokkhim, H., Bansal, N., Grøndahl, L., & Bhandari, B. (2016). In vitro digestion of different forms of bovine lactoferrin encapsulated in alginate micro-gel particles. *Food Hydrocolloids, 52*, 231–242.
Bougrier, C., Delgenes, J. P., & Carrere, H. (2007). Impacts of thermal pre-treatments on the semi-continuous anaerobic digestion of waste activated sludge. *Biochemical Engineering Journal, 34*, 20–27.
Bowen, W. R., Hall, N. J., Pan, L.-C., Sharif, A. O., & Williams, P. M. (1998). The relevance of particle size and zeta-potential in protein processing. *Nature Biotechnology, 16*, 785–787.
Britigan, B. E., Serody, J. S., & Cohen, M. S. (1994). The role of lactoferrin as an anti-inflammatory molecule. In H. T. William, B. Lonnerdal, & V. S. Rumball (Eds.), *Lactoferrin: Structure and function* (pp. 143–156). New York, NY, USA: Plenum Press.
Cao, L., & Maas, H. (2015). *U.S. Patent No. 8,999,923*. Washington, DC: US Patent and Trademark Office.
Costa, F. F., Brito, M. A. V. P., Furtado, M. A. M., Martins, M. F., de Oliveira, M. A. L., de Castro Barra, P. M., et al. (2014). Microfluidic chip electrophoresis investigation of major milk proteins: Study of buffer effects and quantitative approaching. *Analytical Methods, 6*, 1666–1673.
David-Birman, T., Mackie, A., & Lesmes, U. (2013). Impact of dietary fibers on the properties and proteolytic digestibility of lactoferrin nano-particles. *Food Hydrocolloids, 31*, 33–41.
El-Loly, M. M., & Mahfouz, M. B. (2011). Lactoferrin in relation to biological functions and applications: A review. *International Journal of Dairy Science, 6*, 79–111.
Feng, M., Van Der Does, L., & Bantjes, A. (1995). Preparation of apo lactoferrin with a very low iron saturation. *Journal of Dairy Science, 78*, 2352–2357.
Furlund, C. B., Ulleberg, E. K., Devold, T. G., Flengsrud, R., Jacobsen, M., Sekse, C., et al. (2013). Identification of lactoferrin peptides generated by digestion with human gastrointestinal enzymes. *Journal of Dairy Science, 96*, 75–88.
García-Montoya, I. A., Cendón, T. S., Arévalo-Gallegos, S., & Rascón-Cruz, Q. (2012). Lactoferrin a multiple bioactive protein: An overview. *Biochimica et Biophysica Acta (BBA)-General Subjects, 1820*, 226–236.
Gulão, E. D. S., de Souza, C. J., da Silva, F. A., Coimbra, J. S., & Garcia-Rojas, E. E. (2014). Complex coacervates obtained from lactoferrin and gum Arabic: Formation and characterization. *Food Research International, 65*, 367–374.
Hu, F., Pan, F., Sawano, Y., Makino, T., Kakehi, Y., Komiyama, M., et al. (2008). Studies of the structure of multiferric ion-bound lactoferrin: A new antianemic edible material. *International Dairy Journal, 18*, 1051–1056.
Iafisco, M., Foltran, I., Di Foggia, M., Bonora, S., & Roveri, N. (2010). Calorimetric and Raman investigation of cow's milk lactoferrin. *Journal of Thermal Analysis and Calorimetry, 103*, 41–47.
Kawakami, H., Tanaka, M., Tatsumi, K., & Dosako, S. I. (1992). Effects of ionic strength and pH on the thermostability of lactoferrin. *International Dairy Journal, 2*, 287–298.
Lees, J. G., Miles, A. J., Wien, F., & Wallace, B. A. (2006). A reference database for circular dichroism spectroscopy covering fold and secondary structure space. *Bioinformatics, 22*, 1955–1962.
Levay, P. F., & Viljoen, M. (1995). Lactoferrin: A general review. *Haematologica, 80*, 252–267.
Levine, R. L., Moskovitz, J., & Stadtman, E. R. (2000). Oxidation of methionine in proteins: Roles in antioxidant defense and cellular regulation. *IUBMB Life, 50*, 301–307.
Lönnerdal, B., & Kelleher, S. L. (2009). Micronutrient transfer: Infant absorption. In G. R. Goldberg, A. Prentice, A. Prentice, S. Filteau, & K. Simondon (Eds.), *Breast-feeding: Early influences on later health* (pp. 29–40). New York, NY, USA: Plenum Press.
Majka, G., Śpiewak, K., Kurpiewska, K., Heczko, P., Stochel, G., Strus, M., et al. (2013). A high-throughput method for the quantification of iron saturation in lactoferrin preparations. *Analytical and Bioanalytical Chemistry, 405*, 5191–5200.
Masson, P. L., & Heremans, J. F. (1971). Lactoferrin in milk from different species. *Comparative Biochemistry and Physiology Part B: Comparative Biochemistry, 39*, 119–131.
Mata, L., Sánchez, L., Headon, D. R., & Calvo, M. (1998). Thermal denaturation of human lactoferrin and its effect on the ability to bind iron. *Journal of Agricultural and Food Chemistry, 46*, 3964–3970.
Mead, P. E., & Tweedie, J. W. (1990). cDNA and protein sequence of bovine lactoferrin. *Nucleic Acids Research, 18*, 7167.
Medina, I., Tombo, I., Satué-Gracia, M. T., German, J. B., & Frankel, E. N. (2002). Effects of natural phenolic compounds on the antioxidant activity of lactoferrin in liposomes and oil-in-water emulsions. *Journal of Agricultural and Food Chemistry, 50*(8), 2392–2399.
Minekus, M., Alminger, M., Alvito, P., Ballance, S., Bohn, T., Bourlieu, C., et al. (2014). A standardised static in vitro digestion method suitable for food–an international consensus. *Food and Function, 5*, 1113–1124.
Navarro, F., Harouna, S., Calvo, M., Pérez, M. D., & Sánchez, L. (2015). Kinetic and thermodynamic parameters for thermal denaturation of ovine milk lactoferrin determined by its loss of immunoreactivity. *Journal of Dairy Science, 98*, 4328–4337.
Nicklisch, S. C., & Waite, J. H. (2014). Optimized DPPH assay in a detergent-based buffer system for measuring antioxidant activity of proteins. *MethodsX, 1*, 233–238.
Pan, Y., Rowney, M., Guo, P., & Hobman, P. (2007). Biological properties of lactoferrin: An overview. *Australian Journal of Dairy Technology, 62*, 31.
Pękal, A., & Pyrzynska, K. (2015). Effect of pH and metal ions on DPPH radical scavenging activity of tea. *International Journal of Food Sciences and Nutrition, 66*, 58–62.
Ripolles, D., Harouna, S., Parrón, J. A., Calvo, M., Pérez, M. D., Carramiñana, J. J., et al. (2015). Antibacterial activity of bovine milk lactoferrin and its hydrolysates prepared with pepsin, chymosin and microbial rennet against foodborne pathogen Listeria monocytogenes. *International Dairy Journal, 45*, 15–22.
Saito, H., Takase, M., Tamura, Y., Shimamura, S., & Tomita, M. (1994). Physico-chemical and antibacterial properties of lactoferrin and its hydrolysate produced by heat treatment at acidic pH. In H. T. William, B. Lonnerdal, & V. S. Rumball (Eds.), *Lactoferrin: Structure and function* (pp. 219–226). New York, NY, USA: Plenum Press.
Schaible, U. E., & Kaufmann, S. H. (2004). Iron and microbial infection. *Nature Reviews Microbiology, 2*, 946–953.
Sreedhara, A., Flengsrud, R., Langsrud, T., Kaul, P., Prakash, V., & Vegarud, G. E. (2010). Structural characteristic, pH and thermal stabilities of apo and holo forms of caprine and bovine lactoferrins. *Biometals, 23*, 1159–1170.
Stănciuc, N., Aprodu, I., Râpeanu, G., van der Plancken, I., Bahrim, G., & Hendrickx, M. (2013). Analysis of the thermally induced structural changes of bovine lactoferrin. *Journal of Agricultural and Food Chemistry, 61*, 2234–2243.
Tomita, M., Wakabayashi, H., Shin, K., Yamauchi, K., Yaeshima, T., & Iwatsuki, K. (2009). Twenty-five years of research on bovine lactoferrin applications. *Biochimie, 91*, 52–57.
Troost, F. J., Steijns, J., Saris, W. H., & Brummer, R. J. M. (2001). Gastric digestion of bovine lactoferrin in vivo in adults. *Journal of Nutrition, 131*, 2101–2104.
Uchida, T., Oda, T., Sato, K., & Kawakami, H. (2006). Availability of lactoferrin as a natural solubilizer of iron for food products. *International Dairy Journal, 16*, 95–101.
Van Berkel, P. H. C., Geerts, M. E. J., van Veen, H. A., Kooiman, P. M., Pieper, F. R., de Boer, H. A., et al. (1995). Glycosylated and unglycosylated human lactoferrins both bind iron and show identical affinities towards human lysozyme and bacterial lipopolysaccharide, but differ in their susceptibilities towards tryptic proteolysis. *Biochemical Journal, 312*, 107–114.
Wakabayashi, H., Yamauchi, K., & Takase, M. (2006). Lactoferrin research, technology and applications. *International Dairy Journal, 16*, 1241–1251.
Wang, B., Timilsena, Y. P., Blanch, E., & Adhikari, B. (2016). Drying and denaturation characteristics of three forms of bovine lactoferrin. *Drying Technology*. http://dx.doi.org/10.1080/07373937.2016.1196699. article in press.
Whitmore, L., & Wallace, B. A. (2008). Protein secondary structure analyses from circular dichroism spectroscopy: Methods and reference databases. *Biopolymers, 89*, 392–400.
Yao, X., Bunt, C., Cornish, J., Quek, S. Y., & Wen, J. (2013). Oral delivery of lactoferrin: A review. *International Journal of Peptide Research and Therapeutics, 19*, 125–134.
Zhang, R., Zhang, Z., Zhang, H., Decker, E. A., & McClements, D. J. (2015). Influence of lipid type on gastrointestinal fate of oil-in-water emulsions: In vitro digestion study. *Food Research International, 75*, 71–78.

CHAPTER 6

Complex Coacervation and In-vitro Digestion Study of Lactoferrin

Published in *Journal of Functional Foods*, 2017, 37, 97-106

Journal of Functional Foods 37 (2017) 97–106

Contents lists available at ScienceDirect

Journal of Functional Foods

journal homepage: www.elsevier.com/locate/jff

Preparation and study of digestion behavior of lactoferrin-sodium alginate complex coacervates

Bo Wang [a], Ewan Blanch [a], Colin J. Barrow [c], Benu Adhikari [a,b,*]

[a] School of Science, RMIT University, Melbourne, VIC 3083, Australia
[b] CSIRO Manufacturing Flagship, Clayton South, VIC 3169, Australia
[c] Centre for Chemistry and Biotechnology, Deakin University, Geelong, VIC 3217, Australia

ARTICLE INFO

Article history:
Received 29 April 2017
Received in revised form 30 June 2017
Accepted 21 July 2017

Keywords:
Lactoferrin
Sodium alginate
Complex coacervation
In-vitro digestion
Iron release/binding
Antioxidant capacity

ABSTRACT

Complex coacervates of bovine lactoferrin (LF) and sodium alginate (NaAlg) were prepared aiming to protect the structure and associated function of LF in gastric stage of digestion. The parameters affecting the formation of complex coacervates (pH, LF-to-NaAlg ratio) were optimized using electrostatic charge density, turbidity and yield of the complex coacervates. The breaking down of LF structure into smaller peptides, antioxidant capacity and iron release/binding properties of LF and LF-NaAlg were determined in oral, gastric and intestinal stages of *in-vitro* digestion. The highest yield of LF-NaAlg complex coacervates was achieved at pH 4.5 and the LF-to-NaAlg ratio of 8:1. UP to 30% LF was delivered to the intestinal stage in complex coacervate form while the entire uncomplexed LF was degraded at the gastric stage. The antioxidant capacity of LF in complex coacervate was increased by 12%. The iron binding/release property of LF was not affected in LF-NaAlg complex coacervates.

1. Introduction

Lactoferrin (LF) is an iron-binding protein which is commercially extracted and manufactured from bovine milk (Tomita et al., 2009). It protects breast-fed infants against bacterial infection and inflammation (Artym & Zimecki, 2005; Britigan, Serody, & Cohen, 1994; Sun, Ren, Xiong, Zhao, & Guo, 2016). LF delivers iron to and promotes its absorption in the human body (Paesano et al., 2010). LF modulates cell growth, scavenges harmful free radicals and inhibits the formation of several toxic compounds (Baveye, Elass, Mazurier, Spik, & Legrand, 1999). Because of these functional properties, LF is added in a variety of commercial products including functional foods, therapeutic drinks, fermented milk, chewing gums, cosmetics and toothpaste (Shi et al., 2012; Tomita et al., 2009).

In order to benefit from the bio-functional properties of LF, it must be delivered to targeted absorption sites of the human digestive system in a structurally intact form (Lönnerdal & Kelleher, 2009). Our previous digestion study (Wang, Timilsena, Blanch, & Adhikari, 2017a) showed that bovine LF cannot pass through the gastric stage of digestion in its intact form and 80–90% of its iron binding ability is irreversibly lost in the gastric stage of digestion. Thus, LF must be protected to a suitable degree when it is delivered through the oral route. It has been shown that when protein is complex-coacervated with gum, it becomes more resistant to thermal degradation and gastro-intestinal digestion, compared to the un-complexed or free form (Mouécoucou, Villaume, Sanchez, & Méjean, 2004; Timilsena, Adhikari, Barrow, & Adhikari 2017). Hence, it is expected that complex coacervation of LF with a polysaccharide (gum) can increase its stability during gastrointestinal delivery (Gulão, de Souza, da Silva, Coimbra, & Garcia-Rojas, 2014; Yan et al., 2013). In this study, native LF and sodium alginate (NaAlg) were used to synthesize LF-NaAlg complex coacervates.

The choice of NaAlg is based on its wide commercial availability and desirable characteristics, such as good affinity with water and highly anionic charge density at pH values > 2.0 (Harnsilawat, Pongsawatmanit, & McClements, 2006). The pH-dependent electrostatic characteristics are important parameters to be considered during the formation of complex coacervates. It has been demonstrated that LF is a cationic protein at neutral pH and remains positively charged below pH 8.0 (Bokkhim, Bansal, Grøndahl, & Bhandari, 2013; Wang et al., 2017a). Given the highly cationic nature of LF, the selected polysaccharide has to be highly anionic to achieve high level of complex coacervation efficiency. Given the highly anionic nature of NaAlg, it is expected to form highly stable complex coacervates with LF over a wide pH range.

* Corresponding author at: School of Science, RMIT University, Melbourne, VIC 3083, Australia.
E-mail address: benu.adhikari@rmit.edu.au (B. Adhikari).

http://dx.doi.org/10.1016/j.jff.2017.07.044
1756-4646/

The complex coacervation process is affected by several intrinsic and extrinsic factors including pH, ratio of biopolymers used and ionic charge densities of biopolymers. Due to this reason, optimization of the complex coacervation parameters, especially pH, biopolymer ratio and ionic strength, is essential. These parameters affect both the yield and stability of the complex coacervates and ultimately affect the degradation of the complexed biopolymers during gastrointestinal digestion (Eratte, Dowling, Barrow, & Adhikari, 2017; Timilsena et al., 2017).

In the above context, the aim of this research was to determine the optimum condition (pH, LF-to-NaAlg ratio) for the formation of LF-NaAlg complex coacervates and investigate the degradation behavior and bio-functionality of LF-NaAlg complex coacervates in the simulated (*in-vitro*) gastrointestinal tract (GIT). The overarching purpose was to better preserve the structure and functional characteristics of LF, especially from the adverse effect of gastric digestion. The changes in molecular weight, secondary structural features, antioxidant capacity and iron release/binding properties of LF and LF-NaAlg complex coacervates at oral, gastric and intestinal digestion stages were determined. The research findings will provide better insights into the digestion pattern of complex coacervated (with polysaccharides) LF and the release profile of iron in the GIT so that formation of these complex coacervates could be tailored to deliver LF to the intestinal stage of digestion in the most effective way. These modified microcapsules could be increasingly used in food and pharmaceutical industries to benefit consumer health.

2. Materials and methods

2.1. Materials

Bovine lactoferrin (90% purity and 13% iron saturation) was donated by Tatura Milk Industries Ltd. (Subsidiary of Bega Cheese, Australia). α-amylase (Catalogue no: 9000855), mucin, pepsin (Catalogue no: 77151), bile salts and 2, 2-Diphenyl-1-picrylhydrazyl (DPPH) were obtained from Sigma-Aldrich (NSW, Australia). Sodium Alginate (Manucol® DMF, >99% purity) was purchased from IMCD Australia Ltd. (Victoria, Australia), Pancreatin (Catalogue no: 02102557) was purchased from MP Bio-medicals (Welland, Australia). Transglutaminase was bought from Food Ingredient Depot (Victoria, Australia). Mini-PROTEAN® TGX™ gels, WesternC blotting protein standards (Catalogue no: 1610376), Laemmli sample buffer, Tris/Glycine/SDS buffer, β-mercaptoethanol and Coomassie Brilliant Blue R-250 solution were purchased from Bio-Rad (Victoria, Australia). All chemicals used in this study were of analytical grade and were used as received.

2.2. Determination of the optimum pH and LF-NaAlg ratio for complex coacervation

The optimum condition for the formation of complex coacervates between LF and NaAlg were determined by following the previously reported method (Timilsena, Wang, Adhikari, & Adhikari, 2016; Wang, Adhikari, & Barrow, 2014). This method uses measurement of electrostatic charge (zeta potential), turbidity and yield of complex coacervates as dependent variables and pH and polymeric ratio as independent variables.

2.2.1. Measurement of zeta potential

The zeta potential values of LF and NaAlg were measured by using a Malvern NanoZS (Malvern Instruments Ltd., Worcestershire, UK). Briefly, LF and NaAlg samples were dissolved in Milli-Q water at a concentration of 2 mg mL^{-1}. Then, the pH of these samples was adjusted between 2.0 and 10.0 by drop-wise addition of either 1.0 M HCl or 1.0 M NaOH. The strength of electrostatic interaction (SEI) for complex coacervation was determined using Eq. (1).

$$SEI = \varepsilon(LF) \times \varepsilon(NaAlg) \quad (1)$$

where, $\varepsilon(LF)$ and $\varepsilon(LF)$ are absolute zeta potential values of LF and NaAlg, respectively. The pH value at which SEI reached a maximum value was considered the optimum pH for the formation of LF-NaAlg complex coacervates (Timilsena et al., 2016).

2.2.2. Determination of turbidity and yield of complex coacervates

The turbidity values of LF, NaAlg and their complex coacervates were determined by using a turbidity meter (Turbidity Meter: HI93703, Hanna Instruments Inc, Hungary). For this purpose, 1.5% (w/v) LF and NaAlg solutions were mixed with different LF-to-NaAlg ratios (1:4, 1:1, 4:1, 8:1, 16:1 and 24:1) at pH 4.5. Similarly, another set of samples were prepared by mixing 1.5% (w/v) LF and NaAlg solutions with a LF-to-NaAlg ratio of 16:1 at different pH conditions (2.0, 3.0, 3.5, 4.0, 4.5, 5.0, 6.0, 7.0 and 8.0). The pH (4.5) and LF-to-NaAlg ratio (16:1) was selected based on the highest yield of LF-NaAlg complex coacervates. The LF and NaAlg mixtures were stirred at 500 rpm for 2 h at ambient temperature (25 °C). In order to stabilize the newly formed complex coacervates, transglutaminase (0.25%, w/v) was added into the LF-NaAlg solutions and stored at 4 °C overnight. The crosslinked LF-NaAlg solutions were diluted 30 times for turbidity measurement.

For yield measurement, cross-linked LF-NaAlg complex coacervates (1.5%, w/v) were centrifuged at 10,000 × *g* for 10 min (20 °C) and then washed with Milli-Q water to remove any remaining soluble components. The precipitate was freeze-dried by using a laboratory scale freeze dryer (FreeZone™, LabconcoInc, USA). The yield of the LF-NaAlg complex coacervates was calculated using Eq. (2).

$$CY(\%) = m_i/m_0 \times 100\% \quad (2)$$

where, CY is the yield of coacervates (%), m_i and m_0 are masses (mg) of dried coacervates and dry solid matter used in the formulation, respectively.

2.3. Determination of LF-to-NaAlg molecular ratios in complex coacervates

In order to determine the LF-to-NaAlg molar ratios in the complex coacervates, 10 mL of crosslinked LF-NaAlg complex coacervate slurries with LF-to-NaAlg ratios of 16:1 and 8:1 (pH 4.5) were centrifuged at 10,000 × *g* for 10 min (20 °C). The supernatant was withdrawn for bicinchoninic acid (BCA) protein analysis (Smith et al., 1985) and the precipitate was freeze-dried. LF and NaAlg contents in the supernatant and precipitate were determined using Eqs. (3)–(5).

$$M_p \times V_p = M_t \times V_t - M_s \times V_s \quad (3)$$

$$m_p \times V_p = m_t \times V_t - m_s \times V_s \quad (4)$$

$$N_p = M_p \times V_p + m_p \times V_p \quad (5)$$

where M_p, M_t and M_s are the protein concentrations (g L^{-1}) in the precipitate, complex coacervate slurry and supernatant, respectively. Similarly, m_p, m_t and m_s are the NaAlg concentration (g L^{-1}) of the precipitate, complex coacervates slurry and supernatant, respectively. V_p, V_t and V_s represents the volume (L) of precipitate, complex coacervate slurry and supernatant, respectively. N_p is the weight (g) of the precipitate after freeze drying. The molecular weights of LF and one NaAlg residue (–$C_6H_8NaO_6$–) were taken to be 78 kDa (Moore, Anderson, Groom, Haridas, & Baker, 1997) and 199 Da, respectively.

2.4. Drying of LF-NaAlg complex coacervates

LF-NaAlg complex coacervate slurries were converted into powders using freeze and spray drying. For the spray drying process, 1000 mL of complex coacervate slurries (total solid content of 3.4–8.5%, w/v) prepared as described in Section 2.2.2 above. Two LF-to-NaAlg ratios (16:1 and 8:1) were used in these spray drying trials. The slurries were diluted as required to avoid the blocking of the atomizing nozzle and dried using a laboratory scale spray dryer (Spray dryer FT30 MKII, Armfield, UK). The dryer inlet and outlet temperatures and flow rates in these trials were 180 °C, 95 °C and 1000–1200 mL h^{-1}, respectively. The pressure of the atomizing (compressed) air was maintained at 138 kPa.

2.5. Acquiring the surface morphological features of complex coacervate powders

The surface morphology of spray- and freeze-dried LF and LF-NaAlg complex coacervate powders was captured using a scanning electron microscope (SEM) (FEI Quanta200 ESEM, Japan). The dried powders were deposited on aluminum stubs using double-sided adhesive carbon tape, gold coated and observed under SEM. An accelerating voltage of 15 kV was applied during these measurements.

2.6. In-vitro digestion of LF and LF-NaAlg complex coacervates

The digestion patterns of LF and LF-NaAlg complex coacervates were monitored using an *in-vitro* digestion system that consisted of oral, gastric and intestinal phases. A digitally controlled shaking water bath (MaXturdy 30, Daihan Scientific, South Korea) was used to maintain the temperature (37 °C) and provide continual agitation of the sample (95 rpm).

Simulated digestion fluid for each digestion stage was prepared according to a previously reported method (Minekus et al., 2014). Simulated oral fluid (SOF) was prepared by dissolving 521 mg $NaHCO_3$, 137 mg $K_2HPO_4{\cdot}3H_2O$, 88 mg NaCl, 48 mg KCl and 41 mg $CaCl_2$ in 100 mL Milli-Q water. Then, 216 mg mucin and 20,000 U α-amylase were added to the above solution and the pH was adjusted to 7.0 using 1.0 M HCl or 1.0 M NaOH. Simulated gastric fluid (SGF) was prepared by mixing 200 mg NaCl and 106 mg pepsin in 100 mL Milli-Q water to maintain the final pepsin activity of 2000 U mL^{-1}. The pH of SGF was adjusted to 2.0 using 1.0 M HCl. Similarly, 680 mg KH_2PO_4, 876 mg NaCl, 500 mg bile salts and 640 mg pancreatin (1 U mg^{-1}) were dissolved in 100 mL Mili-Q (pH 7.0) to prepare simulated intestinal fluid (SIF).

In-vitro digestion was initiated by adding 1 mL pre-warmed SOF (37 °C) to 1 mL LF/LF-NaAlg solutions. This mixture was incubated at 37 °C for 2 min in a shaking water bath. This oral digesta was subjected to gastric digestion by adding 2 mL of pre-warmed SGF solution to 2 mL of oral digesta. This mixture was incubated at 37 °C for 2 h during which the pH was maintained at 2.0 by intermittent addition of 1.0 M HCl. In the same way, intestinal digestion was initiated by adding of 4 mL of pre-warmed SIF to the SGF digesta. This mixture was incubated at 37 °C for 2 h and the pH was maintained at 7.0 by drop-wise addition of 1.0 M NaOH. After completion of digestion in each digestion stage (2 min oral digestion, 2 min oral digestion + 2 h gastric digestion; and 2 min oral + 2 h gastric + 2 h intestinal digestion), the digesta were diluted so as to maintain the solid content to 20 mg mL^{-1} with Milli-Q water. Then, the pH value of the gastric digesta was adjusted to 7.0 and the pH values of oral and intestinal digesta were adjusted to 4.0 to terminate the enzyme-substrate reaction (Genevieve, 1995). These digesta were instantly frozen after pH adjustment and stored at −20 °C before further analysis.

2.7. Acquiring degradation patterns of the complex coacervated LF

The degradation patterns and changes in molecular weights of LF and LF-NaAlg complex coacervate at different digestion stages were examined using sodium dodecyl sulphate polyacrylamide gel electrophoresis (SDS-PAGE). The experiment was performed with a 4–15% precast polyacrylamide gel under reducing conditions. The oral, gastric and intestinal digesta were diluted to 2 mg mL^{-1} by adding Milli-Q water. Then, 100 μL of this diluted slurry was mixed with an equal volume of SDS-loading buffer (95% of 2 × Laemmli buffer and 5% of β-mercaptoethanol). These mixtures were heated at 95 °C for 10 min. Five microliters (5 μL) of the heated samples were loaded onto the precast gels. Ten microliters (10 μL) of WesternC™ blotting protein standard was also loaded onto each gel as a molecular weight marker. The Mini-PROTEAN Tetra Cell was equilibrated at 100 V for 10 min before sample loading. The experiment was further run at 15 V for 10 min with standards and samples. Then, the voltage of SDS-PAGE was raised to 100 V and maintained at this level for 75 min. The precast gel was removed and dyed with 0.1% (w/v) Coomassie Brilliant Blue R-250 solution on a shaker (40 rpm) overnight at ambient temperature. It was then de-stained using a de-staining solution containing 10% (w/v) acetic acid and 40% (w/v) methanol for 2 h. Multiple washing was performed with frequent changes of de-staining solution. The image of the washed gel was captured by using a digital camera and the band intensity measurements were performed using Image J software (Abràmoff, Magalhães, & Ram, 2004).

2.8. Determination of the secondary structural features of complex coacervated LF at different stages of digestion

The changes in secondary structural features of complex coacervated LF after completion of each stage of digestion (oral, oral + gastric, oral + gastric + intestinal) were determined by using Far-UV circular dichroism (CD) spectra (Jasco International Co., Ltd., Tokyo, Japan). For this purpose, 60 μL of each sample (0.5%, w/v) was loaded into a cylindrical quartz cell with optical path length of 0.1 mm. The spectral data was recorded over the wavelength range of 190–250 nm with 5 accumulations.

2.9. Measurement of antioxidant capacity of LF-NaAlg complex coacervates

The antioxidant capacity of LF and LF-NaAlg complex coacervate was measured at different digestion stages by using 2, 2-diphenyl-1-picrylhydrazyl radical (DPPH) method (Nicklisch & Waite, 2014). This method is based on the electron-transfer reaction between DPPH and antioxidants and is commonly used to measure the radical scavenging activity of proteins (Huang, Ou, & Prior, 2005). Briefly, 1 mL of LF and LF-NaAlg samples before, and after, digestion (2%, w/v) was added to 2.17 mL citrate/phosphate buffer (0.1 M, pH 2.0 or pH 7.0) containing 1% (v/v) polysorbate-20 (Tween 20™). The pH of gastric digesta was maintained at 2.0 to simulate the gastric condition, whereas the pH of oral and intestinal digesta was maintained at 7.0. The radical scavenging reaction was initiated by adding 160 μL of 2 mM freshly prepared methanolic DPPH solution to the above mixtures to achieve a final DPPH concentration of 0.1 mM. The citrate/phosphate buffers (pH 2.0 and pH 7.0) were used as the control. The absorbance values were taken at 517 nm using Milli-Q water as the blank. All samples were gently mixed and stored in the dark at ambient temperature (25 °C) and the absorbance of each sample was measured once again after 120 min. The radical scavenging activity was calculated by the percentage loss of absorbance at a wavelength of 517 nm using Eq. (6).

$$I\% = [(A_{s0} - A_{s1})/A_{s0} - (A_{c0} - A_{c1})/A_{c0}] \times 100\% \quad (6)$$

where, A_{s0} and A_{c0} are the absorbance of samples and the buffer, respectively, at the beginning of the incubation (2 min). A_{s1} and A_{c1} are the absorbance values of samples and buffer, respectively, after storing them in the dark for 120 min.

2.10. Measurement of iron release and iron binding properties of LF and LF-NaAlg complex coacervates during digestion

Spectroscopic analysis was used to quantify the release profile of iron from LF and its complex coacervates during digestion (Feng, Van Der Does, & Bantjes, 1995; Majka et al., 2013). Briefly, digested samples of LF and LF-NaAlg were diluted to 1% (w/v) and then centrifuged at 10,000 × *g* for 10 min at ambient temperature (20 °C). The supernatant was withdrawn and the extent of decrease in absorbance at 466 nm, compared to that of LF/LF-NaAlg complex coacervate at the same concentration (1%, w/v), was used to determine the iron release profile of LF. The iron binding ability was measured by mixing the above-mentioned supernatant with freshly prepared ferric nitrilotriacetate (FeNTA) solution (9.9 mM ferric nitrate and 8.5 mM nitrilotriacetic acid in Milli-Q water) at an iron to LF molar ratio of 2:1. This mixture was stirred at 400 rpm for 1 h (20 °C) and then dialyzed against Milli-Q water at a sample to water ratio of 1:50 (v/v) for 48 h (4 °C) with three changes of water. The absorbance value measured at 466 nm was also used to quantify the iron binding ability.

2.11. Statistical analysis

The statistical analysis was performed using IBM's statistical software (SPSS®, version 21, IBM Corp.). The results obtained from three replicate runs were expressed as the mean ± standard deviation where feasible. Significant difference, at the 95% ($p < 0.05$) level of confidence, was determined according to the results from analysis of variance (ANOVA) and post hoc comparison tests (Duncan's Multiple Range Test, DMRT, P = 0.05).

3. Results and discussion

3.1. Optimization of LF-NaAlg complex coacervation parameters

The LF-NaAlg complex formation process is expected to be affected by the LF-to-NaAlg ratio, pH, temperature and ionic strength (De Kruif, Weinbreck, & de Vries, 2004; Liu, Low, & Nickerson, 2009). We determined the optimum pH, LF-to-NaAlg ratio as the starting point.

The zeta potential values of LF and NaAlg in the pH range of 2.0–10.0 are given in Fig. 1. As can be seen, LF possessed negative charges above pH 8.5, and below which it remained positively charged, while NaAlg remained negatively charged throughout the tested pH range. Due to these opposite charge characteristics, the strength of electrostatic interaction (SEI) increased continuously when pH decreased from 8.0 to 5.0, remained constant between pH 5.0 to 4.0 and decreased sharply below this pH. This indicates that electrostatic interactions between the positively charged groups at the protein's surface ($-NH_3^+$) and the negatively charged groups in the alginate ($-COO^-$) occurred at every pH between 2.0 and 8.0. However, the highest electrostatic interaction occurred in a relatively narrow range (pH 4.0–5.0). Beyond this range, the SEI value (indicating electrostatic attractive forces) dropped sharply, indicating to a substantial decrease in driving force LF-NaAlg required for complex coacervate formation.

In order to confirm what LF-to-NaAlg ratio and pH most readily produced the stable complex coacervates (the point at which strongest electrostatic interaction between LF and NaAlg occurs), the yield and turbidity values of complex coacervates at 3.5–7.0 pH range and 4:1–24:1 LF-to-NaAlg ratios were determined (Fig. 2). As can be seen (Fig. 2), the yield (w/w) and turbidity values of LF-NaAlg complex coacervates reached the highest level (83% and 59 FTU, respectively) at pH 4.5 (Fig. 2A), whereas these values are slightly lower in a pH 5.0 at the same LF-to-NaAlg ratio. Interestingly, when the pH was dropped to 4.0, both the yield and turbidity values decreased sharply to 44% and 20 FTU, respectively. It may be due to the fact that LF tends to open its iron-binding domain below pH 4.0 (Baker & Baker, 2004; Hu et al., 2008). Consequently, negatively charged amino acids (i.e. aspartic acid, $pK_a = 3.65$) in the iron-binding domain of LF are exposed to the solvent (water in this case), reducing the strength of positive charges surrounding the iron-binding domain. This subsequently weakens the electrostatic binding force between LF and NaAlg and hence decreased the yield and turbidity values. At and below pH 4.0, the zeta potential value of LF did not increase in the same way it had increased from pH 8.0 to pH 5.0. In fact, the zeta potential value at and below pH 4.0 has almost flat lined. This might be due to the release of Fe^{3+} ion from the iron binding domain, which generated additional hydrogen ions. These additional hydrogen ions neutralized some of the negative charge generated by the exposure of negatively charge amino acids. We determined the preferred pH for LF-NaAlg complex coacervation to be 4.5.

After determining the optimum pH value for complex formation, the optimum LF-to-NaAlg ratio was also determined (Fig. 2B). As can be seen, the yield (w/w) and turbidity values increased significantly (91%, 69 FTU) ($p < 0.05$) at the LF-to-NaAlg ratio of 8:1. Nearest yield and turbidity values (85%, 57 FTU) were achieved at a LF-to-NaAlg ratio of 16:1. Since the higher LF-to-NaAlg ratio possesses a lesser proportion of the non-LF component in the final LF products, an LF-to-NaAlg ratio of 16:1 could be a preferred ratio for industrial productions. However, the higher LF-to-NaAlg ratio also indicates higher number of LF molecules in the complex coacervates to be protected by each NaAlg molecule, which might not provide enough protection for LF during digestion. Therefore, LF-to-NaAlg ratios of either 16:1 or 8:1 can be taken as optimum conditions depending on the application of the complex coacervates.

3.2. Morphological features of LF and LF-NaAlg complex coacervate powders

The composition (%) of LF and NaAlg in LF-NaAlg complex coacervates produced at two LF-to-NaAlg ratios (16:1 and 8:1) are shown in Table 1. As expected, more alginate molecules (9 NaAlg residues per LF molecule) interacted with LF and formed an insoluble complex coacervate at the LF-to-NaAlg ratio of 8:1. In contrast, only 1.6% of available alginate molecules (6 NaAlg residues per LF molecule) participated in forming the insoluble LF-NaAlg complex coacervates at the LF-to-NaAlg ratio of 16:1. This difference in composition was reflected on the morphological features of the spray- and freeze-dried LF-NaAlg complex coacervate powders (Fig. 3). The spray-dried LF powders were spherical, hollow and uniform with the mean particle size of 2–20 μm. However, when the LF formed complex coacervates with NaAlg and was cross-linked by transglutaminase, the powders were more compact, irregular in shape and they had rougher surface topography. Interestingly, when the LF-to-NaAlg ratio was 8:1, the hollow interior of the spray-dried powder disappeared. The buckled shape and hollow interior were caused by the formation of a glassy skin in the early stage of drying. The glassy skin usually possesses low moisture diffusivity, resists outward diffusion of water and results into internal vaporization and leads to the formation of hollow interior in spray dried powders polymeric materials (Adhikari, Howes, Shrestha, & Bhandari, 2007). The absence of hollow interior in

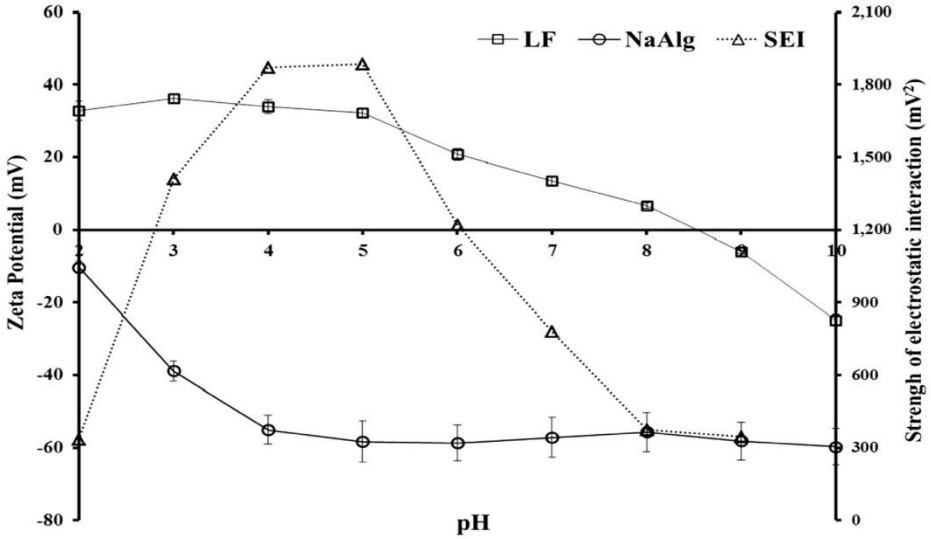

Fig. 1. Zeta potential and strength of electrostatic interaction (SEI) of 0.2% (w/v) lactoferrin (LF) and sodium alginate solution at zero ironic strength. SEI is the product of absolute values of the zeta potentials of the protein and polysaccharide (secondary Y-axis).

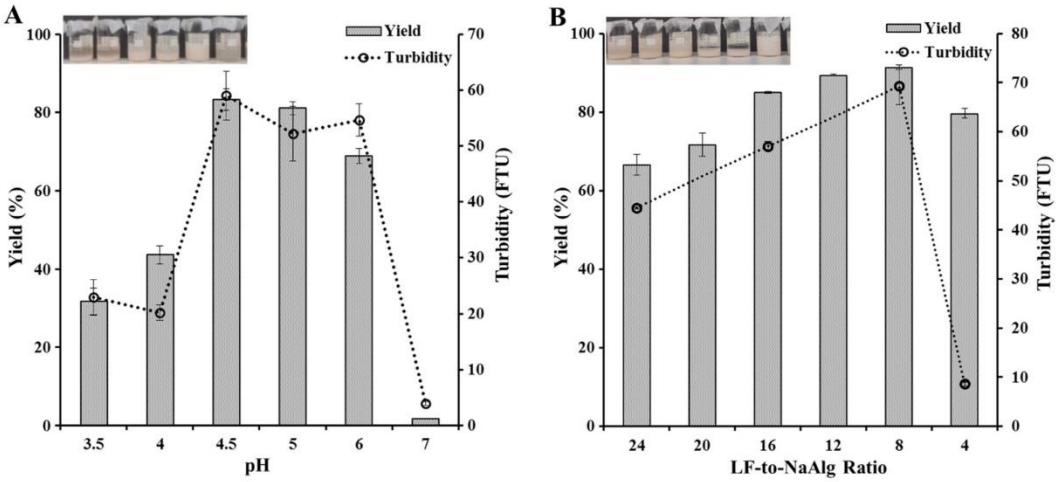

Fig. 2. Yield and turbidity value of LF-NaAlg complex coacervation (**A**) as a function of pH at LF-to-NaAlg ratio of 16:1 and (**B**) as a function of LF-to-NaAlg ratio at pH 4.5. The concentration of proteins and polysaccharide in the system was fixed to 1.5% and 0.06% (w/v) during the yield and turbidity measurements, respectively. The inserted image shows the direct view of turbidity of samples with LF to NaAlg at 1.5% (w/v) concentration.

Table 1
The molecule compositions of LF-NaAlg complex coacervates with LF-to-NaAlg ratios of 16:1 and 8:1 at pH 4.5. The molecular weight of LF is 78 kDa and the molecular weight of one NaAlg residue ($-C_6H_8NaO_6-$) is 199 Da.

LF-to-NaAlg ratio	Yield (%, w/w)	LF in LF-NaAlg complex coacervate (%, w/w)	NaAlg in LF-NaAlg complex coacervate (%, w/w)	NaAlg residues per LF molecule in the complex coacervates (mol/mol)
16:1	85.1 ± 0.2	98.4 ± 0.3	1.6 ± 0.3	6.4 ± 1.3
8:1	91.4 ± 0.6	97.8 ± 0.1	2.2 ± 0.1	9.0 ± 0.4

spray-dried LF-NaAlg powders suggests that the complex coacervate matrix makes it easier for water molecules to diffuse out compared to the LF matrix. The freeze-dried LF powders had smoother surface morphology compared to spray dried ones. The surface morphology of freeze-dried LF-NaAlg at LF-to-NaAlg ratio of 16:1 was very close to that of the freeze-dried LF. However, the surface became uneven when the NaAlg content increased in the composition (LF-to-NaAlg ratio of 8:1).

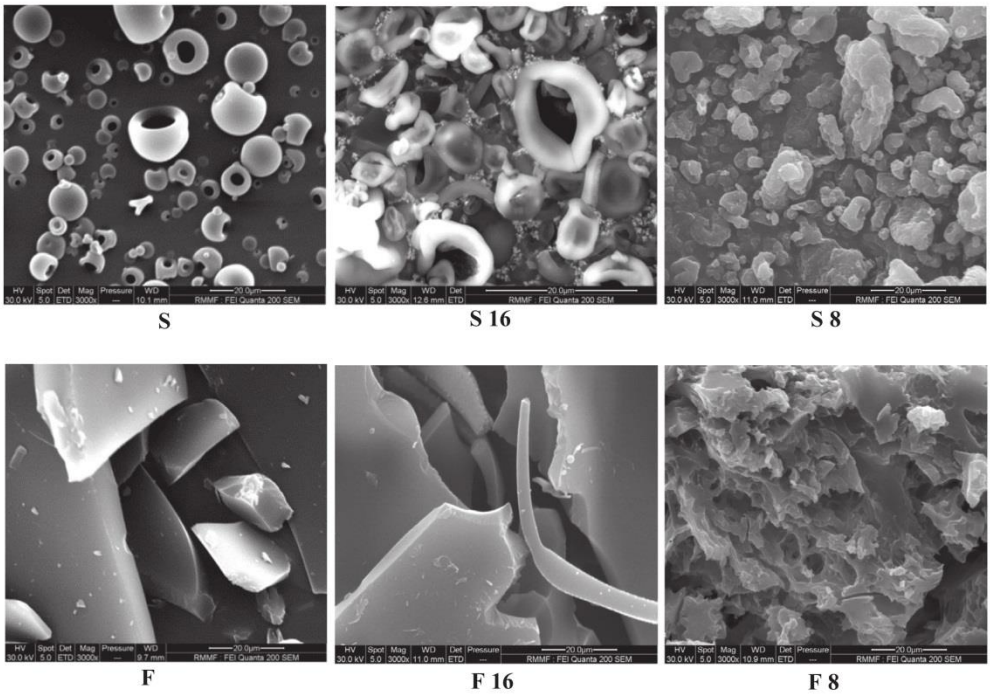

Fig. 3. SEM micrographs of spray-dried (**S**) LF, freeze-dried (**F**) LF and LF-NaAlg complex coacervates powders produced at LF-to-NaAlg ratios of 8:1 (**S8**, **F8**) and 16:1 (**S16**, **F16**). The images S and F for pure or uncomplex coacervated LF are taken from our previous study (Wang, Timilsena, Blanch, & Adhikari, 2017b) for comparison purpose.

3.3. Digestion behavior of LF and LF-NaAlg complex coacervates

Digestion and structure-breakdown of LF and LF-NaAlg complex coacervates during digestion were determined by SDS-PAGE (Fig. 4). In agreement with both the literature and our previous study (Furlund et al., 2013; Wang et al., 2017a), it was found that the structure of unprotected LF was completely broken down to less than 10 kDa fragments after gastric digestion and these fragments were degraded further during the intestinal digestion. The structure of LF in the complex coacervates at LF-to-NaAlg ratio of 16:1 was similar to that of LF during oral digestion. However, the structure of the complex coacervates was disrupted during gastric digestion due to the low pH (2.0) and proteolysis (action of pepsin). Seventy three percent of LF in the complex coacervates was degraded to less than 10 kDa peptides with a weak band showing at 15 kDa. The band of intact LF (at 75 kDa) had 27% more intensity compared to that of the un-complex coacervated LF indicating that the native structure of 27% of LF was protected in LF-NaAlg complex coacervates at the gastric stage of digestion. This is due to the protection provided by NaAlg as it formed insoluble complexes and blocked some of the sites which pepsin would attack for proteolysis. The results of oral digestion of the LF-NaAlg complex

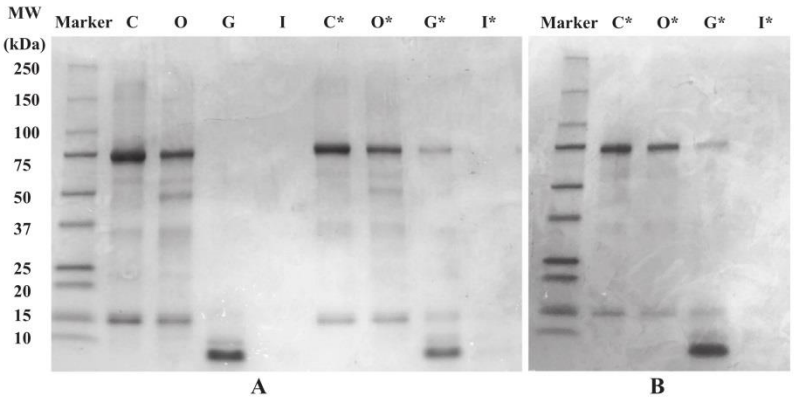

Fig. 4. Digestion patterns of LF and LF-NaAlg complex coacervate with LF-to-NaAlg ratio of 16:1 (**A**) and 8:1 (**B**). Where "C" indicates the control samples, "O" indicates the samples after oral digestion. "G" and "I" are the samples after successive oral + gastric and oral + gastric + intestinal digestion, respectively. LF-NaAlg complex samples are labeled by "*".

coacervates were similar at both ratios. However, the protection of LF, in the case of LF-to-NaAlg ratio 8:1 during gastric digestion was increased as the band intensity was 34% higher compared to that of the LF alone. This increased protection is due to the increased coverage of proteolytically sensitive sites of LF by alginate molecules as there are 9 alginate residues to each LF molecule. As reported by Chater, Wilcox, Brownlee, and Pearson (2015), alginate significantly inhibits the proteolytic activity of pepsin; hence, the LF-NaAlg complex coacervates with a higher NaAlg-to-LF ratio could protect LF from proteolysis more effectively. Another reason for the increased protection of LF in the complex coacervated form during gastric digestion is due to the higher viscosity of the complex coacervates at higher NaAlg content. According to Rebholz and Northrop (1991), an increase of viscosity of pepsin-substrate matrix reduced the diffusion of reactants to and from the enzyme and ultimately slowed down the enzyme-substrate reaction. However, alginate cannot survive from trypsin attack (Chater et al., 2015), and this is why the LF that remained intact in LF-NaAlg complex coacervate matrix during gastric digestion was completely degraded during intestinal digestion.

3.4. Secondary structural features of LF and LF in LF-NaAlg complex coacervates during digestion

Far-UV circular dichroism (CD) spectra of LF and LF-NaAlg are presented in Fig. 5. The ellipticity in the spectra is reported in mdeg (millidegrees). The secondary structural features of LF during complex formation and gastrointestinal digestion processes were reflected by the changes in ellipticity of control (LF not subjected to complex coacervation and/or digestion) and treated sample solutions. As can be observed, LF and the LF-NaAlg complex coacervates exhibit similar negative peak at ~210 nm (α-helix structure) and the positive peak at ~195 nm (β-sheet structure). This similarity in the spectral features indicates that LF did not change its secondary structural conformation when it formed complex coacervates with NaAlg. After gastric digestion, the conformation of LF changed substantially as indicated by the shifting of the negative peak to 198 nm ('random coil' or disordered structure) and the disappearance of positive β-sheet peak. LF-NaAlg complex coacervates showed a similar trend as the negative spectral peaks shifted to ~203 nm, which is a smaller shift compared to the one shown by uncoacervated LF. This observation indicated that pepsinolysis caused less secondary structural changes in the coacervated LF. There are almost no spectral differences between LF and LF in LF-NaAlg complex coacervates after intestinal digestion. This observation suggested that the complex coacervation with NaAlg did not provide any protection to LF during the intestinal digestion, which is in accordance with SDS-PAGE results (Fig. 4) described in Section 3.3.

3.5. Effect of digestion on the antioxidant capacities of LF and LF-NaAlg complex coacervates

The DPPH inhibition profiles of LF and LF-NaAlg complex coacervates at different pH and digestion stages are shown in Fig. 6. As can be observed, both LF and LF-NaAlg complex coacervates possessed much higher DPPH inhibition (30% and 39%, respectively) at pH 2.0 (gastric environment) compared to when they were at pH 7.0 (oral and intestinal environments). This is because the lower pH increases the scavenging process of DPPH in proteins as the antioxidant capacity is determined by a proton-coupled electron transfer mechanism instead of electron-transfer reactions (Pękal & Pyrzynska, 2015). Interestingly, LF-NaAlg complex coacervates possessed similar antioxidant capacity to that of LF at the end of gastrointestinal tract (pH 7.0). The antioxidant capacity of LF-NaAlg complex coacervates was increased by 30% compared to that of LF during the gastric conditions (pH 2.0). After gastric digestion, the antioxidant capacity of LF was decreased by ~12%, which is due to the breakdown of peptides. However, there is no significant difference ($p > 0.05$) in the antioxidant capacity of LF-NaAlg complex coacervates after the same digestion stage. This preservation of free radical scavenging capacity might be due to the higher resistance of LF-NaAlg complex coacervates to proteolysis, as described previously (Section 3.3). Another reason for the higher antioxidant capacity observed in LF-NaAlg complex coacervates during gastric digestion is due to the breakdown of the NaAlg content. It has been reported that NaAlg and its low molecular weight fractions possess moderate antioxidant properties (Sellimi et al., 2015; Şen, 2011). In the case of intestinal digestion, there are no observable difference in antioxidant capacity between the LF and LF-NaAlg digesta. This is because both LF and NaAlg degraded completely during intestinal digestion (Fig. 4). The antioxidant capacity of intestinal digested LF and LF-NaAlg complex coacervates was slightly higher than that of the control samples without any treatment (pH 7.0).

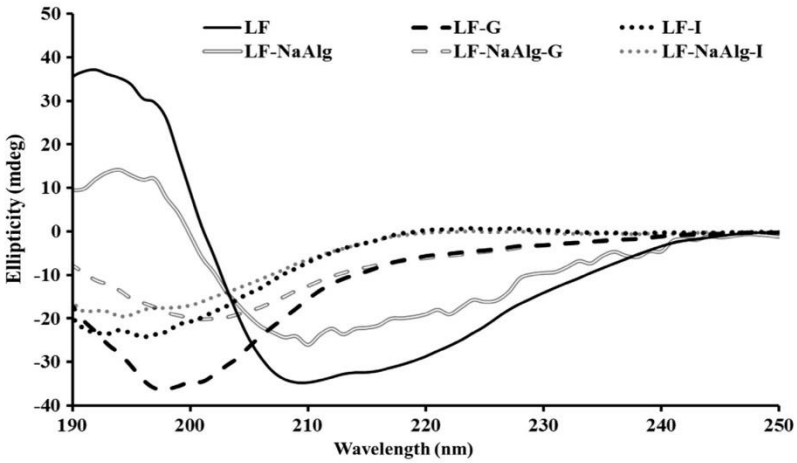

Fig. 5. Far-UV circular dichroism spectra of LF (black color) and LF-NaAlg coacervate with LF-to-NaAlg ratio of 16:1 (gray color), where solid, dashed and dotted lines indicate control, gastric digested (G) and intestinal digested (I) samples, respectively.

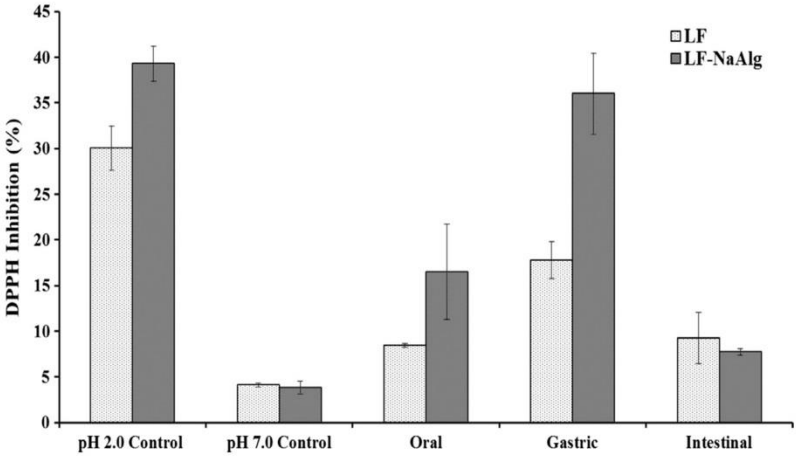

Fig. 6. Antioxidant capacity of LF and LF-NaAlg complex coacervates (6 mg mL^{-1}) at LF-to-NaAlg ratio of 16:1 at orgal, gastric and intestinal digestion stages.

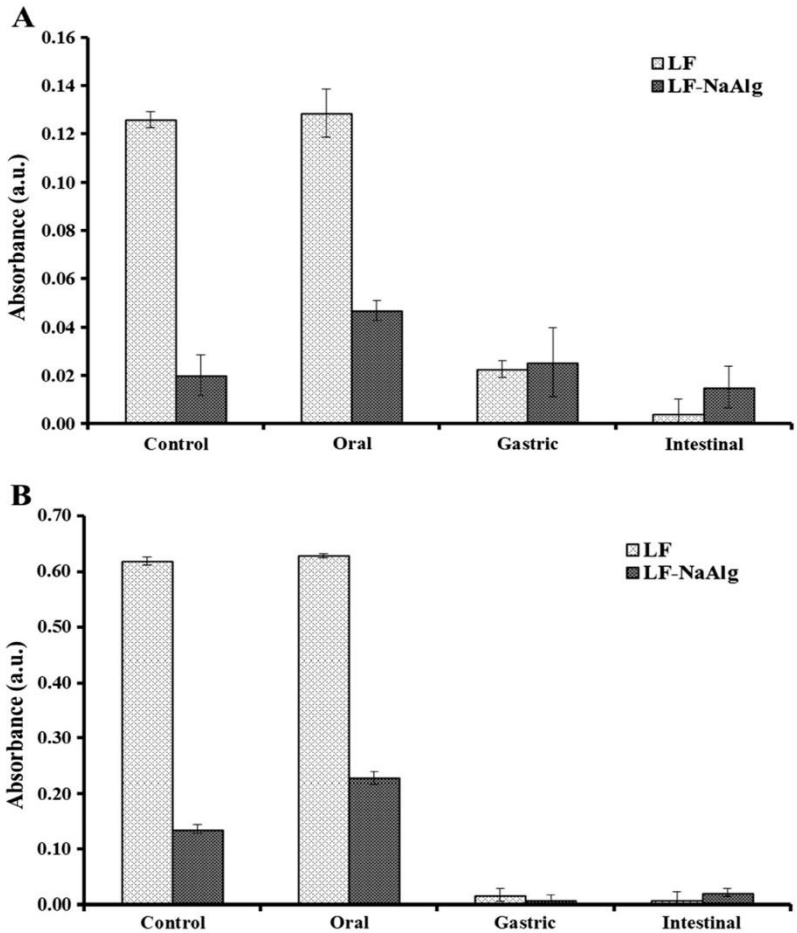

Fig. 7. Iron release (**A**) and iron binding (**B**) profiles of LF and LF-NaAlg complex coacervate (LF-to-NaAlg ratio of 16:1) at different digestion stages. The light absorbance was measured at 466 nm wavelength.

This higher antioxidant capacity can be attributed to the released amino acids (e.g., methionine and cysteine) as they exhibit a higher DPPH inhibition ability than the protein itself (Levine, Moskovitz, & Stadtman, 2000).

3.6. The release of iron by LF and LF-NaAlg complex coacervates during digestion

Iron in its insoluble form cannot be metabolized by human body, whereas the free iron catalyzes reactions that produce free oxygen radicals that are highly toxic to cells (Schaible & Kaufmann, 2004). The iron bound to LF which shows light absorbance at 466 nm wavelength can be utilized and provides benefits to the human body. The iron release profiles of LF and LF-NaAlg are presented in Fig. 7A. As can be observed, more than 80% of the iron bound to the LF was released after gastric digestion due to the highly acidic condition (pH 2.0). This is due to the breakdown of LF structure that almost completely destroyed the iron-binding domains, which is consistent with the literature (Baker & Baker, 2004; Wang et al., 2017a). When LF was complex coacervated with NaAlg (LF-to-NaAlg ratio of 16:1, pH 4.5), the amount of iron bound to LF (in soluble form) decreased sharply to 16% compared to that of the control sample (LF, without any treatment). This is because the LF-NaAlg complex coacervate is insoluble in water at around the optimum pH. Interestingly, no significant difference ($p > 0.05$) was observed between LF and LF-NaAlg after gastric digestion. This indicates that although 27% of LF remained intact during peptic hydrolysis (Fig. 4), its iron-binding structural domains would have been irreversibly altered due to which LF was unable to retain iron in its structure at the end of gastric digestion. Similar effect of digestion on the iron binding behavior of LF was observed when it was in complex coacervated form with NaAlg (Fig. 7B). The amount of iron in the LF-NaAlg complex coacervate (LF-to-NaAlg ratio of 16:1, pH 4.5) that can be utilized in human bodies was 22% of that of the control samples (LF, without any treatment). Both LF and LF-NaAlg completely lost their iron binding ability after gastric digestion. In this study, LF was not entirely covered by NaAlg (encapsulation) and hence its surface could be partially exposed to the harsh pH condition (pH 2.0) in gastric digestion stage. When LF is exposed to this level of low pH, its conformation is substantially altered with the loss of ~20% α-helix structure (Sreedhara et al., 2010). As the α-helix (121-131 residues in N lobe and 395-407 in C lobe) is an essential structural component in the iron binding domain (Moore et al., 1997), the iron binding ability of LF could be significantly reduced in this low pH environment. Therefore, the effectiveness of LF as an iron transferring protein (during gastrointestinal delivery) was not improved even when it formed complex coacervates with NaAlg. Higher level protection of LF's structure and associated functions requires additional treatments.

4. Conclusions

LF and NaAlg were able to form complex coacervates over a wide pH range (pH 2.0–8.0) and LF-to-NaAlg ratios (4:1–24:1); however, the highest yield of LF-NaAlg complex coacervate occurred at pH 4.5 and at LF-to-NaAlg ratios of 8:1 and 16:1. LF-NaAlg complex coacervation provided 27%–34% protection to LF and its antioxidant ability was fully retained. The un-coacervated LF was completely broken-down to less than 10 kDa fragments at the gastric stage of digestion and its antioxidant capacity was decreased by 12%. No significant difference in iron release and iron binding properties was observed between un-coacervated LF and LF-NaAlg complex coacervates as almost all of the iron bound to LF and LF-NaAlg was released and the iron binding ability of LF/LF-NaAlg was completely lost during gastric stage of digestion. The iron-binding structural domains of LF were irreversibly broken down at the gastric stage of digestion whether or not LF was coacervated with NaAlg.

Acknowledgements

The authors acknowledge Tatura Milk Industries Ltd. (Subsidiary of Bega Cheese, Australia) for kindly donating freshly produced lactoferrin solution for this research. The authors wish to acknowledge the assistance of Dr Yakindra Timilsena, Nyok Ling Tai and Arissara Phosanam in some of the experiments. This work was partially supported by the ARC Linkage grant (LP140100722).

References

Abràmoff, M. D., Magalhães, P. J., & Ram, S. J. (2004). Image processing with ImageJ. *Biophotonics International, 11*(7), 36–42.
Adhikari, B., Howes, T., Shrestha, A. K., & Bhandari, B. R. (2007). Development of stickiness of whey protein isolate and lactose droplets during convective drying. *Chemical Engineering and Processing: Process Intensification, 46*(5), 420–428.
Artym, J., & Zimecki, M. (2005). The role of lactoferrin in the proper development of newborns. *Advances in Hygiene and Experimental Medicine, 59*, 421–432.
Baker, H. M., & Baker, E. N. (2004). Lactoferrin and iron: Structural and dynamic aspects of binding and release. *BioMetals, 17*, 209–216.
Baveye, S., Elass, E., Mazurier, J., Spik, G., & Legrand, D. (1999). Lactoferrin: A multifunctional glycoprotein involved in the modulation of the inflammatory process. *Clinical Chemistry and Laboratory Medicine, 37*, 281–286.
Bokkhim, H., Bansal, N., Grøndahl, L., & Bhandari, B. (2013). Physico-chemical properties of different forms of bovine lactoferrin. *Food Chemistry, 141*(3), 3007–3013.
Britigan, B. E., Serody, J. S., & Cohen, M. S. (1994). The role of lactoferrin as an anti-inflammatory molecule. In H. T. William, B. Lonnerdal, & V. S. Rumball (Eds.), *Lactoferrin: Structure and function* (pp. 143–156). New York, USA: Plenum Press.
Chater, P. I., Wilcox, M. D., Brownlee, I. A., & Pearson, J. P. (2015). Alginate as a protease inhibitor in vitro and in a model gut system; selective inhibition of pepsin but not trypsin. *Carbohydrate Polymers, 131*, 142–151.
De Kruif, C. G., Weinbreck, F., & de Vries, R. (2004). Complex coacervation of proteins and anionic polysaccharides. *Current Opinion in Colloid & Interface Science, 9*(5), 340–349.
Eratte, D., Dowling, K., Barrow, C. J., & Adhikari, B. P. (2017). In-vitro digestion of probiotic bacteria and omega-3 oil co-microencapsulated in whey protein isolate-gum Arabic complex coacervates. *Food Chemistry, 227*, 129–136.
Feng, M., Van Der Does, L., & Bantjes, A. (1995). Preparation of apo lactoferrin with a very low iron saturation. *Journal of Dairy Science, 78*, 2352–2357.
Furlund, C. B., Ulleberg, E. K., Devold, T. G., Flengsrud, R., Jacobsen, M., Sekse, C., et al. (2013). Identification of lactoferrin peptides generated by digestion with human gastrointestinal enzymes. *Journal of Dairy Science, 96*, 75–88.
Genevieve, S. (1995). Isolation of glycopeptides and glycosylation sites. In A. Verbert (Ed.), *Methods on glycoconjugates* (pp. 41–47). Florida, USA: CRC Press.
Gulão, E. D. S., de Souza, C. J., da Silva, F. A., Coimbra, J. S., & Garcia-Rojas, E. E. (2014). Complex coacervates obtained from lactoferrin and gum Arabic: Formation and characterization. *Food Research International, 65*, 367–374.
Harnsilawat, T., Pongsawatmanit, R., & McClements, D. J. (2006). Characterization of β-lactoglobulin–sodium alginate interactions in aqueous solutions: a calorimetry, light scattering, electrophoretic mobility and solubility study. *Food Hydrocolloids, 20*(5), 577–585.
Hu, F., Pan, F., Sawano, Y., Makino, T., Kakehi, Y., Komiyama, M., et al. (2008). Studies of the structure of multiferric ion-bound lactoferrin: A new antianemic edible material. *International Dairy Journal, 18*, 1051–1056.
Huang, D., Ou, B., & Prior, R. L. (2005). The chemistry behind antioxidant capacity assays. *Journal of Agricultural and Food Chemistry, 53*(6), 1841–1856.
Levine, R. L., Moskovitz, J., & Stadtman, E. R. (2000). Oxidation of methionine in proteins: Roles in antioxidant defense and cellular regulation. *IUBMB Life, 50*, 301–307.
Liu, S., Low, N. H., & Nickerson, M. T. (2009). Effect of pH, salt, and biopolymer ratio on the formation of pea protein isolate–gum arabic complexes. *Journal of Agricultural and Food Chemistry, 57*(4), 1521–1526.
Lönnerdal, B., & Kelleher, S. L. (2009). Micronutrient transfer: infant absorption. In G. R. Goldberg, A. Prentice, S. Filteau, & K. Simondon (Eds.), *Breast feeding: Early influences on later health* (pp. 29–40). New York, NY, USA: Plenum Press. Majka.
Majka, G., Śpiewak, K., Kurpiewska, K., Heczko, P., Stochel, G., Strus, M., et al. (2013). A high-throughput method for the quantification of iron saturation in lactoferrin preparations. *Analytical and Bioanalytical Chemistry, 405*(15), 5191–5200.
Minekus, M., Alminger, M., Alvito, P., Ballance, S., Bohn, T., Bourlieu, C., et al. (2014). A standardised static in vitro digestion method suitable for food-an international consensus. *Food and Function, 5*, 1113–1124.
Moore, S. A., Anderson, B. F., Groom, C. R., Haridas, M., & Baker, E. N. (1997). Three-dimensional structure of diferric bovine lactoferrin at 2.8 Å resolution. *Journal of Molecular Biology, 274*(2), 222–236.

Mouécoucou, J., Villaume, C., Sanchez, C., & Méjean, L. (2004). Effects of gum arabic, low methoxy pectin and xylan on in vitro digestibility of peanut protein. *Food Research International, 37*(8), 777–783.

Nicklisch, S. C., & Waite, J. H. (2014). Optimized DPPH assay in a detergent-based buffer system for measuring antioxidant activity of proteins. *MethodsX, 1*, 233–238.

Paesano, R., Berlutti, F., Pietropaoli, M., Pantanella, F., Pacifici, E., Goolsbee, W., et al. (2010). Lactoferrin efficacy versus ferrous sulfate in curing iron deficiency and iron deficiency anemia in pregnant women. *BioMetals, 23*(3), 411–417.

Pękal, A., & Pyrzynska, K. (2015). Effect of pH and metal ions on DPPH radical scavenging activity of tea. *International Journal of Food Sciences and Nutrition, 66*, 58–62.

Rebholz, K. L., & Northrop, D. B. (1991). Effects of viscosity and solvent deuterium identify multiple partially rate-limiting steps in the kinetics of porcine pepsin. In M. D. Ben (Ed.), *Structure and function of the aspartic proteinases: Genetics-structures-mechanisms* (pp. 139–142). New York, USA: Plenum Press.

Schaible, U. E., & Kaufmann, S. H. (2004). Iron and microbial infection. *Nature Reviews Microbiology, 2*, 946–953.

Sellimi, S., Younes, I., Ayed, H. B., Maalej, H., Montero, V., Rinaudo, M., et al. (2015). Structural, physicochemical and antioxidant properties of sodium alginate isolated from a Tunisian brown seaweed. *International Journal of Biological Macromolecules, 72*, 1358–1367.

Şen, M. (2011). Effects of molecular weight and ratio of guluronic acid to mannuronic acid on the antioxidant properties of sodium alginate fractions prepared by radiation-induced degradation. *Applied Radiation and Isotopes, 69*(1), 126–129.

Shi, J., Finckenberg, P., Martonen, E., Ahlroos-Lehmus, A., Pilvi, T. K., Korpela, R., et al. (2012). Metabolic effects of lactoferrin during energy restriction and weight regain in diet-induced obese mice. *Journal of Functional Foods, 4*(1), 66–78.

Smith, P. K., Krohn, R. I., Hermanson, G. T., Mallia, A. K., Gartner, F. H., Provenzano, M., et al. (1985). Measurement of protein using bicinchoninic acid. *Analytical Biochemistry, 150*(1), 76–85.

Sreedhara, A., Flengsrud, R., Prakash, V., Krowarsch, D., Langsrud, T., Kaul, P., et al. (2010). A comparison of effects of pH on the thermal stability and conformation of caprine and bovine lactoferrin. *International Dairy Journal, 20*(7), 487–494.

Sun, J., Ren, F., Xiong, L., Zhao, L., & Guo, H. (2016). Bovine lactoferrin suppresses high-fat diet induced obesity and modulates gut microbiota in C57BL/6J mice. *Journal of Functional Foods, 22*, 189–200.

Timilsena, Y. P., Adhikari, R., Barrow, C. J., & Adhikari, B. (2017). Digestion behaviour of chia seed oil encapsulated in chia seed protein-gum complex coacervates. *Food Hydrocolloids, 66*, 71–81.

Timilsena, Y. P., Wang, B., Adhikari, R., & Adhikari, B. (2016). Preparation and characterization of chia seed protein isolate–chia seed gum complex coacervates. *Food Hydrocolloids, 52*, 554–563.

Tomita, M., Wakabayashi, H., Shin, K., Yamauchi, K., Yaeshima, T., & Iwatsuki, K. (2009). Twenty-five years of research on bovine lactoferrin applications. *Biochimie, 91*, 52–57.

Wang, B., Adhikari, B., & Barrow, C. J. (2014). Optimisation of the microencapsulation of tuna oil in gelatin–sodium hexametaphosphate using complex coacervation. *Food Chemistry, 158*, 358–365.

Wang, B., Timilsena, Y. P., Blanch, E., & Adhikari, B. (ng et al., 2017 b). Characteristics of bovine lactoferrin powders produced through spray and freeze drying processes. *International Journal of Biological Macromolecules, 95*, 985–994.

Wang, B., Timilsena, Y. P., Blanch, E., & Adhikari, B. (2017a). Mild thermal treatment and *in-vitro* digestion of three forms of bovine lactoferrin: Effects on functional properties. *International Dairy Journal, 64*, 22–30.

Yan, Y., Kizilay, E., Seeman, D., Flanagan, S., Dubin, P. L., Bovetto, L., et al. (2013). Heteroprotein complex coacervation: bovine β-lactoglobulin and lactoferrin. *Langmuir, 29*(50), 15614–15623.

CHAPTER 7

General Discussion, Overall Conclusions, and Recommendations

7.1. Introduction

This thesis documents a series of research work carried out to study the structure-function relationships of bovine lactoferrin (LF) during thermal processing and gastrointestinal digestion, aiming to preserve its structural integrity and functional properties. The new findings contribute to the body of underpinning science which can be applied to protect LF against harsh environmental conditions prevailing in powder formation and digestion. This thesis started hypothesising that the environmental stresses prevailing in drying and digestion environments alter LF's three dimensional structure and compromise its functional properties. It further hypothesised that the undesirable changes in LF's structure and subsequent impact on function can be reduced by a) optimising processing parameters and b) forming complex coacervates as more acid-stable matrix. These hypotheses were tested and the outcomes are documented in Chapter 3 to Chapter 6. Regarding the effect of drying, it was found that denaturation of LF occurred at convective drying environments if the exposure time was longer. However, denaturation was avoided in convective drying process with short residence time (spray drying) and in low temperature drying process (freeze-drying) even when the residence time was longer. The above findings imply that industries can produce LF powders without losing its structural integrity and functional properties by selecting suitably optimised spray- and freeze-drying processes. In the digestion studies, it was found that the LF was completely hydrolysed at the gastric stage of digestion. The findings in these studies showed conclusively that LF must be protected by suitable means to deliver its functional attributes (e.g. iron transferring property) to human body. Complex coacervation between LF and sodium alginate (NaAlg) was carried out in order to preserve LF's structure and functions in the gastrointestinal tract. It was found that this approach was partially successful as ~30% of LF in complex coacervated form was delivered to the intestinal absorption sites in the functionally intact forms.

This thesis commenced with the study of the powder formation process of LF. Single droplet drying experiments were conducted to obtain the fundamental information such as the drying rate, drying kinetics and the nature and extent of changes in secondary structural features (denaturation) during convective air drying. This information was used to design or formulate a spray drying process so that lowest possible denaturation of LF was achieved. The physicochemical and functional characteristics of the spray-dried LF powders were determined and compared with those of freeze-dried ones. In order to understand the effect of thermal stress on the digestion behaviours of LF, the structural and functional properties of

both mild thermal treated and untreated (not heated) LF at different stages of digestion (*in-vitro*) were determined. As final part of the experimental work, LF-NaAlg complex coacervates were synthesised and the efficacy of this method in protecting LF's structure and functional properties at different stages of digestion was examined.

The research outcomes in this thesis provide fundamental insight into the drying and digestion behaviours of LF and LF-NaAlg complex coacervates. The understanding of the drying and denaturation behaviours of LF, documented in this thesis, provides essential underpinning science as well as validated process parameters to produce LF powders using spray drying which is much cost effective than freeze drying. This would increase the availability and affordability of LF powders and broaden their application in many food and pharmaceutical formulations. The advances made on the science of digestion and LF-NaAlg complex coacervation shall facilitate much effective delivery of LF through oral route as LF-NaAlg can be easily incorporated in high-value food products such as infant formula and nutritional supplements. Altogether, this study will contribute to the good health and wellbeing of human population.

7.2. Main research findings, overall discussion and conclusions

The structure-function aspects of all three forms of LF (iron depleted apo-LF, iron saturated holo-LF and native-LF with 12.6% iron saturation) were studied. The apo- and holo-LF were prepared in the laboratory. The iron saturation level of apo- and holo-LF was 1.4 and 100.0%, respectively. The native-LF was obtained by using membrane filtration technology and was received in solution form from a local manufacturer. The purity of these LFs was >90%. At the first stage of this study, all the three forms of LF were subjected to convective air drying and *in-vitro* digestion conditions. Mild thermal treatment, which simulated the thermal stress that could be encountered in the pre-processing of the drying process, was also carried out to investigate its effect on the drying and digestion behaviours of LF. It was found that 20-30% of apo-LF and 10-20% of holo-LF was denatured during convective air drying of 70 and 95^{o}C when the drying (or residence) time was 10 min. These observations showed that iron saturation increased the thermal stability of LF during convective air drying process. However, in adult digestion conditions, all the three forms of LF were completely degraded to <10 kDa small peptides/amino acids. The iron binding ability of all the three forms of LF was decreased by ~80%. The mild thermal treatment did

not exert significant effect on the digestion behaviours of LF. These findings indicate that iron saturation or an increase in iron saturation level did not increase the stability of LF's structure in gastrointestinal tract. Based on the facts that native-LF is primary product obtained industrially and that the digestion pattern of LF is not affected by the degree of iron saturation, native-LF was used for the further spray/freeze drying and complex coacervation studies. Both spray and freeze drying processes produced high quality (native-) LF powders with <2% denaturation. The antioxidant capacity of the spray-dried LF powders was comparable to that of liquid ones indicating the fact that the spray-drying process did not affect this important functional attribute. The LF-NaAlg complex coacervates were produced with ease in 4.0-5.0 pH range and 8:1 to 16:1 LF-to-NaAlg mass ratios with yield values of >85%. Thus, this is highly feasible method to replicate in industrial settings. The secondary structural features of LF were not affected when it was complex coacervated with NaAlg. These complex coacervates protected ~30% of LF from hydrolysis during gastric digestion. The key findings obtained from the above studies and their significance to the body of knowledge and real-life application are articulated in the ensuing sections

7.2.1. Convective air drying and denaturation characteristics of lactoferrin

Currently, there is limited research on spray drying of LF owing to the difficulty of measuring drying and denaturation kinetics of aqueous LF droplets in the spray drying chamber. Hence, single droplet drying, which mimics the spray drying environment, was used to determine the drying and denaturation characteristics of LF in industrially applicable convective air drying (spray drying) conditions.

The key findings of the drying and denaturation characteristics of LF are documented in **Chapter 3**. The thermal properties of LF were determined by using differential scanning calorimeter. The data revealed that the thermal denaturation temperature of holo-LF is 22ºC higher than that of apo-LF. The denaturation temperature of native-LF lies in between that of holo- and apo-LF. This higher thermal stability of holo-LF is attributed to its more compact conformation formed by binding two iron atoms (Rastogi *et al.*, 2016). For this reason, two convective air drying temperatures (70 and 95ºC) were selected to investigate the drying and denaturation profiles of all three forms of LF. The relative humidity values at these two temperatures ranged from 6 to 7% and the air velocities past the droplet were maintained at 0.5-1.0 m/s. This is realistic slip velocity range in co-current spray dryers as air and particles

move in the same direction. Single droplet of 1,200 µm was created and dried for 10 min. Denaturation kinetics of LF was measured at both temperatures. The thermal stability of the iron-saturated holo form was the highest (10-20% denaturation), that of iron-depleted apo from was the lowest (20-30% denaturation), and that of native form remained in between these two forms at both drying air temperatures (~20% denaturation). As determined by circular dichroism, the alteration of secondary structural features (α-helix, β-sheet, β-turn, and random coil) of all the three forms of LF was of the order of 10% in both medium temperatures (70 and 95°C) and exposure time (10 min). However, in the spray drying process, even the largest droplet size of LF was smaller than 100 µm diameter and it dried much faster due to higher surface area to volume ratio. As high drying rates prevail at high surface area to volume ratio, it is expected much less conformational changes (denaturation) of LF to occur during spray drying process. The insights gained from the single droplet drying study led to the conclusion that the spray drying process can be effectively used to produce LF powders.

7.2.2. Denaturation and physicochemical characteristics of spray- and freeze-dried LF

Fresh aqueous bovine LF solution obtained from membrane processing (16–18%, w/v) that obtained directly from industry was used as staring material for spray and freeze drying. This aqueous LF solution was spray dried as received without dilution or concentration. The physicochemical and functional properties of the spray- and freeze-dried LF powders were measured, compared and explained. The findings of this part of study are documented in **Chapter 4**.

Spray drying was carried out at 180^{o}C inlet temperature and two outlet temperatures of 70 and 95^{o}C. These two outlet temperatures were found to be optimum through single droplet drying experiments and also covered the denaturation temperature of apo-LF (66^{o}C) and holo-LF (88^{o}C) mentioned above. The freeze drying process was comprised of pre-freezing (-20^{o}C, 24 h), primary (0^{o}C, 12 h) and secondary (20^{o}C, 6 h) drying stages. These drying parameters are within the range of industrially preferred freeze drying conditions (Tang & Pikal, 2004). Both spray- and freeze-dried LF powders showed negligible denaturation (<2%) and had no significant ($p>0.05$) changes in their secondary structural features. The antioxidant activity of both spray- and freeze-dried powders was also comparable to that of fresh membrane processed aqueous LF solution. The solubility of both spray- and freeze-

dried LF were >94%. The moisture sorption properties of spray and freeze-dried LF were similar to each other with identical type II sorption behaviour. All the dried-LF powders demonstrated typical amorphous characteristics with <2.1% crystallinity. Only minor differences in the physical properties (e.g. moisture content and water activity) were observed between the spray- and freeze-dried LF powders. The findings documented in Chapter 4 indicate that, under suitably optimised drying conditions, spray drying can be confidently used to produce amorphous LF powders with intact molecular configuration and high antioxidant capacities. The characteristic short drying time (<17 s) (Schmitz-Schug, Foerst & Kulozik, 2013) and rapid evaporative cooling prevailing in spray drying process are attributed in preserving the structural configuration and functional properties of spray-dried LF powders. The combination of low temperature and direct sublimation of solid water (ice) into water vapour during freeze drying also avoided the denaturation of LF.

7.2.3. Fate of lactoferrin in simulated gastrointestinal digestion

In order to study the fate or breakdown of lactoferrin powders during simulated gastrointestinal digestion, spray- and freeze-dried LF powders produced as detailed in Chapter 4 are used. These powders were dissolved in Milli-Q water and subjected to *in-vitro* adult digestion. The change of structure and functional properties of LF at oral, gastric and intestinal stages of digestion were measured, interpreted and documented in **Chapter 5**. The effects of mild thermal stress (isothermal heating at 70^{o}C for 10 min) and iron saturation/depletion on the digestion behaviour of LF were also studied and documented in **Chapter 5**. The Sodium dodecyl sulphate polyacrylamide gel electrophoresis tests revealed that hydrolytic degradation of LF occurred primarily during the gastric stage of digestion. All the three forms of LF were degraded to <10 kDa fractions due to the acidic (pH <2.0) hydrolysis and pepsinolysis by pepsin. The breakdown of LF also altered secondary structural features. It was found that >10% of the α-helix structure of LF was converted into random coil during the gastric stage of digestion. Due to this alteration in conformation coupled with hydrolysis of LF into peptides in the gastric stage, most of the iron (>80%) was dissociated from the LF's structure in this stage and its iron binding ability was irreversibly lost. The antioxidant capacity of LF was also decreased in this digestion stage. These findings indicated that LF is not able to deliver its biologically active iron and other important functional properties to the absorption sites located at the small intestine. The isothermal heat

treatment and the degree of iron saturation in LF had no significant difference in its digestion. Therefore, thermal treatment usually applied during the pre-processing of LF (before spray or freeze drying) was found to exert no significant effect on the digestion behaviours of LF. Iron saturation, which results into a more compact structure of LF, is also not adequately effective in delivering LF to the small intestine through oral route. The above findings suggested that more effective protection is required to preserve the structural and functional properties of LF during digestion and that LF must be adequately encapsulated in order to deliver it as part of food.

7.2.4. Complex coacervation and its effect on the digestion behaviours of LF

Electrostatic complexation (complex coacervation) of LF with NaAlg was used in this thesis to slow down or minimise the premature digestion of LF in gastric digestion stage. The choice of NaAlg as oppositely charged biopolymer is based on the fact that it is readily available in the market and its desirable characteristics such as good affinity with water and highly anionic charge density at pH values > 2.0 (Carneiro-da-Cunha *et al.,* 2011; Harnsilawat, Pongsawatmanit, & McClements, 2006). Furthermore, NaAlg is also resistant to pepsin hydrolysis (Chater *et al.,* 2015). This is also a temperature and acid stable polysaccharide, hence, NaAlg was used to synthesise LF-NaAlg complex coacervates. The LF-NaAlg complex coacervates were prepared at the optimised pH and LF-to-NaAlg ratios (**Chapter 6**). The physicochemical properties and the digestion behaviour of the LF-NaAlg complex coacervates are documented in **Chapter 6**.

The LF-NaAlg complex coacervate formation process is affected by the LF-to-NaAlg ratio, pH, temperature and ionic strength (De Kruif, Weinbreck, & de Vries, 2004; Liu, Low, & Nickerson, 2009). The optimum pH and the LF-to-NaAlg ratio were determined as the starting point. The measured electrostatic charge density (zeta potential) indicated that LF is positively charged below pH 8.0 and NaAlg is negatively charged above pH 2.0; therefore, LF and NaAlg were able to form complex coacervates over a wide pH range (pH 2.0–8.0) and LF-to-NaAlg ratios (4:1–24:1). However, the highest yield (91%) and turbidity (61 FTU) of LF-NaAlg complex coacervate were observed at pH 4.5 and at LF-to-NaAlg ratios of 8:1. Slightly lower, yet realistic yield and turbidity values (85%, 57 FTU) were achieved at a LF-to-NaAlg ratio of 16:1. Since the higher LF-to-NaAlg ratio contains lower concentration of NaAlg in the final LF-NaAlg complex coacervates, the LF-to-NaAlg ratio of 16:1 could be a

preferred parameter for industrial production. Therefore, LF-to-NaAlg ratios of either 16:1 or 8:1 can be chosen as the optimum ratio depending on the application of the resultant complex coacervates. It has to be stated here that no change in the secondary structural features of LF occurred due to the formation of electrostatically driven LF-NaAlg complex coacervates. Furthermore, these LF-NaAlg complex coacervates provided 27%–34% protection to LF during the gastric stage of digestion. It is worth noting here that structure feature of un-complex LF is completed destroyed at this stage of digestion. This level of protection provided by the NaAlg is due to the fact that formed insoluble complex coacervates and blocked some of the sites which would otherwise be available to pepsin for proteolysis. As a consequence, significantly less alteration of secondary structural features of LF was observed at the gastric stage of digestion. Interestingly, the antioxidant capacity of LF was fully retained during gastrointestinal tract. However, the effectiveness of LF as an iron transferring protein was not improved when it formed complex coacervates with NaAlg. This is because LF was not entirely covered when it was coacervated with NaAlg and hence its surface was partially exposed to the acid and enzymes prevailing during gastric digestion stage. These exposing patches provide sites for acid and enzymes to penetrate the coacervate structure. Once the enzymes and acids are able to access the sites, they are able to irreversibly break down the iron binding structural domains of LF and ultimately compromise its iron binding ability. Therefore, forming complex coacervates with NaAlg only slowed down or reduced the premature digestion of LF in gastric digestion stage to some extent. Much stronger or effective protection of LF's structure and associated functions (e.g. iron binding ability) requires additional treatments such as forming complex coacervates with a more digestion-resistant matrix or application of completely different microencapsulation method. Nevertheless, the above findings provide useful insights of digestion of LF in complex coacervated state.

7.3. Contribution made by this Thesis to the community and industry

The major contributions made by this Thesis are listed below.

1. This research is important to industry as well as to the academic community. The findings documented in Chapter 3 (Wang *et al.*, 2017a) and Chapter 4 (Wang *et al.*, 2017b) show, conclusively, that structurally and functionally intact LF powders can be produced through spray drying and these powders possess either similar or better

physicochemical properties compared to the LF powders produced through freeze-drying. When an industry implements the process protocols developed in this study, it can produce spray-dried LF powders at significantly low cost. Upon implementation of these findings in industry, LF powders will be more readily available. This will broaden the application of LF in many food and pharmaceutical formulations.

2. The understanding of nature and extent of digestion of LF in human digestive system is important for industry as well to the end-users. This understanding will help develop encapsulating shell material and encapsulation method that can produce encapsulated LF powder that resist the premature digestion of LF in the gastric stage of digestion. Such encapsulated LF powders can then be used to deliver LF in structurally and functionally intact form to the desired sites of human intestine for its absorption. For example, the findings from Chapter 5 (Wang *et al.*, 2017c) showed that all forms of LF were completely hydrolysed or digested in gastric phase of digestion, which indicates that this protein must be protected from premature digestion in order to effectively deliver it to the small intestine.

3. The findings documented in Chapter 6 (Wang *et al.*, 2017d) indicated that the LF-sodium alginate complex coacervates can be synthesized easily and efficiently if the specific pH range and LF-to-NaAlg ratios proposed in this work are used. This complex coacervation process can be replicated or scaled up easily in industrial setting. The structure and function of LF are better protected in complex coacervated form with NaAlg in the digestion stage of human digestion upon oral intake. Thus, this study will ultimately contribute to the good health of human population.

Four research articles and a review paper were generated from this thesis. All the research articles have been published in peer-reviewed journals. The review article forms the Literature Review chapter. It has been accepted for publication in a well-regarded refereed journal. Overall, the findings of this study provide sound basis for producing high quality LF powders using convective air drying/spray drying. It also provides insightful knowledge for preserving the structure-function properties of LF during digestion by using complex coacervation.

7.4. Recommendations for the future work

Due to constraints in time and resources, the following lines of research could not be pursued and are recommended for future research.

1. Fresh membrane processed native-LF donated by Tatura-Bega company was used, as received, as the starting material to produce spray-and freeze-dried LF powders. The spray and freeze drying studies of holo- and apo-LF could not be undertaken as these two forms of LF were synthesised in small quantities. The holo-LF provides more iron content in LF-fortified products and apo-LF possesses stronger iron binding capacity compared to the native form. A systematic study on the science of powder formation and greater understanding of the functional properties of apo- and holo-LF would help them produce commercially and make them available in the market.

2. Industrially obtained native-LF was used to form LF-NaAlg complex coacervates. The science of formation of complex coacervates of holo-/apo-LF and NaAlg and their digestion behaviour could not be studied as part of this thesis. Studies on these two aspects would provide better understanding of molecular level of interaction between LF and NaAlg.

3. Preliminary results have shown that calcium chloride ($CaCl_2$) could displace the iron content in LF. The interaction of calcium ion with LF and/or LF-NaAlg complex coacervate may displace iron ion and may make LF nutritionally inferior. The displacement of iron from LF and encapsulated LF structure by any ion is important from scientific and application perspective.

4. The LF-NaAlg complex coacervates provided up to 34% protection of LF during digestion. However, there are many acid-stable polysaccharides such as guar gum, xanthan gum and pectin. These polysaccharides could form complex coacervates with LF but could not be studied in this thesis. Thus, synthesis of complex coacervates of LF with broad range of acid-stable polysaccharides and their digestion study could be an interesting line of research.

5. Secondary structural features of LF were used as indicators of changes in its structure-function relationship during drying and digestion. The higher order structure can be realistically used for this purpose. Three-dimensional modelling can provide a holistic

picture of the structure-function correlations of LF and its complexes and complex coacervates.

6. Adult intestinal digestion was simulated in this thesis in preparing simulated digestion fluids. The digestion condition in infant intestinal tract was not simulated. Since the digestive systems of infants and newborns are different than that of adult (e.g. intragastric pH and the gastric empting rate is higher), LF could exhibit different digestion patterns. Understanding of the digestion and absorption properties of LF and its complexes and coacervates in simulated infant digestion conditions would provide important insights on the digestion of LF used in infant products.

7.5. References

Bokkhim, H., Bansal, N., GrØndahl, L., & Bhandari, B. (2013). Physico-chemical properties of different forms of bovine lactoferrin. *Food Chemistry*, 141(3), 3007-3013.

Carneiro-da-Cunha, M. G., Cerqueira, M. A., Souza, B. W., Teixeira, J. A., & Vicente, A. A. (2011). Influence of concentration, ionic strength and pH on zeta potential and mean hydrodynamic diameter of edible polysaccharide solutions envisaged for multinanolayered films production. *Carbohydrate Polymers*, 85(3), 522-528.

Chater, P. I., Wilcox, M. D., Brownlee, I. A., & Pearson, J. P. (2015). Alginate as a protease inhibitor in vitro and in a model gut system; selective inhibition of pepsin but not trypsin. *Carbohydrate Polymers*, 131, 142–151

De Kruif, C. G., Weinbreck, F., & de Vries, R. (2004). Complex coacervation of proteins and anionic polysaccharides. *Current Opinion in Colloid & Interface Science*, 9(5), 340–349

Harnsilawat, T., Pongsawatmanit, R., & McClements, D. J. (2006). Characterization of b-lactoglobulin–sodium alginate interactions in aqueous solutions: a calorimetry, light scattering, electrophoretic mobility and solubility study. *Food Hydrocolloids*, 20(5), 577–585.

Liu, S., Low, N. H., & Nickerson, M. T. (2009). Effect of pH, salt, and biopolymer ratio on the formation of pea protein isolategum arabic complexes. *Journal of Agricultural and Food Chemistry*, 57(4), 1521–1526.

Rastogi, N., Singh, A., Singh, P. K., Tyagi, T. K., Pandey, S., Shin, K *et al.*, (2016). Structure of iron saturated C-lobe of bovine lactoferrin at pH 6.8 indicates a weakening of iron coordination. *Proteins: Structure, Function, and Bioinformatics*, 84(5), 591-599.

Schmitz-Schug, I., Foerst, P., & Kulozik, U. (2013). Impact of the spray drying conditions and residence time distribution on lysine loss in spray dried infant formula. *Dairy Science & Technology*, 93(4–5), 443–462

Steijns, J. M., & Van Hooijdonk, A. C. M. (2000). Occurrence, structure, biochemical properties and technological characteristics of lactoferrin. *British Journal of Nutrition*, 84(S1), 11-17.

Tang, X. C., & Pikal, M. J. (2004). Design of freeze-drying processes for pharmaceuticals: practical advice. *Pharmaceutical research*, 21(2), 191-200.

Wang, B., Timilsena, Y. P., Blanch, E., & Adhikari, B. (2017a). Drying and denaturation characteristics of three forms of bovine lactoferrin. *Drying Technology*, 35(5), 606-615.

Wang, B., Timilsena, Y. P., Blanch, E., & Adhikari, B. (2017b). Characteristics of bovine lactoferrin powders produced through spray and freeze drying processes. *International Journal of Biological Macromolecules*, 95, 985-994.

Wang, B., Timilsena, Y. P., Blanch, E., & Adhikari, B. (2017c). Mild thermal treatment and in-vitro digestion of three forms of bovine lactoferrin: Effects on functional properties. *International Dairy Journal*, 64, 22-30.

Wang, B., Blanch, E., Barrow, C., & Adhikari, B. (2017d). Preparation and study of digestion behavior of lactoferrin-sodium alginate complex coacervates. *Journal of Functional Foods*, 37, 97-106.